Ana Rita Queiroz da Cruz

Gene Therapy-Based Strategies for Glioblastoma Towards Chemosensitization: Use of Gemini Surfactants as Drug Delivery Systems

Dissertação apresentada à Universidade de Coimbra para cumprimento dos requisitos necessários à obtenção do grau de Mestre em Biotecnologia Farmacêutica.

Coimbra

Setembro, 2015

Front Cover: RNA silencing.
http://losnuevosguerreros.org/mod/glossary/view.php?id=93&mode=date&hook=&sortkey=UPDATE&sortorder=asc&fullsearch=0&page=12

This work was performed at the Center for Neuroscience and Cell Biology, University of Coimbra, Portugal, in the Group of Vectors and Gene Therapy, under the supervision of Professor Maria Amália da Silva Jurado, Professor Maria da Conceição Monteiro Pedroso de Lima and Professor Luís Fernando Morgado Pereira de Almeida.

This work is funded by FEDER funds through the Operational Programme Competitiveness Factors - COMPETE and national funds by FCT - Foundation for Science and Technology under the strategic project UID/NEU/04539/2013.

Toda a ciência está aqui,
na maneira como esta mulher (…)
rega quatro ou cinco leiras
de couves: mão certeira
com a água,
intimamente com a terra,
empenho do coração.
(…)

Eugénio de Andrade

Agradecimentos

Quero agradecer à Professora Doutora Maria Amália da Silva Jurado e à Professora Doutora Maria da Conceição Pedroso de Lima por me terem orientado desde o projecto da licenciatura, por não desistirem dos textos que eu ia enviando, por terem tido a paciência de me explicar o que estava errado e me darem a oportunidade de melhorar, pelas suas preciosas sugestões e pelo seu rigor científico.

À Doutora Sandra Silva, à Professora Doutora Luísa do Vale e ao Professor Doutor Eduardo Marques, obrigada pela colaboração no que se refere à síntese dos tensioativos.

À Professora Doutora Maria Paula Matos Marques, por ter preparado a solução de cisplatina e pelos conselhos relativos à sua utilização.

À Catarina, pelas técnicas laboratoriais que me foste ensinando e pela parceria ao aprender outras, pelas tuas sugestões semanais, pelas tuas perguntas sempre tão pertinentes e tão desafiantes. À Ana Maria, por teres lido todos os rascunhos deste trabalho, por me dizeres que não devia ser assim e por teres a paciência de me explicar como devia ser. Às duas muito obrigada pelos cafés com ciência, que muitas vezes incluíam as minhas dúvidas e revoltas, obrigada por me ajudarem nesses momentos e por arranjarem sempre uma solução.

Às Ritas, as maiores amigas que Coimbra me trouxe, por me terem acompanhado nesta caminhada, por me ouvirem resmungar e terem o poder de me animar, e por ter a certeza que a saga das Ritas não acaba aqui.

Aos meus amigos da terrinha, às Ineses, Joana, Sara, Mafalda e Catarina, por me obrigarem a fazer uma pausa que, de seguida e com mais energia, se transformava num avanço.

À Susana, a minha maior surpresa neste último ano em Coimbra, por teres sido a minha companheira de escrita, de casa e de dúvidas, obrigada também pelos lenços.

Ao Diogo, por teres o dom de fazer com que tudo pareça mais fácil, por todas as conversas sem fim, conselhos e também pelos ralhetes.

Aos meus pais, irmão e avós, por partilharem a minha atenção com as minhas células, que eu tinha de "alimentar", por acreditarem que seria capaz, às vezes mais do que eu.

Esta tese não seria possível sem vocês, por isso é-vos dedicada.

TABLE OF CONTENTS

Abbreviations

A

AAV - adeno-associated virus

ABC - ATP-binding cassette

Ad - adenovirus

AGO2 - Argonaute 2

B

BBB - blood-brain barrier

BII - Bliss interaction index

BIR - baculoviral IAP repeat domain

BIRC5 - baculoviral IAP repeat containing 5

***bis-quats* -** bis-quaternary ammonium salts

C

CDDP - cisplatin

cDNA - complementary DNA

CGS - cationic gemini surfactants

CMC - critical micellar concentrations

CMV - cytomegalovirus

CNS - central nervous system

CSC - cancer stem cells

D

DLS - dynamic light scattering

DOPE - dioleoylphosphatidylethanolamine

dsRNA - double-stranded RNA

E

EGFR - epidermal growth factor receptor

ETO - etoposido

F

FDA - Food and Drug Administration

G

GBM - glioblastoma

GFP - green fluorescent protein

H

H_{II} - inverted hexagonal phase

HL - helper lipids

HPRT1- hypoxanthine phosphoribosyltransferase 1

I

IAP - inhibitor-of-apoptosis proteins

L

L_o - liquid-ordered

M

MET - mesenchymal-epithelial transition

MGMT - O6-methylguanine-DNA methyltransferase

miRNAs - microRNAs

MLV - multilamellar vesicles

MMP - mitochondria-penetrating peptides

mRNA - messenger RNA

MRP2, cMOAT or ABCC2 - multidrug resistance-associated protein 2

mtDNA - mitochondrial DNA

MTS - mitochondrial targeting sequences

N

ncDNA - nuclear DNA

NER - nucleotide excision repair

NRT - no reverse transcription control

NTC - No Template Control

P

PCS - photon correlation spectroscopy

PDGFR - platelet-derived growth factor receptors

pDNA - plasmid DNA

PE - phosphatidylethanolamines

pmtGFP - plasmid DNA encoding mitochondrial GFP

pncGFP - plasmid DNA encoding nuclear GFP

Q

QELS - quasi-elastic light scattering

qRT-PCR - quantitative real time PCR

R

Rb - retinoblastoma protein

RISC - RNA-induced silencing complex

RNAi - RNA interference

Rv - retrovirus

S

siGFP - siRNA duplex against GFP

siRNA DY547 - DY547 labeled non-targeting siRNA duplex

siRNAs - small interfering RNAs

siSURV - anti-survivin siRNA duplex

siMUT - non-targeting siRNA duplex

SRB - sulforhodamine B

T

TKR - receptor tyrosine kinase

TMZ – temozolomide

Topo IIa - Topoisomerase Iia

TTP - triphenylphosphonium cation

W

WHO - World Health Organization

Resumo

O glioblastoma é o tipo de tumor cerebral mais comum e agressivo, caraterizando-se por alta capacidade proliferativa, elevados níveis de angiogénese e grande resistência à quimioterapia. O tratamento médico habitual envolve a remoção do tecido tumoral através de cirurgia, seguida de radioterapia com concomitante ou subsequente administração do agente alquilante temozolomida (TMZ). No entanto, a evolução clínica está longe de ser satisfatória, sendo a taxa de sobrevivência média dos doentes de apenas 15 meses após o diagnóstico. Tendo em consideração que a maior causa de insucesso do tratamento desta patologia reside na resistência intrínseca e adquirida aos fármacos, este trabalho teve por principal objectivo o desenvolvimento de estratégias terapêuticas capazes de sensibilizar as células de GBM a agentes quimioterapêuticos. Com este propósito, foram implementadas duas estratégias de terapia génica não-viral, envolvendo o uso de tensioativos gemini catiónicos (CGS) e explorando o seu potencial para a vectorização de ácidos nucleicos e fármacos. Numa das estratégias foram utilizados CGS como vectores de siRNAs em células humanas de glioblastoma (U87), a fim de diminuir a expressão da proteína anti-apoptótica survivina, sobre-expressa em tecidos tumorais, e aumentar, consequentemente, a susceptibilidade das células a agentes quimioterapêuticos. A segunda estratégia usufruiu da vantagem dos GSC promoverem a transferência de pDNA tanto para o núcleo como para as mitocôndrias de células de uma linha de glioblastoma estabelecida a partir de um tumor recorrente (DBTRG-05MG), e explorou a capacidade desses mesmos sistemas de entrega induzirem a libertação, em ambos os organelos, do fármaco anticancerígeno cisplatina (CDDP), cuja ação farmacológica envolve a formação de aductos com moléculas de DNA.

Neste trabalho ficou patente que a redução da expressão de survivina potencia sinergisticamente a acção tóxica dos compostos TMZ e etopósido nas células U87. Por outro lado, a exposição de células DBTRG-05MG a CDDP incorporada em complexos de pDNA e tensioativos gemini derivados de serina conduziu a uma diminuição drástica da viabilidade e da proliferação das células, bem como à paragem do ciclo celular na fase S, efeitos que mostraram ser mais severos do que os induzidos por CDDP na forma livre, na mesma concentração. Adicionalmente, o pDNA usado como veículo de CDDP, complexado com tensioativos gemini, demonstrou não ter perdido a capacidade de promover expressão génica, quando transferido para o núcleo ou para a mitocôndria. Desta forma, as estratégias implementadas neste estudo revelaram a possibilidade de reduzir as doses terapêuticas de fármacos anticancerígenos, contribuindo para prevenir o desenvolvimento de quimiorresistência e obviar efeitos colaterais dos fármacos. Além disso, demonstrando a versatilidade e o elevado potencial das formulações contendo tensioativos gemini para a

vectorização de ácidos nucleicos e fármacos em células de GBM, este estudo abre caminho a abordagens terapêuticas multi-modais que, aliando a quimioterapia à terapia génica, permitem vencer com elevada eficiência a quimiorresistência de GBM.

Abstract

Glioblastoma (GBM) is the most common and aggressive primary brain tumor, being characterized by its propensity for proliferation, strong angiogenesis and resistance to chemotherapy. The standard treatment involves maximal surgical resection, radiotherapy and adjuvant or concomitant administration of the alkylating drug temozolomide (TMZ). However, the clinical outcome has proven to be far from being satisfactory, patients having a median survival of only 15 months after diagnosis. Taking into account that the major cause of treatment failure in GBM patients is the intrinsic and acquired drug resistance, the objective of the present work was centered in the development of therapeutic strategies aiming at sensitizing GBM cells to chemotherapeutics. To accomplish this objective, two gene therapy-based approaches were developed, involving the use of cationic gemini surfactants (CGS) and exploiting their potential for drug delivery. The first strategy took advantage of the ability of CGS to deliver siRNA, in order to promote downregulation of the anti-apoptotic protein survivin, aberrantly expressed in tumor tissues, so that GBM cells (U87) become more susceptible to chemotherapeutics. The second strategy benefited from the potential of GCS to deliver pDNA into nucleus and mitochondria in human recurrent glioblastoma cells (DBTRG-05MG), exploring their capacity to promote in both organelles a co-delivery of the anti-cancer drug cisplatin (CDDP), whose pharmacological activity is based on the formation of adducts with DNA molecules.

Significant results were obtained showing that survivin knockdown combined with temozolomide or etoposide administration resulted in a synergistic toxic effect on U87 cells. Additionally, the delivery of CDDP formulated in serine-derived gemini surfactant-based complexes led to a drastic decrease of viability of DBTRG-05MG cells, an efficient inhibition of cell growth and a significant arrest of the cell cycle in the S phase, effects that showed to be much more severe than those induced by free CDDP, at the same concentrations. Moreover, it was observed that the pDNA, used as a vehicle of CDDP formulated in gemini surfactant-based complexes, did not lose its capacity to promote gene expression, when delivered both in the nucleus and in mitochondria.

Therefore, both strategies implemented in this study revealed the possibility of reducing the doses of anti-cancer drugs to prevent the emergence of chemoresistance and drug side-effects. Additionally, benefiting from the versatility and potential of gemini surfactant-based formulations for drug delivery in GBM cells, this study opens windows towards the establishment of multimodal therapeutic approaches, allying chemotherapeutics to gene therapy, aiming at surpassing the chemoresistance of GBM.

Chapter 1

Introduction

Introduction

1.1. Glioblastoma

The central nervous system (CNS) is composed of two types of cells: neurons (or nerve cells) and neuroglia (or glia), the latter being three times more abundant than the former. Physically, glial cells are similar to neurons, but their less prolonged branches do not have the same functions as axons and dendrites. Neurons are responsible for receiving, processing and sending electrical signals, through synaptic interactions. Glial cells support neurons' functions: preserve the ionic milieu of nervous system, modulate signal transmission, synaptic action and neural development, and also assist the recovery of injured neurons (Purves *et al.*, 2004). Glial cells can be divided into three cell types: astrocytes, oligodendrocytes and microglial cells.

Tumors that arise from glial cells are named gliomas and the ones that emerge from astrocytes (astrocytomas) are the most common form of glioma, accounting for 75% of all primary CNS gliomas (Adamson *et al.*, 2009). Glioblastoma (GBM), which is classified by the World Health Organization (WHO) as a grade IV glioma, being therefore the most malignant and challenging astrocytoma to treat, represents > 51% of all primary CNS gliomas (Adamson *et al.*, 2009). The etiology of gliomas is still unknown, but two risk factors have been pointed as possible causes for their development: the exposure to high doses of ionizing radiation and hereditary mutations associated with syndromes such as Cowden's disease, Li–Fraumeni syndrome and neurofibromatosis (Adamson *et al.*, 2009; Schwartzbaum *et al.*, 2006). The most common symptoms of GBM are progressive focal neurologic deficits, headaches, and seizures (Adamson *et al.*, 2009).

1.1.1. Grading

WHO grading, which is a "malignancy scale" based on the histology of tumors of the CNS, when combined with other parameters such as age, tumor location, proliferation rate and genetic alterations, allows to predict the neoplasm behavior, establish a prognosis, choose the appropriate therapy and predict the response to this therapy (Louis *et al.*, 2007). Table 1.1 shows the WHO grading of astrocytic gliomas, the predictive prognosis and neoplasm behavior.

Besides the four WHO grades, in which gliomas are divided, two different classes of astrocytic gliomas are considered regarding their capacity for invasion and propensity for malignancy progression: diffuse astrocytic tumors, which include WHO grades II, III and IV that are described as tumors with a high potential for invasion, with diffuse infiltration, and

with a propensity to develop into higher grades of malignancy; and low grade infiltrative astrocytomas, which correspond to WHO grade I and are characterized by their limited invasion and propensity for malignancy progression (Ware, Berger and Binder, 2003).

Table 1.1 - WHO grading of astrocytic gliomas Louis *et al.*, 2007; Ware *et al.*, 2003.

WHO grading	Astrocytic gliomas	Prognosis	Neoplasm behavior
Grade I	juvenile pilocytic astrocytoma	treatable with resection	low proliferation
Grade II	diffuse astrocytoma	> 5 years	low proliferation, infiltrative, nuclear atypia, possibility of malignancy progression
Grade III	anaplastic astrocytoma	2 – 3 years	nuclear atypia, mitotic activity, possibility of malignancy progression
Grade IV	glioblastoma	1 year	nuclear atypia, mitotic activity, endothelial proliferation, necrosis

Based on the origin of the tumor, GBMs can also be classified as primary and secondary GBMs. Primary GBM accounts for 90% of all GBM cases, occurring in older patients, and arise in an isolated manner, without clinical or histological signals of a previous less malignant astrocytoma (Ohgaki and Kleihues, 2007, 2013). Secondary GBM occurs in patients with less than 45 years and arises from a lower grade astrocytoma, commonly from WHO grade II, which progressively becomes a higher malignancy astrocytoma (WHO grades III or IV) (Furnari *et al.*, 2007). Interestingly, their morphology is indistinguishable but their genetic and epigenetic profiles reveal differences, which probably indicates that these two classes of GBM require different therapeutic strategies (Furnari *et al.*, 2007; Ohgaki and Kleihues, 2007, 2013). For this reason and also because tumors of the same WHO grade behave differently towards therapy, an extensive research has been conducted to identify different chromosomal abnormalities, genetic alterations and impaired molecular pathways of the astrocytic tumors (Furnari *et al.*, 2007; Ohgaki and Kleihues, 2007; Tanaka *et al.*, 2013;

Verhaak *et al.*, 2010). This may allow a more detailed classification of gliomas and also the design of new molecular targeted therapies.

1.1.2. Common hallmarks and impaired signaling pathways

GBM is characterized by uncontrolled cellular proliferation and widespread invasion, resistance to apoptosis, strong angiogenesis, and propensity to impair adjacent normal tissue (Furnari *et al.*, 2007). In addition, GBM exhibits cellular heterogeneity, presenting a subpopulation of cancer stem cells (CSC) that seems to be responsible for tumor resistance to chemotherapy. Therefore, GBM patient prognosis remains poor, the disease culminating in death 12 to 15 months after diagnosis.

Genetic alterations, specifically the activation of oncogenes and the downregulation of tumor-suppressor genes, have been identified in all types of cancers, as contributors to tumor proliferation. A great number of these genetic abnormalities have been found in GBM, favoring cell proliferation, cell migration and apoptosis inhibition. These features have been correlated with the capability of low grade astrocytic tumors to achieve higher levels of malignancy (secondary GBM).

Regarding GBM molecular expression, GBM can be divided into four subtypes: proneural, neural, classical and mesenchymal, and the response to therapy is dependent on the subtype, the classical subtype being the most susceptible and the proneural subtype being the most resistant (Verhaak *et al.*, 2010). Nevertheless, there are three signaling pathways that are proven to be impaired in all subtypes of GBM: the receptor tyrosine kinase (TKR)/Ras/PI3K, the retinoblastoma protein (Rb) and p53 signaling (Tanaka *et al.*, 2013). These three pathways ensure the balance between cell proliferation and cell death, acting in different manners.

TKR/RAS/PI3K signaling is impaired in 88% of GBM cases (Cancer Genome Atlas Research Network, 2008; Tanaka *et al.*, 2013) and the overexpression of the TRK epidermal growth factor receptor (EGFR) is present in 40%-50% of patients with GBM (Stommel *et al.*, 2007; Tanaka *et al.*, 2013; Ware *et al.*, 2003). Among them, 50% present the EGFRIII variant, which causes a constitutive activation of this signaling pathway, leading to cell growth, proliferation and survival. Besides EGFR, other TKRs can be amplified, namely platelet-derived growth factor receptors (PDGFR) and mesenchymal-epithelial transition (MET) (Snuderl *et al.*, 2011; Stommel *et al.*, 2007; Szerlip *et al.*, 2012), which reflects intratumoral heterogeneity (Szerlip *et al.*, 2012) and likely results in tumor-resistance to targeted therapies (Stommel *et al.*, 2007).

A high percentage of GBM patients (78%) present Rb signaling impairment. Rb protein mediates G1/S cell cycle arrest, and the loss of function of this protein in GBM favors G1/S progression and, consequently, cancer development (Cancer Genome Atlas Research Network, 2008; Tanaka *et al.*, 2013).

The p53 signaling pathway is altered in 87% of GBM patients (Cancer Genome Atlas Research Network, 2008; Tanaka *et al.*, 2013). In response to DNA damage, the tumor suppressor protein p53 causes G1 and/or G2 cell cycle arrest, leading to apoptosis (Tanaka *et al.*, 2013). In addition, wild-type p53 downregulates, at the transcriptional level, survivin expression, which is one of the nine members of the family of inhibitor-of-apoptosis proteins (IAP) (George, Banik and Ray, 2010; Mita *et al.*, 2008). Therefore, due to p53 function impairment in GBM, overexpression of survivin is potentiated and, consequently, the cancer progresses.

Survivin overexpression

Survivin is a 16.4-kDa protein encoded by the BIRC5 (baculoviral IAP repeat containing 5) gene, which is overexpressed in the majority of cancers, including GBM (George *et al.*, 2010). Survivin, the smallest protein of the IAP family, contains a single BIR (baculoviral IAP repeat domain) and acts through inhibition of mitochondrial-dependent apoptosis. However, its function is not limited to cell death blocking, since it also plays an important role in the regulation of mitosis (Okada and Mak, 2004), angiogenesis (Duffy *et al.*, 2007; Ryan, B.; O'Donovan, N.; Duffyg, 2009) and chemoresistance (Mita *et al.*, 2008; Pennati, Folini and Zaffaroni, 2008).

After transcription, survivin mRNA undergoes alternative splicing, originating four protein variants: wild-type survivin, survivin-2β, survivin-ΔEx3 and survivin-3β. Survivin-2β differs from wild-type survivin by an additional exon of 23 amino acids; the lack of the exon 3 generates survivin-ΔEx3; and survivin-3B results from the addition of an extra exon (exon 3B) (Caldas *et al.*, 2005; Noton *et al.*, 2006). Therefore, the amino acid sequence of each survivin isoform is remarkably different, which has an impact on protein molecular weight (Table 1.2), tertiary structure and, probably, on the anti-apoptotic function. Additionally, these isoforms have different subcellular locations: survivin, survivin-2β and survivin-3B are preferentialy localized in the cytoplasm, while survivin-ΔEx3 is localized in the nucleus (Mahotka *et al.*, 2002).

Table 1.2 - Features and preferential localization of the four protein isoforms. Adapted from Caldas *et al.*, 2005.

	Survivin	**Survivin-2β**	**Survivin- ΔEx3**	**Survivin-3B**
Preferential localization	cytoplasm	cytoplasm	nucleus	cytoplasm
Protein size (aa)	142	165	137	120
Predicted molecular weight (kDa)	16.4	18.6	15.6	13.8

Survivin constitutes an attractive target for cancer therapies because it is rarely detected in normal tissues (Altieri, 2008; Duffy *et al.*, 2007; Mita *et al.*, 2008) and is highly expressed in tumors (Altieri, 2008), revealing different expression levels of protein isoforms, which can be correlated with tumor aggressiveness (Caldas *et al.*, 2005).

The effect of therapeutic strategies involving survivin silencing on cell death has proven to be cell type-dependent (Trabulo *et al.*, 2011). In fact, survivin depletion can suffice for observing a cell death phenotype, or can result in cancer cell sensitization to apoptosis by chemotherapeutic drugs. In the latter situation, an additional therapy is required to induce cell death, a survivin silencing strategy combined with chemotherapy or with another targeted therapy being more effective in this case (Mita *et al.*, 2008).

1.1.3. Therapeutic approaches

The standard treatment for patients with GBM involves maximal surgical resection followed by radiotherapy and adjuvant or concomitant temozolomide (TMZ) administration. This combined treatment prolongs survival in 2.5 months, when compared with radiotherapy alone (Stupp *et al.*, 2005; Zhang, Stevens and Bradshaw, 2012).

Chemotherapy

a. Temozolomide

Temozolomide (Figure 1.1) was approved by the Food and Drug Administration (FDA) on March, 2005 for treatment of patients with primary GBM (Anton, Baehring and Mayer, 2012). Currently, TMZ is the first-line chemotherapeutic agent for treating GBM patients.

Therapies targeting brain tumors have to overcome blood-brain barrier (BBB) to be effective, and TMZ, an alkylating agent, can cross the BBB, due to its lipophilicity. TMZ is a prodrug that undergoes spontaneous chemical conversion at a physiological pH (Kaina *et al.*, 2007; Zhang *et al.*, 2012). Its active form subsequently acts through the delivery of a methyl

group to the purine bases of DNA, thus methylating O6-guanine, N7-guanine and N3-adenine, the O6 position of guanine being the main site that upon methylation causes cytotoxic lesions (Zhang *et al.*, 2012).

However, this drug has shown to induce chemoresistance, losing its efficiency to treat GBM patients. The main mechanism responsible for the acquired chemoresistance is the increased expression of the DNA-repair enzyme O6-methylguanine-DNA methyltransferase (MGMT) (ESTELLER *et al.*, 2000; Kaina *et al.*, 2007; Pan *et al.*, 2012), which repairs guanine through the removal of the methyl adducts. Therefore, the majority of primary GBM submitted to standard therapy recurs and currently there is no accepted therapeutic approach to treat patients with secondary GBM (Sevim, Parkinson and McDonald, 2011).

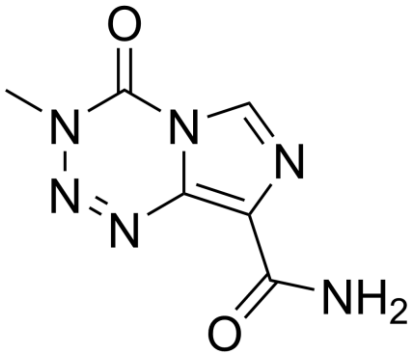

Figure 1.1 - Chemical structure of temozolomide, an alkylating agent used as the first-line treatment of GBM.

b. Etoposide

Etoposide (ETO, Figure 1.2) acts against Topoisomerase II enzyme, specifically targeting Topoisomerase IIa (Topo IIa) (Sevim *et al.*, 2011). Topo IIa transiently cleaves both DNA strands to relax supercoiled DNA (Liu, 1989), facilitating DNA access to enzymes and allowing its replication or transcription. Therefore, ETO interferes with DNA metabolism, limiting cancer progression.

The therapeutic potential of ETO has been tested in patients with recurrent malignant glioma but only 20% of the patients with GBM responded to this treatment (Fulton, Urtasun and Forsyth, 1996).

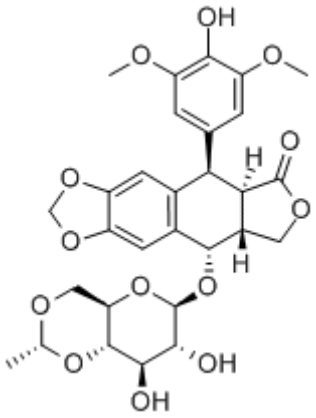

Figure 1.2 - Chemical structure of Etoposide, a DNA topoisomerase poison.

c. Cisplatin

Cisplatin or cis-diamminedichloroplatinum II (CDDP; Figure 1.3), a platinum anticancer drug, was approved by FDA in 1978, to treat testicular and bladder cancer (Galluzzi *et al.*, 2012). Currently, it is also used as a first-line treatment for a broad range of solid tumors such as ovarian, cervical, head and neck, esophageal and lung (Rocha *et al.*, 2014; Todd and Lippard, 2010) and as an adjuvant therapy in recurrent GBM (Brandes *et al.*, 2004). CDDP has been used in combination with TMZ in patients with recurrent GBM (Brandes *et al.*, 2004), due to the fact that CDDP reduces MGMT activity (Wang, L. and Setlow, 1989). Several other approaches have been used to treat GBM using CDDP in combination with other chemotherapeutics or other molecular agents (Kondo *et al.*, 1995; Li, H. *et al.*, 2012; Rocha *et al.*, 2014).

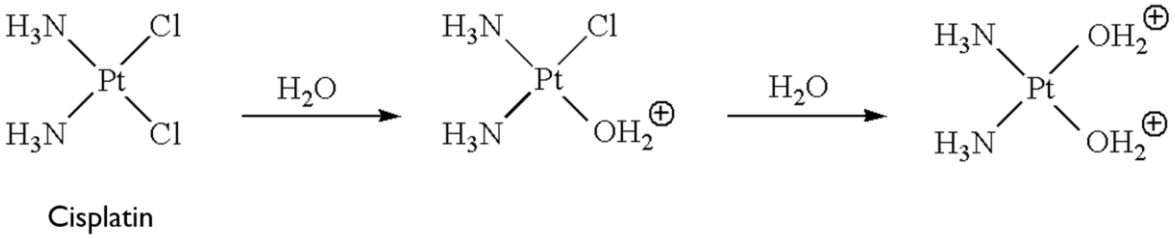

Figure 1.3 - Generation of mono- and bi-aquated cisplatin forms (aquation).

CDDP is formed by one platinum ion surrounded by two chloride ions and two amine groups. Once in the intracellular environment, CDDP undergoes a process known as aquation, in which one or both of its chloride atoms are replaced by water (Figure 1.3). This phenomenon activates its action, since CDDP becomes positively charged and, consequently, capable of interacting with nuclear DNA and with other nucleophiles (Cullen *et al.*, 2007; Rocha *et al.*, 2014). Therefore, CDDP binds covalently to DNA, forming CDDP-DNA

adducts promoting a connection between two bases from the same DNA strand (intrastrand cross-links) or from opposite strands (interstrand cross-links) (Eastman, 1987). Consequently, the impairment of DNA structure results in cell-cycle arrest, through transcription and replication inhibition, which, in turn, triggers cell apoptosis (Todd and Lippard, 2010), or induces cell resistance to CDDP when drug lesions are recognized and removed by nucleotide excision repair (NER) (Martin, Hamilton and Schilder, 2008), present in the nuclear DNA (ncDNA).

In addition to the mechanism of DNA damage repair, the increase of drug efflux, mediated by a member of ATP-binding cassette (ABC) transporters, particularly the multidrug resistance-associated protein 2 (MRP2, also known as cMOAT or ABCC2), limits the efficacy of CDDP during the course of the treatment (Szakács *et al.*, 2006), leading to tumor relapse. In fact, MRP2 was found to be overexpressed in the plasma membrane of CDDP-resistant cells (Szakács *et al.*, 2006).

Mitochondrial DNA (mtDNA) emerges as a promising alternative cellular target for CDDP, since it is also sensitive to DNA intercalation agents (Li, W. *et al.*, 2014) and lacks NER (Cullen *et al.*, 2007). Moreover, once enclosed in mitochondria, CDDP would overcome cellular extrusion, since ABC efflux pumps only act on cytosolic substrates. Additionally, it was reported that mitochondria of cancer cells are more susceptible to injury than those of normal cells, which would enable to selectively target tumor tissues, through mitochondrial impairment (Fulda, Galluzzi and Kroemer, 2010). In fact, Wisnovsky and coworkers (Wisnovsky *et al.*, 2013) demonstrated that the specific delivery of CDDP into mitochondria of ovarian tumor cells was sufficient to cause cell death and, importantly, the induced cytotoxicity affected both wild-type and CDDP-resistant ovarian cancer cells.

Noteworthy, mitochondria are surrounded by a double-membrane that effectively protects the function of their machinery, restricting the access of a wide range of ions and molecules to their interior. Therefore, there is a need for designing vectors that can surpass this barrier, in order to aid drugs to enter into mitochondrial matrix, when this is the local they exert their activity, namely targeting mitochondrial DNA (Smith *et al.*, 2012).

Due to the advances in molecular biological research in the GBM field, cytotoxic agents have been used in combination with molecular approaches, which render cells more susceptible to drug toxicity. In this regard, gene therapy has emerged as a very promising alternative/complementary approach to chemotherapy, due to its potential for regulating gene expression.

Gene Therapy

Gene therapy consists of the delivery of exogenous nucleic acid molecules into abnormal cells, in order to modulate genes that are aberrantly expressed as a consequence of a disease (Opalinska and Gewirtz, 2002). This therapy has potential to treat or impair the progression of several pathologies involving genetic deregulation, such as cancer, cardiovascular, infectious and neurodegenerative diseases (Opalinska and Gewirtz, 2002; Verma and Somia, 1997).

Gene therapy includes three different strategies: gene insertion, gene replacement and gene silencing (Kay, 2011). The primary concept of gene therapy involves gene insertion, a strategy that attempts to induce the expression of a missing protein, through the delivery of a plasmid DNA (pDNA). Gene replacement takes advantage from technologies like zinc finger nucleases and DNA recombination, to repair a genetic mutation. Gene silencing approach benefits from RNA interference (RNAi) technology, which involves the usage of small interfering RNAs (siRNAs) or microRNAs (miRNAs), in order to interfere with a target messenger RNA (mRNA) that is typically overexpressed, owing to a genetic mutation (Hannon, 2002; Kay, 2011).

a. Plasmid DNA (pDNA)

Plasmid DNA is designed as a circular DNA molecule containing a therapeutic and/or a reporter gene under the control of a strong promoter, often that from cytomegalovirus (CMV). Therefore, through the use of plasmid DNA encoding a reporter gene, such as the green fluorescent protein (pGFP), information can be extracted about the percentage of cells that are efficiently transfected, by using a certain gene delivery system. Similarly, plasmid DNA can be delivered to mitochondria inside eukaryotic cells. A novel strategy to track GFP expression into the mammalian mitochondria has been described (Lyrawati, Trounson and Cram, 2011). Taking advantage of the fact that the translation system of mitochondria does not follow the "universal genetic code" (Anderson *et al.*, 1981; Yoon, Koob and Yoo, 2010), Lyrawati and co-workers (Lyrawati *et al.*, 2011) designed a plasmid DNA encoding GFP (pmtGFP) that can only be translated by mitochondrial machinery.

b. Small interfering RNAs (siRNAs)

RNAi is a natural process of gene silencing, which was firstly observed in 1998, in the nematode *Caenorhabditis elegans* (Fire *et al.*, 1998). After that, it was demonstrated that synthetic siRNAs of about 21 nucleotides in length were also effective in mediating sequence-specific gene silencing in a mammalian cell line (Elbashir *et al.*, 2001).

SiRNAs are endogenously produced in mammalian cells (Figure 1.4). Cytoplasmic long double-stranded RNA (dsRNA) is processed by Dicer, which is an RNAse III enzyme, generating double-stranded siRNA. Then, siRNA duplexes bind to Argonaute 2 (AGO2) and are loaded into RNA-induced silencing complex (RISC), the sense (passenger) strand being discarded. After integration into RISC, the siRNA antisense (guide) strand pairs with a complementary sequence of the target mRNA, mRNA is cleaved by AGO2 and, consequently, mRNA translation is blocked (Fougerolles *et al.*, 2007; Hannon and Rossi, 2004; Kim and Rossi, 2007).

Exogenous synthetic double-stranded siRNAs can be added to the cells, to promote suppression of specific genes. Once in the cytoplasm, these molecules are incorporated into the AGO2-RISC complex, circumventing the first steps of the endogenous dsRNA processing pathway, taking advantage of the cellular machinery to accomplish their task (Hannon and Rossi, 2004).

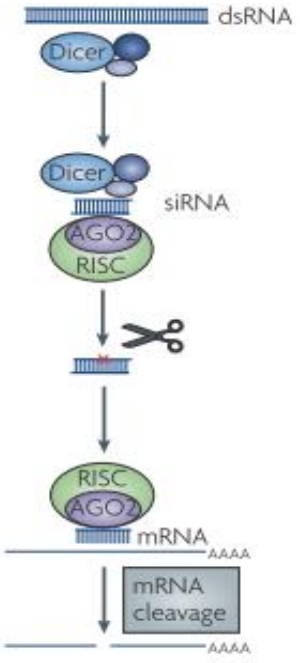

Figure 1.4 - siRNA pathway in mammalian cells. Adapted from Fougerolles *et al.*, 2007.

After choosing the most adequate nucleic acid molecules for the desired gene therapy approach, the next step consists of the design of delivery systems able to reach the required intracellular target (cytosol, nucleus or mitochondria).

c. Nucleic acid delivery systems

Due to the inability of nucleic acids to circulate in the organism fluids without being degraded, and to surpass the membrane barriers so that they can reach the intracellular

target, there is a need to design nucleic acid delivery systems. These systems are divided into two categories: viral and non-viral.

Retrovirus (Rv), adenovirus (Ad) and adeno-associated virus (AAV) are the most used viral-vectors in the gene therapy field. In fact, viral vectors are the most effective gene carriers, although their potential is restricted by some aspects: Ad triggers immunogenic reactions; AAV presents a small size, which limits the genetic cargo capacity; and Rv, which integrates randomly the exogenous DNA into the host genome, can induce the expression of oncogenes by inserting upstream of these sequences and putting them under the control of the promoter contained in the exogenous plasmid DNA (Mountain, 2000). Consequently, non-viral vectors, characterized by their simplicity and safety features, have been developed as an alternative for viral vectors. In contrast with viral vectors, which take advantage of the innate ability of viruses for infection and release of nucleic acids into the infected cells, non-viral vectors have to overcome several physiological and cellular barriers to introduce the genetic material into the target cells. Therefore, an efficient non-viral carrier should condense the nucleic acids, prevent their degradation by serum nucleases and confer them colloidal stability, so that nucleic acids circulate in blood stream before reaching the target cells. The next step involves the interaction of the delivery system with the cell surface, promoting its translocation into the cell. If complexes are taken up through endocytosis, gene carriers should promote destabilization of the endosomal membrane and nucleic acid escape, thus avoiding lysosomal degradation. In the case of siRNA delivery, complexes carrying these molecules must be disassembled in the cytoplasm, so that siRNA will become available to target mRNA. The delivery systems carrying pDNA should also be able to promote its translocation across nuclear or mitochondrial membranes, in order to ensure gene expression (Simões *et al.*, 2005).

Cationic gemini surfactants (CGS) constitute an example of non-viral nucleic acid delivery systems, which interact with the nucleic acids through electrostatic and hydrophobic interactions and were shown to mediate efficient delivery of plasmid DNA (pDNA), both to the nucleus and to mitochondria (Bell *et al.*, 2003; Cardoso *et al.*, 2011, 2014, 2015a, 2015b; Fielden *et al.*, 2001; Rosenzweig, Rakhmanova and Macdonald, 2001). Since CGS were used in the present work to deliver siRNA and pDNA, they will be described in more detail in the next sections.

i. Cationic gemini surfactants: properties and structural features

Gemini or dimeric surfactants are amphiphilic molecules containing two identical polar headgroups and two identical hydrophobic chains, connected by a rigid (*e.g.* stilbene) or

flexible (*e.g.* methylene) spacer, in contrast to the conventional surfactants, which have a single alkyl tail bound to a polar headgroup (Menger, Fredric and Keiper, 2000). Therefore, gemini surfactants are highly versatile molecules, being designed with different number of carbons in the alkyl chains and in the spacer, as well as with different polar headgroups, which can be nonionic (*e.g.* polyether sugar) or positively (*e.g.* ammonium) or negatively (*e.g.* phosphate, sulfate, carboxylate) charged. The spacer can vary in its nature, being polar (*e.g.* polyether) or nonpolar (*e.g.* aliphatic, aromatic), and rigid (*e.g.* stilbene) or flexible (*e.g.* methylene chain) (Menger, Fredric and Keiper, 2000; Weihs *et al.*, 2005).

Since the spacer and the tails have a hydrophobic character and the headgroups are hydrophilic, gemini surfactants can adopt different conformations when exposed to an air/water interface, depending on the electrostatic repulsion established between the two headgroups and the length and flexibility of the spacer. Thus, gemini surfactants assume an orientation in which they extend their tails above the water surface when the spacer is short, to minimize the electrostatic repulsions between the charged heads (Figure 1.5A), but acquire a conformation in which both tails are projected into the air if the spacer is long enough (Figure 1.5B); gemini surfactants may also assume a linear conformation, in which one of their hydrophobic tails is extended into the air and the other one is immersed into the water (Figure 1.5C). In contrast, monomeric surfactants assume only one orientation, in which they locate their headgroup at the air/water interface and extend their hydrophobic tail into the air (Figure 1.5D) (Karaborni *et al.*, 1994; Menger, F and Littau, 1993).

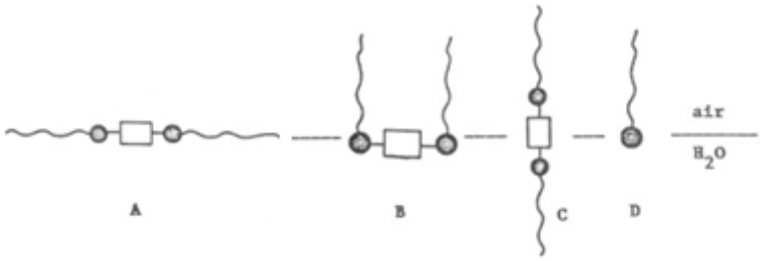

Figure 1.5 - Schematic representation of the possible orientations adopted by gemini surfactants (A-C) and monomeric surfactants (D) at an air/water interface. Adapted from Menger and Littau, 1993.

Regarding micellization, it is remarkable that gemini surfactants have critical micellar concentrations (defined as the concentration above which the surfactant abruptly aggregates in water forming micelles; CMC) lower than monomeric surfactant analogs containing the same number of carbon atoms in the hydrophobic tail, being around two orders of

magnitude more efficient in forming micellar structures than their monomeric counterparts (Menger, F and Littau, 1993; Menger, Fredric and Keiper, 2000). On the other hand, while a monomeric surfactant forms spherical micelles in water, the analogue gemini surfactant can present a much richer phase diagram, forming spherical, worm-like or thread-like micelles, vesicles and/or other structures, depending on the concentration (Karaborni *et al.*, 1994; Pérez *et al.*, 2007). Taking into account that micellization is a highly cooperative process, driven by attractive hydrophobic interactions, which compensate the electrostatic repulsions established between surfactant ionic headgroups, it is not surprising that the CMC of gemini surfactants with short chains is higher than that of surfactants with long chains. Indeed, the increasing hydrophobicity of surfactants with long chains decreases their solubility, promoting gemini self-assembly, in order to reduce the hydrocarbon/water contact (Grosmaire *et al.*, 2002; Menger, Fredric and Keiper, 2000). Less intuitive is the role played by the length and flexibility of the spacer in the surfactant aggregation behavior. In this regard, whereas gemini surfactants containing a rigid spacer avoid self-assembly into micelles, since the spacer inhibits the interaction between the alkyl tails, those having a short and flexible spacer, which allows to chain/chain association, are more prone to adopt a micellar structure (Menger, F and Littau, 1993). Interestingly, the molecular packing of gemini surfactants in micelles and monolayer is also dependent on the length of their spacer, short spacers inducing close packing, due to the hydrophobic forces established between the alkyl tails (Groth *et al.*, 2004). Figure 1.6 illustrates schematically the packing displayed by aggregates of two gemini surfactants differing in the spacer length (12–2–12 and 12-4-12).

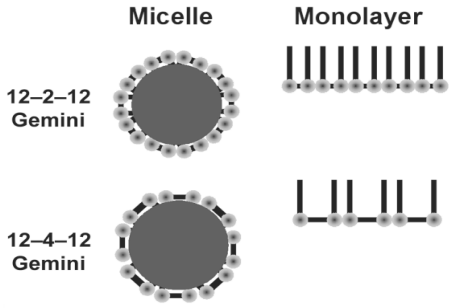

Figure 1.6 - Schematic representation of two gemini surfactants differing in the spacer length. 12-2-12 reveals a more tight packing in a micelle and in a monolayer than 12-4-12 surfactants. Adapted from Groth *et al.*, 2004.

Gemini surfactants also present a surface efficiency (as assessed by the quantity of surfactant required to decrease the surface tension by a given amount) three orders of magnitude higher than that displayed by the corresponding monomeric surfactants (Menger, F and

Littau, 1993). The superior surfactant properties exhibited by gemini surfactants as compared to those of monomeric counterparts (lower CMC values and higher surfactant efficiency) are allied to a higher efficiency in condensing nucleic acids, therefore requiring lower amounts of gemini surfactants than those necessary of the monomeric analogs to induce the same level of nucleic acid condensation (Karlsson, Eijk, van and Söderman, 2002). In fact, promising properties have been found in gemini surfactants, which, although known since 1971 (Robinson, 1971), were only rediscovered two decades ago, regarding their biomedical application as drug and gene delivery systems, as well as their usefulness for household products, cosmetic and food, among others (Kumar and Tyagi, 2014). The number of patents that cover this large range of gemini surfactant applications have strikingly increased in the last years.

The possibility for structure modulation, including the high variety of molecules that can be linked to the spacer, has allowed the synthesis of a large range of different gemini surfactants with different structural features and, consequently, different physicochemical properties. In this regard, CGS of bis-quaternary ammonium salts (*bis-quats*) (Figure 1.7) have been the most extensively studied and characterized. This family of gemini surfactants is commonly designated by m-s-m (m and s for the number of carbon atoms in the hydrophobic chains and in the spacer group, respectively) and is represented by the general structure $[C_mH_{29}(CH_3)_2N^+\text{-}(CH_2)_s\text{-}N^+(CH_3)_2C_mH_{29}]2Br^-$ (Cardoso *et al.*, 2011). As mentioned above, gemini surfactants reveal excellent properties for biomedical applications, although they present poor biocompatibility and biodegradability due to the absence of cleavable linkages in their structure (Pérez *et al.*, 2007; Weihs *et al.*, 2005). Natural surfactants have been used to overcome this problem, but their extraction and isolation involve high costs, are time-consuming and inefficient (since small quantities of surfactants are recovered) (Silva *et al.*, 2009). Therefore, novel classes of surfactants have been synthesized, employing natural structural motifs, namely, amino acids, sugars and lipids. These classes of gemini surfactants combine the characteristic properties of the conventional gemini surfactants with an enhanced biocompatibility and biodegradability, inducing less cytotoxicity than the conventional *bis-quats* analogues (Brito *et al.*, 2009; Silva *et al.*, 2012; Singare and Mhatre, 2012).

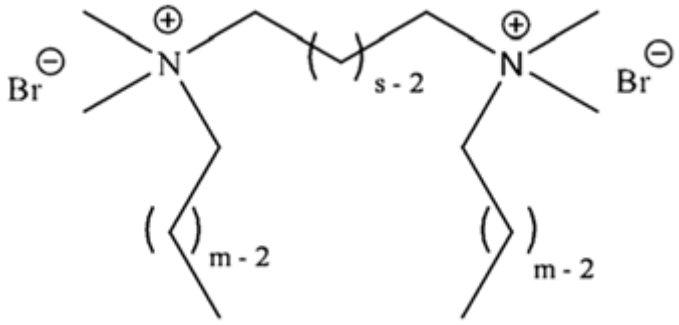

Figure 1.7 - Schematic representation of the general structure of cationic gemini surfactants of the alkanediyl-α,ω-bis(alkyldimethylammonium bromide) family.

CGS derived from the amino acid arginine have been the most studied, revealing to be less toxic than the corresponding *bis-quats*, and to be readily biodegradable, while maintaining the outstanding self-assembling properties that are characteristic of gemini surfactants (Singare and Mhatre, 2012). Silva and coworkers synthesized cationic gemini surfactants based on serine (Figure 1.8) (Silva *et al.*, 2012), following their observation that from three monomeric surfactants they synthesized, differing in the amino acid residue (tyrosine, serine and 4-hydroxyproline) linked to the alkyl chain through an N-alkyl linkage, the one based on serine was that showing the best toxicological profile and the lowest cmc (Silva *et al.*, 2009). This family of CGS is often referred to as $(mSer)_2Xs$ surfactants, where m and s are the number of carbon atoms in the alkyl tails and in the spacer group, respectively; Ser refers to the serine residue; the subscript 2 corresponds to the two chains and two polar headgroups that constitute a gemini surfactant and X refers to the type of chemical linkage between the amino acid and the spacer.

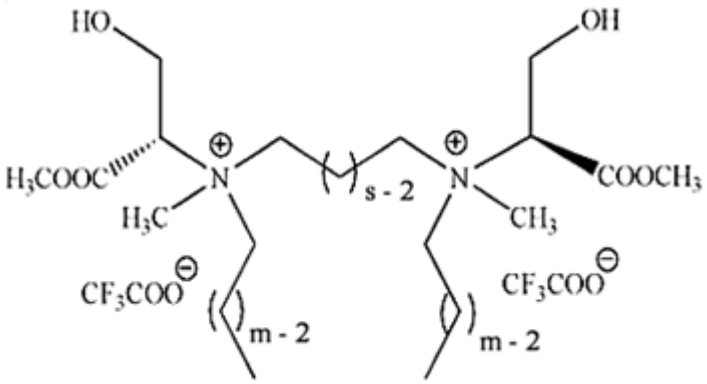

Figure 1.8 - Schematic representation of the general structure of serine-derived gemini surfactants.

ii. Cationic gemini surfactant-based delivery systems: transfection efficiency

CGS have been shown to promote efficient delivery of pDNA into the nucleus (Bell *et al.*, 2003; Fielden *et al.*, 2001; Rosenzweig *et al.*, 2001) and siRNA in the cytoplasm (Zheng *et al.*, 2014), in different types of cells. Moreover, recent studies performed in our laboratory have shown that gemini surfactants can mediate pDNA delivery into mitochondria (Cardoso *et al.*, 2015b). Remarkably, these amphiphilic molecules proved to mediate similar or higher levels of transfection than the commercial transfection reagent Lipofectamine 2000 (Bell *et al.*, 2003; Fielden *et al.*, 2001; Rosenzweig *et al.*, 2001), their efficiency revealing to be dependent on their structural features, the presence of helper lipids (described below) and the ratio between the positive charges of cationic gemini surfactants and the negative charges of nucleic acid phosphate groups. It was observed that gemini surfactant-nucleic acid binding strength is influenced by the spacer length, the most efficient complexation being achieved with gemini surfactants containing 2-3 carbon atoms-long spacer (Kirby *et al.*, 2003), probably because it favors the best accommodation of nucleic acid phosphate groups for interacting with the positively charged headgroups of the gemini surfactants. The positive charges of gene carriers are needed not only to establish electrostatic interactions with the nucleic acids, promoting their condensation, but also to interact with the negatively charged membrane components at the cell surface, inducing cellular internalization of the nucleic acid delivery systems.

Addition of CGS to nucleic acids results in the formation of complexes with different structures, depending on the nucleic acid employed (Figure 1.9), the complexation occurring due to the combination of electrostatic and hydrophobic interactions, the latter being established between surfactant apolar alkyl tails and the nucleic acid backbone (Fielden *et al.*, 2001).

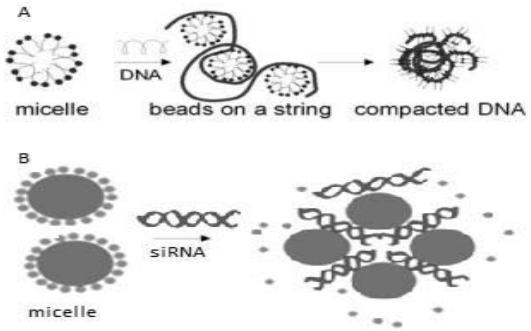

Figure 1.9 - Schematic representation of gemini/pDNA (A) and gemini/siRNA (B) complexation processes. Adapted from Wang, C. *et al.*, 2007 and Falsini *et al.*, 2014.

Endocytosis has been proposed as the preferred mechanism by which the gemini surfactant/DNA complexes are taken up by the cells. Thus, the complexes need to escape from endosomes, in order to prevent nucleic acid degradation in the lysosomal compartment. Bell and co-workers (Bell *et al.*, 2003) suggested that gemini surfactant-based complexes adopt an inverted hexagonal phase (H_{II}) in endosomal lumen, triggered by the low pH, which is characteristic of this organelle. The formation of this structure would contribute to destabilize the endosomal membrane (Figure 1.10), and, hence, to promote the escape from the endosome and the release of the nucleic acids into the cytoplasm, explaining the highly efficient transfection mediated by these surfactants.

In fact, cationic gemini surfactants present an inverted cone molecular geometry due to the larger area of the headgroup cross-section as compared to that of the alkyl chains, being hence arranged in structures with positive curvature (micelles) in aqueous dispersions. Therefore, to adopt a fusogenic inverted hexagonal phase, these molecules must undergo a decrease of the headgroup cross-section area. In this regard, it was proposed that the decrease of pH during endosome maturation promotes a strong interaction between the doubly positive headgroup and the phosphate groups of the DNA, which results in charge neutralization and a further dehydration of both groups and, consequently, in a decrease of the headgroup cross-section (Bell *et al.*, 2003; Kirby *et al.*, 2003).

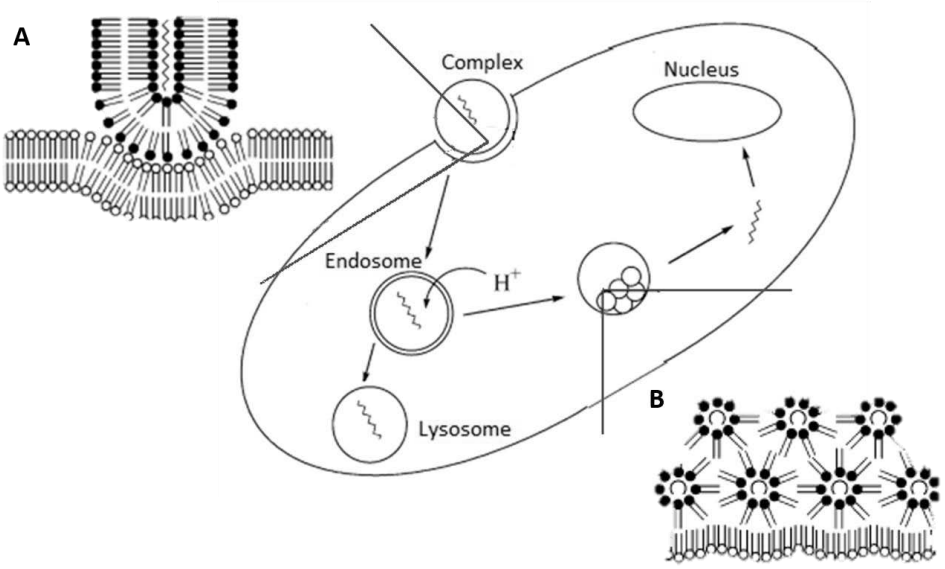

Figure 1.10 - Proposed mechanism by which nucleic acids in gemini surfactant-based complexes escape from the endosome. Following cell internalization and once in the endosome, complexes undergo conformational changes, assuming a fusogenic inverted

hexagonal phase, which leads to endosomal membrane destabilization and, consequently, to nucleic acid release. If this conformational change does not occur, the complexes remain entrapped in the endosomal compartment as the endosomes mature into lysosomes, leading to nucleic acid degradation. **A** shows the endocytosis of the complex by cell membrane invagination and **B** depicts the formation of the inverted hexagonal phase in the endosome. Adapted from Bell *et al.*, 2003.

Nevertheless, Rosenzweig and collaborators (Rosenzweig *et al.*, 2001) observed that transfection activity mediated by gemini surfactants is reduced or even abolished in the presence of serum. It was hypothesized that the addition of colipids (also known as helper lipids) to gemini surfactants could overcome this inhibitory effect of serum, allowing their widespread application, namely *in vivo*. Since then, several studies have revealed that the addition of helper lipids to the gemini surfactant/nucleic acid complexes can further increase their biological activity (Cardoso *et al.*, 2014, 2015a; Grosmaire *et al.*, 2002; Wang, C. *et al.*, 2007)

iii. Role of helper lipids in transfection activity

Cationic liposomes, the most extensively used non-viral vectors, are usually mixed with "helper lipids", in order to enhance gene delivery. Unsaturated phosphatidylethanolamines (PE), such as dioleoylphosphatidylethanolamine (DOPE), have been the most widely employed helper lipids (Hui *et al.*, 1996) and shown to improve the ability of cationic liposomes to transfect a large number of cells *in vitro*. This fact has been attributed to the propensity of DOPE to undergo a transition from a bilayer to a hexagonal phase under acidic pH (Hafez and Cullis, 2001; Koltover, Salditt and Ra, 1998), which may facilitate fusion with or destabilization of target membranes, namely the endosomal membrane (Koltover *et al.*, 1998; Siegel and Epand, 1997; Zuhorn *et al.*, 2005), following cell internalization of cationic liposome-based complexes through endocytosis. The hexagonal phase formation can also contribute to the destabilization of the complexes (Bell *et al.*, 2003), leading to the dissociation of the nucleic acids from their carrier (Zuhorn *et al.*, 2005). These two events contribute to the escape of nucleic acids from the endosomal compartment, which allow them to gain access to the cytoplasm, being ready to perform their task (in the case of siRNA) or to cross the nuclear or mitochondrial membranes (in the case of pDNA).

Cholesterol is another helper lipid commonly employed, particularly in *in vivo* studies, in order to enhance transfection mediated by cationic vectors. When added to a bilayer, cholesterol increases the lipid packing and reduces the free volume, inducing a liquid-

ordered (L_o) phase at high concentrations (Almeida, Vaz and Thompson, 1992), and conferring high stability to the lipid/surfactant arrangements. Consequently, cholesterol-enriched complexes, due to their remarkable stability, exhibit a high circulation lifetime, likely owing to their poor interaction with serum proteins (Crook *et al.*, 1998; Maslov and Zenkova, 2011; Semple, Chonn and Cullis, 1996).

In the present work, the potential of gemini surfactants to be used as pDNA and siRNA delivery systems will be fully explored, taking advantage of the high versatility of these molecules and their combination with helper lipids.

Chapter 2

Objectives

Objectives

. Evaluation of the efficiency of cationic gemini surfactants from conventional and serine-derived *bis-quat* families to deliver siRNAs into human U87 GBM cells.

. Employment of a combined approach involving i. survivin downregulation mediated by siRNAs formulated in a cationic gemini surfactant-based delivery system and ii. administration of the chemotherapeutic agents temozolomide and etoposide, aiming at obtaining a synergistic cytotoxic effect in GBM cells.

. Assessment of the ability of serine-derived *bis-quats* to promote nuclear and mitochondrial delivery of plasmid DNA in the human recurrent DBTRG-05MG GBM cells towards successful gene expression.

. Development of a gemini surfactant-based system capable of co-delivering pDNA and CDDP to nucleus and mitochondria in order to enhance drug therapeutic efficacy in GBM.

Chapter 3

Materials and Methods

Materials and methods

3.1. Materials

Gemini surfactants were synthesized, purified and physically characterized in Centro de Investigação em Química, Department of Chemistry and Biochemistry, University of Porto (Porto, Portugal) and kindly provided for our studies thanks to a collaboration with Prof. Eduardo Marques and Prof. Luísa do Vale from that Institution.

The lipids 1,2-dioleoyl-sn-glycero-3-phosphoethanolamine (DOPE) and cholesterol (Chol) were purchased from Avanti Polar Lipids (Alabaster, AL).

Lipofectamine RNAiMAX was acquired from Invitrogen (Carlsbad, CA). The siRNA duplex against GFP (siGFP) (sense: 5′-GCAAGCUGACCCUGAAGUUCdTdT-3′) and the non-targeting siRNA duplex used as control (siMUT) (sense: 5′-UUCUCCGAACGUGUCACGUdTdT-3′) were synthesized by GeneCust (Dudelange, Luxembourg). The DY547-labeled non-targeting siRNA duplex (sense: 5′-UAAGGCUAUGAAGAGAUACdTdT-3′) and the anti-survivin siRNA duplex (sense: 5′-GGACCACCGCAUCUCUACAdTdT-3′) were purchased from Dharmacon (Lafayette, CO, USA). Plasmid DNA (pDNA) encoding nuclear GFP (pEGFP-C1, herein designated pncGFP) was obtained from Clontech (CA, USA) and plasmid DNA encoding mitochondrial GFP (pmtGFP) was synthesized and kindly provided by Prof. Diana Lyrawati, Brawijaya University (East Java, Indonesia). Custom-designed primers for survivin and for the control HPRT-1 were acquired from Qiagen.

Temozolomide and etoposide were acquired from Selleckchem (Munich, Germany) and cisplatin was purchased from Sigma (Germany) as well as DMSO, which was used to prepare drug stock solutions.

The anti-survivin antibody (goat) was purchased from Santa Cruz (Santa Cruz Biotechnology, Inc., Heidelberg, Germany), the anti-β-actin antibody (mouse) and the secondary antibodies were acquired from Sigma (St. Louis, MO, USA).

3.2. Methods

Gemini surfactant-based complexes

i. Preparation of binary (gemini/nucleic acids) and ternary (gemini/nucleic acids/helper lipids) gemini surfactant-based complexes

Gemini surfactant-based complexes were prepared as previously described (Cardoso *et al.*, 2014). Briefly, an aqueous solution of gemini surfactant was prepared at a concentration of

0.5 mM and filtered through 0.22 µm pore-diameter filters (Schleicher & Schuell, BioScience, Germany). Binary complexes were prepared by mixing an aliquot of gemini solution in HBS with a constant amount of siRNA (siGFP or siSURV, to promote GFP or survivin silencing, respectively, or siMUT) or pDNA (pncGFP or pmtGFP, to promote nuclear or mitochondrial GFP expression), in order to obtain the desired surfactant/nucleic acid (+/-) charge ratios, followed by incubation at room temperature for 30 min. To produce ternary complexes, a suspension of MLVs composed of DOPE:Chol (2:1 molar ratio) was previously prepared by mixing, at this molar ratio, the helper lipids (HL) DOPE and Chol dissolved in chloroform. The lipid mixture was dried under vacuum in a rotatory evaporator, and the lipid film was hydrated with HBS (pH 11.0) to a final lipid concentration of 0.5 mM. The resulting multilamellar vesicles (MLV) were then sonicated for 3 min, in a sonication bath, and added to surfactant/nucleic acid complexes previously incubated for 15 min at room temperature, in order to obtain the desired surfactant/helper lipid molar ratios, followed by a further 15 min incubation. Figure 3.1 schematizes the method of complex preparation.

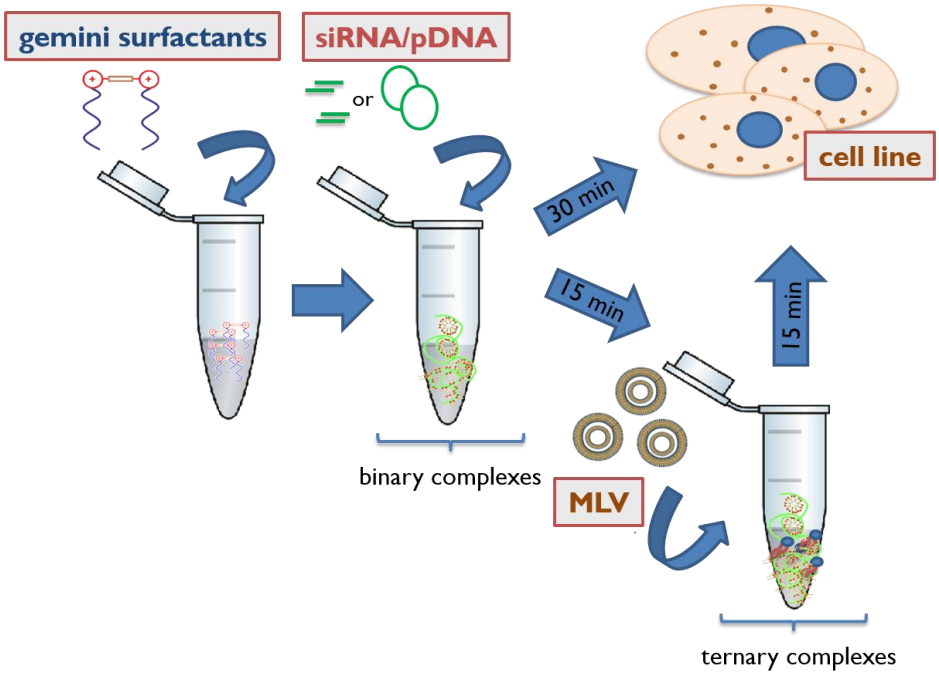

Figure 3.1 – Schematic representation of the methods used for the preparation of binary and ternary complexes based on gemini surfactants. Binary complexes were prepared by mixing an aqueous solution of gemini surfactant with HBS and siRNA or pDNA, to obtain the desired surfactant/nucleic acid (+/-) charge ratios. After 30 min of incubation, at room temperature, complexes were added to plated U87 cells. To produce ternary complexes, a volume of a suspension of MLVs composed of DOPE:Chol (2:1 molar ratio) was added to surfactant/nucleic acid complexes, after 15 min of incubation, at room temperature, to

obtain the desired surfactant/lipid molar ratios. After a further period of 15 min of incubation, these complexes were added to the plated U87 cells.

ii. Preparation of gemini surfactant-based complexes containing cisplatin

For the preparation of gemini/pDNA/cisplatin complexes, a constant amount of plasmid DNA was mixed with a solution of CDDP in HBS at different concentrations (4, 8 and 16 μM). The mixture was left incubating for 10 min to promote association of the plasmid DNA with CDDP and then added to the gemini surfactant, to obtain the 8/1 surfactant/pDNA (+/-) charge ratio. After an incubation period of 30 min, at room temperature, complexes were added to the cells.

Physico-chemical characterization of the complexes

i. Size measurement

The hydrodynamic size distribution of the ternary complexes of surfactant, siRNA and helper lipids was evaluated by dynamic light scattering (DLS), also called photon correlation spectroscopy (PCS) and quasi-elastic light scattering (QELS).

The central concept in DLS, as a technique for determining the size of particles in suspension, is that the scattered light intensity from diffusing particles, whose relative positions undergo Gaussian random changes (i.e. display Brownian motion), fluctuates in time, giving information regarding particle diffusion coefficient, which correlates with particle size. In fact, the hydrodynamic diameter can be determined from the diffusion coefficient using the Stokes-Einstein relationship expressed in the equation:

$$Dh = k_B T / 3\pi\eta D_t$$

where D_h is the hydrodynamic diameter, D_t is the translational diffusion coefficient (obtained by DLS), k_B is the Boltzmann's constant, T is the absolute temperature and η is the viscosity of the medium (Cardoso *et al.*, 2009).

Immediately before analysis, the complexes were prepared as previously described and diluted in HBS. The assay was performed using a Submicron Particle Size Analyzer, Beckman Coulter N4 Plus, at 25 °C. The detection angle was fixed at 90° and D_h calculations were automatically performed by the instrument's software.

ii. Zeta potential determination

In the field of nanotechnology, the interactions established between nanoparticles play an important role in the properties they assume in suspension. If the particles display highly positive or negative charge, electrostatic repulsive forces are generated, which keep each particle discrete and disperse in suspension; on the other hand, particles electrically neutral tend to agglomerate.

An electrical double layer, composed of a Stern layer (inner region) and a diffuse layer (outer region), is formed around each particle (Figure 3.2). The point where these two layers meet forms a boundary, called slip plane. In the presence of an electric field, a charged particle moves with a fixed velocity (electrophoretic mobility). This mobility is related to the Zeta potential, which can be determined using a combination of electrophoresis and Laser Doppler Velocimetry, and corresponds to the electrical potential at the slip plane boundary. The calculation of the zeta potential takes into account the viscosity and the dielectric constant of the medium (Zeta Sizer Nano Series User Manual, Ch. 1.).

Zeta potential measurement of the $(14Ser)_2N5$/siGFP/HL complexes was performed in the aqueous buffer HBS, at 25 °C, using a Zetasizer Nano ZS, ZN 3500, with a 532 nm laser (Malvern Instruments, UK). The complexes were prepared immediately before analysis, placed in the measuring cell and an electric current of 3.0 mA was applied. Measurements were recorded and the zeta potential was calculated for each scattering angle (8.6°, 17.1°, 25.6°, and 34.2°).

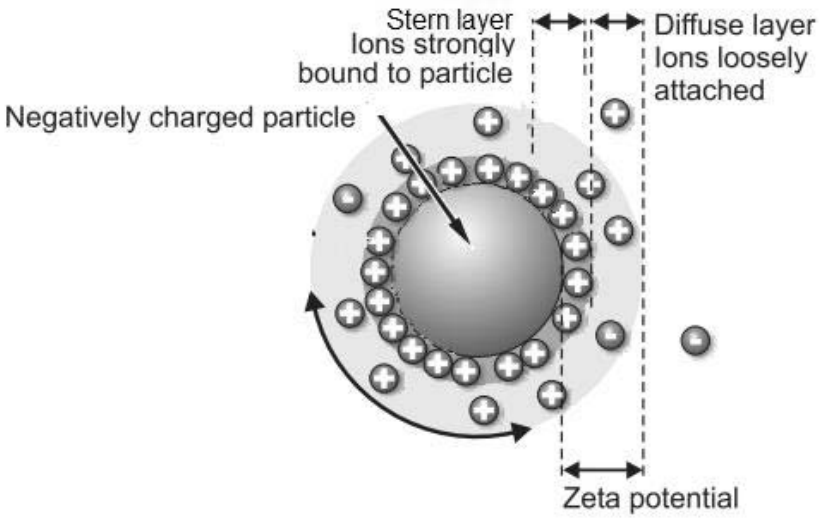

Figure 3.2 - Schematic representation of the distribution of positive and negative ions around a highly negative particle in an aqueous solution. The Stern layer is firmly attached to the particle and is formed by positive ions electrostatically attracted by the particle. Diffuse

layer is composed of loosely attached positive ions, which results from a dynamic equilibrium between attraction by the particle and repulsion by the Stern layer. The ion concentration of positive ions gradually decreases with distance, until the equilibrium with the solution is reached. Modified from Zeta Sizer Nano Series User Manual, Ch. 1.

iii. PicoGreen intercalation assay

PicoGreen intercalation assay was used in this work to evaluate the degree of siRNA protection conferred by gemini surfactant-based delivery systems. PicoGreen is a fluorescent intercalating probe whose fluorescence is enhanced upon binding to nucleic acids, fluorescence intensity reflecting, hence, the amount of accessible/free nucleic acid present in the sample. Therefore, this simple, rapid, and sensitive technique allows to estimate the efficiency of gene carriers in protecting nucleic acids, for example from the access of nucleases.

Complexes containing 14 pmol of siRNA were prepared in a total volume of 100 µL of HBS. After 30 min of incubation, at room temperature, complexes were transferred to a 96-well blackwalled plate (Corning, NY, USA) and 100 µL of PicoGreen (Molecular Probes, Eugene, OR), diluted according to the manufacturer's instructions (1:200 dilution in HBS buffer), were added to each well. Following an incubation period of 5 min, at room temperature, PicoGreen fluorescence was measured using a SPECTRAmax Gemini EM fluorimeter (Molecular Devices, Union City, CA). The excitation and emission wavelengths were set at 485 and 520 nm, respectively. The fluorescence intensity was measured immediately after complex preparation at 25 and 37 °C, and every 10 min for the period of 1 h, at 37 °C. The amount of siRNA available to interact with the probe was calculated by subtracting the values of residual fluorescence (PicoGreen in the absence of siRNA) from those obtained for each measurement, and expressed as a percentage of the maximum fluorescence obtained with naked siRNA, according to the Equation:

$$\% \text{ of free siRNA} = [(F-F_0)/(F_{100}-F_0)]\times 100$$

where F is the fluorescence intensity measured after adding the PicoGreen solution to the complexes, F_{100} (corresponding to 100% of free siRNA) represents the maximum fluorescence intensity obtained using naked siRNA in the same amount as that associated with the complexes, F_0 (corresponding to 0% of free siRNA) is the residual fluorescence intensity, obtained in the absence of siRNA, which represents the maximum protection of the nucleic acid.

Cells culture, transfection and pharmacological treatments

i. Cell lines and culturing conditions

U87 human glioblastoma cell line was kindly donated by Dr Peter Canoll (Columbia University, New York, NY). A modified U87 cell line constitutively overexpressing GFP (U87-GFP) was derived from U87 cells, through infection with a lentiviral vector, as previously described (Costa *et al.*, 2013). The human recurrent glioblastoma cell line DBTRG-05MG, kindly provided by Dr. Massimiliano Salerno (Siena Biotech, Italy), was established from a glioblastoma patient treated with local brain irradiation and multidrug chemotherapy. All GBM cell lines were maintained in culture at 37° C, under a humidified atmosphere containing 5% CO_2. U87 and U87-GFP cells were grown in Dulbecco modified Eagle's medium – high glucose (DMEM–HG; Sigma, D5648) and DBTRG-05MG cells were grown in Roswell Park Memorial Institute 1640 (RPMI, Sigma, R4130) medium. Both media were supplemented with 10% (v/v) heat-inactivated fetal bovine serum (FBS; Sigma, St. Louis, MO, USA), 100 units/mL penicillin (Sigma) and 100 µg/mL streptomycin (Sigma).

U87, U87-GFP and DBTRG-05MG cells grown in monolayer were detached using enzyme-free cell dissociation buffer at 50–70% confluence. Cell suspensions were diluted 1:1 with trypan blue and cells were counted with a hemocytometer. For flow cytometry, qRT-PCR and Western blot analyzes, U87 and DBTRG-05MG cells were plated at a density of $7x10^4$ and $6x10^4$ cells/well, respectively, in 1 mL of complete medium supplemented with FBS (10% v/v), in 12-well cell culture plates. For the assays involving the use of chemotherapeutical drugs (temozolamide, etoposide and cisplatin) U87 and DBTRG-05MG cells were seeded at a density of $6x10^3$ and $5x10^3$ cells/well, respectively, in 100 µL of complete medium, onto 96-well plates, and the border wells were filled with 200 µL sterile water.

ii. Cell transfection

Twenty-four hours after plating, cell medium was replaced with fresh medium (serum-free OptiMEM medium or DMEM medium containing 10, 20, 30 or 60% of serum for U87 and U87-GFP cells).

Gemini surfactant-based complexes, prepared at different (+/-) charge ratios and containing siRNAs against the selected target mRNA or pDNA encoding GFP, were added to the cells at a final concentration of 50 nM for siRNA and 1 µg/mL for pDNA. A non-targeting siRNA sequence (siMUT) was also employed to discriminate target-gene silencing from non-specific effects.

Lipofectamine RNAiMAX (Invitrogen, Carlsbad, CA), prepared according to manufacturer's instructions, was used as a positive control for the delivery of the siRNA against survivin.
Following 4 h incubation (in 5% CO_2, at 37 °C), the medium was replaced with fresh medium containing FBS (10% v/v) and antibiotics.

iii. Confocal microscopy studies

Confocal microscopy was used to evaluate the ability of gemini surfactants to mediate an efficient delivery of siRNAs into the cells, in the presence and absence of serum.
Twenty-four hours before transfection, U87 cells ($2x10^4$ cells/well) were plated onto 8-well chambered coverslips (Ibidi, Munich, Germany). After this period, the medium was replaced by fresh serum-free medium (0%) or medium containing 10% of serum and the complexes formulated with D540-labelled siRNAs (50 nM) were added to the cells.
After a further 4 h incubation, cells were rinsed twice with PBS and incubated with the DNA binding dye Hoechst 33342 (1 μg/mL, Molecular Probes, Eugene, OR) for 5 min (protected from light). Cells were washed twice with PBS and the fluorescence distribution was visualized using a Zeiss Axiovert confocal scanning microscope (Zeiss, Jena, Germany), under the 60× oil immersion objective.

iv. Cell incubation with the drugs

In order to determine if survivin silencing sensitized U87 cells to chemotherapeutic agents, 24 h post transfection, the medium was replaced by fresh medium and the drugs temozolomide (400 μM) and etoposide (1.5 μM), prepared in DMEM, were added to the cells. Forty-eight hours after incubation of non-transfected and transfected cells with the drugs, cell viability was evaluated using the Alamar blue assay.

In order to assess the sensitivity of DBTRG-05M cells to the anti-cancar drug cisplatin, 24 h after plating, RPMI medium was replaced with OptiMEM, and CDDP, prepared in HBS, was added to 96-well plates to yield the final concentrations of 2, 4, 8, 16, 31, 62, 125, 250, 500, 1000 μM. After 4 h of incubation, CDDP-containing medium was replaced with fresh RPMI medium.

Evaluation of molecular outcomes of cell transfection

i. Gene silencing and expression evaluated by flow cytometry

Flow cytometry simultaneously measures and analyzes multiple physical characteristics of cells such as relative particle size, relative granularity or internal complexity, and relative fluorescence intensity, as cells pass one at a time through a focused laser beam.

This technique was used to measure the relative fluorescence intensity of the cells after transfection with the different complexes. U87 cells constitutively expressing GFP (U87-GFP) were employed to examine the level of GFP knockdown achieved with siGFP- and siMUT-containing complexes. The efficiency of the transfection mediated by gemini-based formulations carrying pncGFP or pmtGFP was evaluated in DBTRG-05MG cells, by calculating the percentage of cells expressing GFP.

Forty-eight hours after transfection, cells were detached using enzyme-free cell dissociation buffer (5 min, at room temperature). Cells were, then, washed by centrifugation (200 *g*, 4 °C, 5 min) in 950 µL of ice-cold PBS and the resulting pellets were resuspended in 200 µL of ice-cold PBS. The cell suspensions were immediately analyzed by flow cytometry using a FACS-Calibur flow cytometer (BD Biosciences, San Jose, CA). To discriminate viable and dead cells and to exclude doublets, cells were appropriately gated by forward/side scattering from a total of 10,000 events. Data were stored and analyzed using CellQuest software. The mean fluorescence was normalized with the fluorescence intensity of non-transfected cells.

ii. Quantification of survivin mRNA levels by qRT-PCR

Quantitative real time PCR (qRT-PCR) is a useful tool to quantify the alterations of the levels of mRNA for a given target protein upon cell transfection with siRNA or pDNA. Real time PCR consists of the amplification of a specific complementary DNA (cDNA) sequence (complementary to the mRNA of interest), using specific primers. Consecutive cycles of denaturation, primer annealing and elongation, allow for the amplification of the sequence to which the primers are complementary. The PCR mixture contains a fluorophore molecule which intercalates the nucleic acids and fluoresces only in this environment. The real time PCR system, acting as a fluorimeter, detects the increase of fluorescence, which is proportional to the amount of copies of the sequence being amplified, thus providing quantitative data, with no need for further quantification of the target sequence (Freeman, Walker and Vrana, 1999).

RNA was extracted from the whole-U87 cells (24 and 48 h after cell transfection with complexes containing the target siSURV or the non-target siMUT), using the NucleoSpin

RNA Isolation Kit (Macherey-Nagel, Düren, Germany), according to manufacturer's recommendations.

In order to lyse the cells, the Buffer RA1 was mixed with ß-mercaptoethanol (100:1) and the resulting solution was added to the plated cells, followed by a manual disruption. The lysates were filtered through NucleoSpin Filters and centrifuged at 11,000 *g*, for 1 min at room temperature, to reduce viscosity. Then, 350 µL ethanol (70%) were added to the homogenized lysates, mixed by pipetting up and down (8 times) and loaded into a NucleoSpin RNA Column, followed by centrifugation at 11,000 *g*, for 30 s. The silica membrane of NucleoSpin RNA Columns were desalted with 350 µL of Membrane Desalting Buffer and centrifuged at 11,000 g, for 1 min. In order to digest any contaminating DNA present in the samples, 95 µL of rDNase reaction mixture were applied directly onto the center of the silica membrane of the column, followed by incubation for 15 min at room temperature. The silica membrane was then washed and dried by centrifugation twice with buffer RAW2 and once with buffer RA3. RNA was eluted in 30 µL RNase-free water.

Since the complete elimination of genomic DNA from RNA preparations cannot be guaranteed, it is important to include a No Reverse Transcription control (NRT) in the reverse transcription reaction. This control contains all the components of the cDNA synthesis assay except for the reverse transcriptase. Any qRT-PCR amplification signal obtained in this condition corresponds to genomic DNA unspecific products.

After RNA quantification, 300 ng of RNA (extracted from U87 cells 24 or 48 h after cell transfection) were converted to cDNA using the NZY First-Strand cDNA Synthesis Kit (NZYTech, Lisbon, Portugal), by applying the following protocol: 30 min at 50 °C (cDNA synthesis) followed by 5 min at 85 °C (heat-inactivation of the reverse transcriptase). After transcription, the samples were further incubated for 20 min at 37 °C with 0.5 µL of RNase H (from *E. coli*), to specifically degrade the RNA strand in RNA-cDNA hybrids.

The resulting cDNA was further diluted 10 times with RNase-free water prior to quantification by qRT-PCR.

Quantitative PCR was performed in a StepOnePlus Real-Time PCR System (Applied Biosystems, USA) using 96-well microtiter plates and the iQ SYBR Green Supermix Kit (Bio-Rad).

Primers for the target gene (survivin) and housekeeping gene (hypoxanthine phosphoribosyltransferase 1; HPRT1) were custom-designed and acquired from Invitrogen. A master mix was prepared for each primer set, containing a fixed volume of SYBR Green Supermix and the appropriate amount of each primer, to yield a final concentration of 150 nM. For each reaction, performed in duplicate, 6 µL of master mix were added to 4 µL of

cDNA template. In order to detect contaminants that could be present in the reaction components and also to determine dimmer formation between the primers, a No Template Control (NTC) was performed for the target and reference genes, where the cDNA template was replaced by RNase free-water. The NRT control was also performed for both target and reference genes, to detect possible DNA contaminants that could be present in the sample.

The reaction conditions consisted of enzyme activation and well-factor determination for 1 min and 30 s at 95 °C, followed by 45 cycles for 10 s at 95 °C (denaturation), 30 s at 55 °C (annealing), and 30 s at 65 °C (elongation). The melting curve protocol started immediately after amplification and consisted of 1 min heating at 55°C followed by 80 steps of 10 s, with an increase of 0.5 °C in temperature at each step. Threshold values for threshold cycle (Ct) determination were generated automatically by the StepOne Software.

To determine the mRNA fold change, survivin gene expression was compared to the endogenous reference gene (HPRT1 gene), taking into consideration the different amplification efficiencies of both genes in all experiments, according to the Pfaffl method (Pfaffl, 2001):

$$\Delta Ct_{(survivin)} = Ct_{(control)} - Ct_{(sample)}$$

$$\Delta Ct_{(HPRT1)} = Ct_{(control)} - Ct_{(sample)}$$

$$\text{mRNA fold change} = (E_{survivin})^{\Delta CP(survivin)} / (E_{HPRT1})^{\Delta CP(HPRT1)}$$

where $\Delta Ct_{(survivin)}$ and $\Delta Ct_{(HPRT1)}$ represent the Ct deviation of control – sample of the survivin and HPRT1 transcripts, respectively; and $E_{survivin}$ and E_{HPRT1} are the real-time PCR efficiency of survivin and HPRT1 transcripts, respectively, which are determined according to the equation

$$E = 10^{-1/S} - 1$$

where S is the slope of the standard curve of serial sample dilutions.

iii. Quantification of survivin levels by Western blot

To confirm that the decrease of survivin mRNA levels, analyzed by qRT-PCR, resulted in a reduction of the survivin protein expression, Western blot analysis was also performed. Western blot consists of an electrophoretic separation of proteins, based on their molecular weight, followed by an electrotransference of the separated proteins from the

electrophoresis gel to an appropriate membrane for antibody labeling, and protein quantification (Mahmood and Yang, 2012).

Forty-eight hours after U87 cell transfection with siRNA-containing complexes, protein was extracted, at 4 °C, from 12-well microplates using RIPA lysis buffer (50 mM Tris pH 8.0, 150 mM NaCl, 50 mM EDTA, 0.5% sodium deoxycholate, 1% Triton X-100) containing a protease inhibitor cocktail (Sigma), 10 μg/mL DTT and 1 mM PMSF. The protein content of the lysates was quantified using the Bio-Rad protein assay (Bio-Rad) and 30 μg of total protein were resuspended in a loading buffer (20% glycerol, 10% SDS, 0.1% bromophenol blue), denaturated upon 5 min incubation at 95 °C and loaded onto a 12% polyacrylamide gel for electrophoretic separation.

After electrophoresis, the proteins were blotted onto a PVDF membrane according to standard protocols. After 1 h of membrane blocking in 5% nonfat milk, the membrane was incubated with the primary antibody (anti-survivin 1:200, Santa Cruz Biotechnology, Inc., Heidelberg, Germany) overnight, at 4°C. Following this time period, the membrane was washed three times with TBS/T (25 mM Tris-HCl, 150 mM NaCl, 0.1% Tween) and incubated with the appropriate secondary antibody (1:10000) for 2 h, at room temperature. Then, the membrane was washed three times with TBS/T and incubated with the enzyme substrate ECF (alkaline phosphatase substrate; 20 μL of ECF/cm^2 of membrane) for a maximum of 5 min, at room temperature. Fluorescence detection was achieved at 570 nm using a ChemiDoc™ Touch Imaging System (Bio-Rad). Equal protein loading was shown by reprobing the membrane with an anti-β actin antibody (1:1000, Sigma) and with the appropriate secondary antibody. Prior to membrane reprobing, the blots were washed in 40% methanol for 30 min, followed by a fast wash with Milli-Q water. The membrane was then washed with a glycine solution (0.1M, pH 2.5) for 40 min, further washed three times with TBS/T and blocked for 1 h in 5% nonfat milk.

The analysis of band intensity was performed using ImageJ Software (Wayne Rasband National Institutes of Health, USA), and the survivin band intensity was normalized to β-actin in each experiment, in order to correct variations in the total protein content.

Evaluation of cellular outcomes of cell treatment

i. Evaluation of cell viability

The evaluation of the efficacy of gemini-based formulations to mediate gene silencing or expression was accompanied by cytotoxicity assessment, since the toxic effects exerted by the delivery systems on cells can constitute a limitation for their application in *in vitro* and *in*

vivo studies. Cell viability was also assessed in order to evaluate the outcome of cell treatments (therapeutic gene silencing or drug administration).

Cell viability was assessed by a modified Alamar blue assay, as previously described (Konopka *et al.*, 1996). Resazurin (blue) is the active ingredient of the Alamar blue assay, which is reduced by metabolically active cells to resorufin (pink), this technique allowing, hence, to distinguish metabolically active from metabolically inactive cells. This technique is simple, cheap and easy to perform. Moreover, the colorimetric assay can be performed without cell lysis, since resazurin is a cell permeable dye, and without the detachment of adherent cells, which makes possible the use of the cells for additional assays.

An appropriate volume of resazurin dye (10% v/v) in DMEM–HG medium (for U87 cells) or in RPMI medium (for DBTRG-05MG cells) was added to each well. After color development (upon 45 min to 1 h and 2 h to 3 h of incubation at 37 °C, for 12- and 96-well plated cells, respectively), 150 µL of supernatant were collected from each well, transferred to clear 96-well plates, and the absorbance was measured in a SPECTRAmax PLUS 384 spectrophotometer (Molecular Devices, Union City, CA), at 570 and 600 nm. Cell viability (as a percentage of control cells) was calculated according to the equation:

$$\text{Cell viability (\% of control)} = [(A_{570} - A_{600})/(A'_{570} - A'_{600})] \times 100$$

where A570 and A600 are the absorbances of the treated cells, and A'570 and A'600 are those of the control (non-treated cells), at the indicated wavelengths.

ii. Evaluation of cell proliferation

The sulforhodamine B (SRB) assay was conducted to assess the effects of cisplatin, free or included in a surfactant/DNA complex, on the proliferation of DBTRG-05MG cells. This assay is based on the ability of the anionic dye SRB to bind to basic amino acid residues of proteins, forming an electrostatic complex, under moderately acid conditions. Therefore, the amount of bound dye is proportional to the amount of protein and, consequently, to the number of cells, being an indicator of cell proliferation. The color development is rapid and stable and SRB assay only requires simple equipment and inexpensive reagents, being also highly efficient and allowing to test a large number of samples in a short period of time.

Sulforhodamine B assays was performed as previously described (Vichai and Kirtikara, 2006). Briefly, immediately after treatment with cisplatin and 24, 48, 72 and 96 h after treatment, cells were fixed by adding 100 µL of a solution of acetic acid at 1% in methanol to each well, followed by 1 h incubation at -20 °C. Cells were then rinsed and left to dry at 37 °C, for 20

min, before being incubated with 200 µL of 0.05% SRB staining solution containing 1% acetic acid, for 1 h at 37 °C. To remove the unbound dye, cells were washed several times with a 1% solution of acetic acid in Milli-Q water and, then, left to dry at 37 °C, for 20 min. The protein-bound dye was solubilized in 10 mM Tris buffer (pH 10) for 15 min, under gentle agitation, and the absorbance was measured at 540 nm in a microplate reader (SPECTRAmax PLUS 384, Molecular Devices, Union City, CA).

iii. Cell cycle analysis

In order to evaluate the cytostatic effects of cisplatin on DBTRG-05MG cells, the distribution of the cell population along the different phases of the cell cycle was analyzed by quantification of the DNA of each cell. To accomplish that, propidium iodide, which intercalates into the double stranded macromolecule, was used to fluorescently label the nucleus of the cell. Quiescent and G1 cells have one copy of DNA, whereas cells in G2/M phase of the cell cycle have two copies of DNA. Therefore, when cells in G2/M replication phases passed through the focused laser beam, the fluorescence intensity detected was twice that of quiescent or G1 cells. Cells in S phase are synthesizing DNA, thus revealing fluorescence values between those of quiescent or G1 cells and G2/M cells (Figure 3.3).

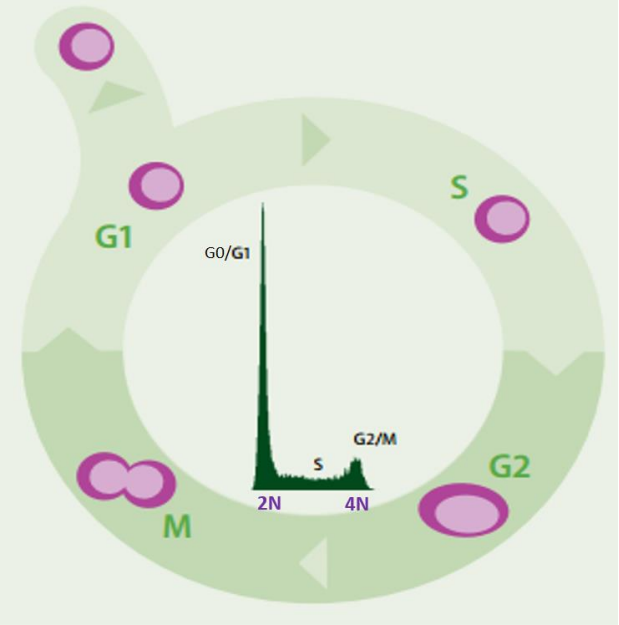

Figure 3.3 - Cell cycle. Cells in G1/G0 phase are diploid (2N) and cells in G2/M phase are tetraploid (4N). DNA content in S phase varies between 2N and 4N. Adapted from https://www.miltenyibiotec.com/~/media/Files/Support/Macs-Technology/AP_MACSQuantApp_CellCycle.ashx.

Twenty-four hours after cells were seeded in 12-well plates, the medium was replaced with a serum free medium and cells were transfected with $(18Ser)_2N5$/pDNA or $(18Ser)_2N5$/pDNA/CDDP complexes (at 8 μM CDDP) or treated with free CDDP, at the same concentrations. After 4 h of incubation, the medium was replaced by complete RPMI medium and, forty-eight hours later, cells were detached using enzyme-free cell dissociation buffer (10 min, at room temperature) and washed by centrifugation (300 g, 4 °C, 5 min) with ice-cold PBS. The supernatant was discarded and cells were fixed by slowly adding 200 μL of 70% ethanol, while vortexing the mixture at low speed. After 24 h incubation at 4 °C, cells were centrifuged to remove ethanol, and washed once with 2% BSA in PBS. The resulting cell pellet was resuspended in 400 μL of propidium iodide/RNAse solution (Immunostep, Salamanca, Spain). After 15 min incubation under dark at room temperature, cell suspensions were immediately analyzed by flow cytometry using a FACS-Calibur flow cytometer (BD Biosciences, San Jose, CA). To discriminate viable and dead cells and to exclude doublets, cells were appropriately gated by forward/side scattering and pulse width. Data were collected from at least 10,000 single cell events, stored in CellQuest software and analyzed using ModFit LT 3.0.

Statistical analysis

Data are presented as mean ± SD of at least three independent experiments. The significance of the results was statistically analyzed by one-way analysis of variance (ANOVA) with Tukey's multiple pairwise comparison, unless stated otherwise. Statistical significance was set at $p < 0.05$.

Chapter 4

Enhancing glioblastoma cell sensitivity to chemotherapeutics: a strategy involving survivin gene silencing mediated by gemini surfactant-based complexes

The results included in this Chapter are part of the following article: Rita Q. Cruz, Catarina M. Morais, Ana M. Cardoso, Sandra G. Silva, Maria L. Vale, Eduardo F. Marques, Maria C. Pedroso de Lima, Amália S. Jurado, *"Enhancing glioblastoma cell sensitivity to chemotherapeutics: a strategy involving survivin gene silencing mediated by gemini surfactant-based complexes"* Submitted for publication in Molecular Pharmaceutics.

4.1. Abstract

Glioblastoma (GBM), the highest grade astrocytoma, is one of the most aggressive and challenging cancers to treat. The standard treatment is usually limited due to the intrinsic resistance of GBM to chemotherapy and drug non-specific effects. Therefore, new therapeutic strategies need to be developed to target tumor cells, sparing healthy tissues. In this context, the inhibitor-of-apoptosis protein (IAP) survivin emerges as an ideal target for a gene silencing approach, since it is sharply differentially expressed in cancer tissues. In this work, two different families of cationic gemini surfactants (*bis-quat* conventional and serine-derived) were tested regarding their efficiency to deliver small interfering RNAs (siRNAs) in a human GBM cell line (U87), in order to select an effective siRNA anti-survivin carrier. Ultimately, a combined approach involving survivin downregulation mediated by siRNAs formulated in a serine-derived gemini surfactant-based vector and administration of the chemotherapeutic agents temozolomide and etoposide was employed, showing to be promising to sensitize GBM cells to chemotherapy.

KEYWORDS: gemini surfactants, gene therapy, survivin, RNA interference, chemotherapy, temozolomide, etoposide, glioblastoma

4.2. Introduction

Glioblastoma (GBM), a grade IV glioma (Adamson *et al.*, 2009), is characterized by its propensity for proliferation and resistance to apoptosis, extensive angiogenesis and widespread invasion (Furnari *et al.*, 2007). Therefore, prognosis of GBM patients remains poor, with a median survival of only 12 to 15 months (Stupp *et al.*, 2005; Zhang *et al.*, 2012). For this reason, it is mandatory to improve the standard therapies or develop new therapeutic interventions.

Survivin, a small inhibitor-of-apoptosis protein (IAP) overexpressed in GBM (George *et al.*, 2010), constitutes an attractive target for cancer therapies because it is rarely detected in normal tissues (Altieri, 2008; Duffy *et al.*, 2007; Mita *et al.*, 2008) and is highly expressed in tumors (Altieri, 2008). Although survivin has been proposed to act through inhibition of mitochondrial-dependent apoptosis, its primary function involves the regulation of the mitosis progression (Okada and Mak, 2004), playing also an important role in angiogenesis [7,](Duffy *et al.*, 2007; Ryan, B.; O'Donovan, N.; Duffyg, 2009) and chemoresistance (Mita *et al.*, 2008; Pennati *et al.*, 2008).

In this context, and considering that an apoptosis deficit renders tumors more chemo- and/or radio-resistant (Fesik, 2005), it is expected that a gene silencing approach, benefiting from RNA interference (RNAi) technology, targeting the anti-apoptotic protein survivin, can enhance cell susceptibility to apoptosis (Pai *et al.*, 2006). Due to the extracellular and intracellular barriers that nucleic acids are unable to surpass by themselves, appropriate carriers are necessary to aid siRNAs to reach the cell cytoplasm, avoiding their degradation. To overcome the safety drawbacks of the highly immunogenic viral vectors (Mountain, 2000), non-viral vectors, characterized by their simplicity and safety, have revealed to be a promising alternative, although their delivery efficiency still needs to be improved towards levels similar to those of their viral counterparts.

In this regard, cationic gemini surfactants, which interact with the nucleic acids through electrostatic and hydrophobic interactions, have been shown to be highly efficient to deliver plasmid DNA (pDNA) (Bell *et al.*, 2003; Cardoso *et al.*, 2015b; Fielden *et al.*, 2001; Rosenzweig *et al.*, 2001). Gemini or dimeric surfactants are amphiphilic molecules characterized by a particular structure containing two identical polar headgroups and two identical hydrophobic chains, connected by a rigid or flexible spacer. This structure differs markedly from that of conventional monomeric surfactants, which have a single alkyl tail connected to a polar headgroup (Menger, Fredric and Keiper, 2000). The gemini structure imparts the compounds significant versatility, since molecules can be designed with different

number of carbons in the alkyl chains and in the spacer, as well as with different polar headgroups (Weihs *et al.*, 2005); in turn, this translates into rich aggregation properties.

Cationic gemini surfactants of the *bis-quaternary* ammonium salt (*bis-quats*) family (Figure 4.1 A), commonly designated m-s-m (m and s standing for the number of carbon atoms in the hydrophobic chains and in the spacer group, respectively) (Cardoso *et al.*, 2011) reveal multifaceted aggregation properties but can present some problems regarding biocompatibility and biodegradability (Pérez *et al.*, 2007; Weihs *et al.*, 2005). Therefore, novel classes of gemini surfactants, containing natural structural motifs (amino acids, sugars and lipids), have been designed to decrease the cytotoxicity associated with conventional *bis-quats* (Brito *et al.*, 2009; Silva *et al.*, 2012; Singare and Mhatre, 2012). In this regard, serine-derived gemini surfactants (Figure 4.1 B), have shown the ability to carry and deliver pDNA (Cardoso *et al.*, 2015a), the transfection efficiency being dependent on surfactant structural features and on the presence of helper lipids (Cardoso *et al.*, 2014, 2015a; Grosmaire *et al.*, 2002; Rosenzweig *et al.*, 2001; Wang, C. *et al.*, 2007).

In the present study, the two different families of gemini surfactants (*bis-quats* and serine-derived gemini surfactants) were studied regarding their potential to deliver siRNAs into the target cells. Subsequently, a combined strategy was employed, involving survivin gene silencing (mediated by the gemini surfactant-based formulation that showed to be the most efficient) and chemotherapeutics, with the overall objective of evaluating the ability of the survivin knockdown approach for sensitizing GBM cells to chemotherapy.

Altogether, our work demonstrated that, through the employment of serine-derived gemini surfactants as anti-survivin siRNA carriers, a significant survivin knockdown was achieved, which rendered U87 cells more susceptible to the chemotherapeutics temozolomide and etoposide.

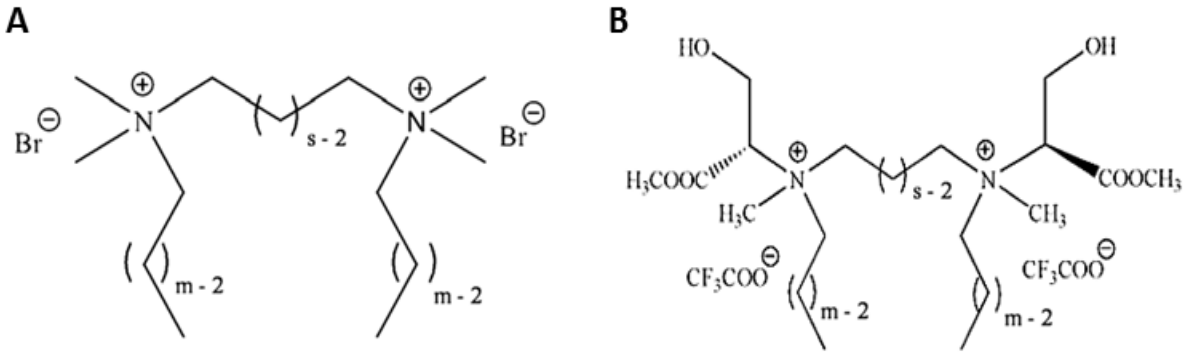

Figure 4.1 - Schematic representation of the general structure of cationic gemini surfactants of the alkanediyl-α,ω-bis(alkyldimethylammonium bromide) family (A) and of the serine-derived gemini surfactant family (B).

4.3. Materials and methods

Conventional gemini surfactants were synthesized by the method reported by Menger (Menger, F and Littau, 1993) and purified by recrystallization. Serine-derived gemini surfactants were synthesized by the method reported by Silva (Silva *et al.*, 2012) and purified by column chromatography. The purity of the compounds was assessed by NMR and mass spectrometry, and the obtained critical micelle concentration values were found to be similar to those already reported in the literature (Burrows *et al.*, 2007; Zana, 2002).

The lipids 1,2-dioleoyl-sn-glycero-3-phosphoethanolamine (DOPE) and cholesterol (Chol) were purchased from Avanti Polar Lipids (Alabaster, AL). Lipofectamine RNAiMAX was acquired from Invitrogen (Carlsbad, CA). The siRNA duplex against GFP (siGFP) (sense: 5′-GCAAGCUGACCCUGAAGUUCdTdT-3′) and the non-targeting siRNA duplex used as control (siMUT) (sense: 5′-UUCUCCGAACGUGUCACGUdTdT-3′) were synthesized by GeneCust (Dudelange, Luxembourg). The DY547-labeled non-targeting siRNA duplex (sense: 5′-UAAGGCUAUGAAGAGAUACdTdT-3′) and the anti-survivin siRNA duplex (5′-GGACCACCGCAUCUCUACAdTdT-3′) were purchased from Dharmacon (Lafayette, CO, USA). Temozolomide and etoposide were acquired from Selleckchem (Munich, Germany) and stock solutions were prepared in DMSO (Sigma, Germany). Custom-designed primers for survivin and for the control HPRT-1 were acquired from Qiagen. The anti-survivin antibody (goat) was purchased from Santa Cruz (Santa Cruz Biotechnology, Inc., Heidelberg, Germany), the anti-β-actin antibody (mouse) and the secondary antibodies were acquired from Sigma (St. Louis, MO, USA).

Cell lines and culturing conditions

U87 human GBM cell line was kindly donated by Dr. Peter Canoll (Columbia University, New York, NY). A modified U87 cell line constitutively overexpressing GFP (U87-GFP) was derived from U87 cells, through infection with a lentiviral vector, as previously described (Costa *et al.*, 2013). Both GBM cell lines were maintained in culture at 37° C, under a humidified atmosphere containing 5% CO_2. Cells were grown in Dulbecco modified Eagle's medium – high glucose (DMEM–HG; Sigma, St. Louis, MO, USA), supplemented with 10% (v/v) heat-inactivated fetal bovine serum (FBS; Sigma, St. Louis, MO, USA), 100 units/mL penicillin (Sigma) and 100 µg/mL streptomycin (Sigma). GBM cells grown in monolayer were detached using enzyme-free cell dissociation buffer at 50–70% confluence. For flow cytometry, QRT-PCR experiments and Western blot analysis, cells were plated at a density of $7x10^4$ cells/well, in 1 mL of complete medium supplemented with FBS (10% v/v), in 12-well culture plates. For the assays involving the use of chemotherapeutical drugs (temozolamide

and etoposide), cells were seeded at a density of $6x10^3$ cells/well, in 100 µL of complete medium, in 96-well plates.

Gemini surfactant-based complexes

Gemini surfactant-based complexes were prepared as previously described (Cardoso *et al.*, 2014). Briefly, an aqueous solution of gemini surfactant was prepared at 0.5 mM and filtered through 0.22 µm pore-diameter filters (Schleicher & Schuell, BioScience, Germany). DOPE and Chol were dissolved in chloroform, mixed at a 2:1 molar ratio and dried under vacuum in a rotatory evaporator. The resulting lipid film was hydrated with HBS (pH 11.0) to a final lipid concentration of 0.5 mM. The resulting multilamellar vesicles (MLVs) were then sonicated for 3 min, in a sonication bath. Binary complexes of gemini/siRNA were prepared by mixing an aliquot of the aqueous gemini solution with HBS and with a constant amount of the aqueous siRNA solution to obtain the desired surfactant/siRNA (+/-) charge ratios, followed by incubation at room temperature for 30 min. To produce ternary complexes (gemini/siRNA/helper lipids), a volume of a suspension of MLVs composed of DOPE:Chol (2:1 molar ratio) was added to surfactant/siRNA complexes, after 15 min of incubation, at room temperature, to obtain the desired surfactant/lipid molar ratios, followed by a further 15 min incubation.

Cell transfection

Twenty-four hours after plating, cell medium was replaced with fresh medium (serum-free OptiMEM medium or DMEM medium containing 10, 20, 30 or 60% of serum).

Gemini surfactant-based complexes prepared at different (+/-) charge ratios and containing siRNAs against the selected target mRNA were added to the cells at a final siRNA concentration of 50 nM. A non-targeting siRNA sequence (siMUT) was also employed to discriminate the target-gene silencing from non-specific effects.

Lipofectamine RNAiMAX (Invitrogen, Carlsbad, CA), prepared according to manufacturer's instructions, was used as a positive control for the delivery of the siRNA against survivin.

Following 4 h incubation (in 5% CO_2 at 37 °C), the medium was replaced with fresh medium containing FBS (10% v/v) and antibiotics. Cells were further incubated to allow gene silencing, for 20 or 44 h before the evaluation of cell viability and siRNA delivery by flow cytometry and mRNA quantification by QRT-PCR, and for 68 h before Western blot analysis.

Cell incubation with the drugs

In order to determine if survivin silencing sensitized U87 cells to chemotherapeutic agents, 24 h post-transfection, the medium was replaced by fresh medium and the drugs temozolomide (400 μM) and etoposide (1.5 μM), prepared in DMEM, were added to the cells. After 48 h of incubation of non-transfected and transfected cells with the drugs, cell viability was evaluated by the Alamar blue assay.

Evaluation of cell viability

Cell viability after gene silencing or after gene silencing plus drug incubation was assessed by a modified Alamar blue assay, as previously described (Konopka *et al.*, 1996). An appropriate volume of resazurin dye in DMEM–HG medium (10% v/v) was added to the cells 48 h after transfection or incubation with the chemotherapeutic drugs. After color development, the absorbance was measured in a SPECTRAmax PLUS 384 spectrophotometer (Molecular Devices, Union City, CA), at 570 and 600 nm, according to the manufacturers' instructions. Cell viability (as a percentage of control cells) was calculated according to the equation:

$$\text{Cell viability (\% of control)} = [(A_{570} - A_{600})/(A'_{570} - A'_{600})] \times 100$$

where A570 and A600 are the absorbances of the treated cells, and A'570 and A'600 are those of the control (non-treated cells), at the indicated wavelengths.

Determination of GFP silencing and expression by flow cytometry

Flow cytometry was used to measure the relative fluorescence intensity of U87 cells after transfection with the different complexes. U87-GFP cells were employed to examine the level of GFP knockdown achieved with siGFP-complexes.

After evaluating cell viability (48 h after transfection), cells were detached using enzyme-free cell dissociation buffer (5 min, at room temperature). Then, cells were washed by centrifugation (200 *g*, 4 °C, 5 min) in 950 μL of ice-cold PBS and the resulting pellets were then resuspended in 200 μL of ice-cold PBS. The cell suspensions were immediately analyzed by flow cytometry using a FACS-Calibur flow cytometer (BD Biosciences, San Jose, CA). Live cells were gated by forward/side scattering from a total of 10,000 events and data were stored and analyzed using CellQuest software. The mean fluorescence was normalized with the fluorescence intensity of non-transfected cells.

Confocal microscopy studies

Confocal microscopy was used to evaluate the ability of gemini surfactants to mediate efficient delivery of siRNAs into the cells, in the presence and absence of serum.

24 h before transfection, U87 cells (2×10^4 cells/well) were plated onto 8-well chambered coverslips (Ibidi, Munich, Germany). After this period, the medium was replaced by fresh serum-free medium (0%) or medium containing 10% of serum and the complexes formulated with DY547-labeled siRNAs (50 nM) were added to the cells.

After a further 4 h incubation, cells were rinsed twice with PBS and incubated with the DNA binding dye Hoechst 33342 (1 μg/mL, Molecular Probes, Eugene, OR) for 5 min (protected from light). Cells were washed twice with PBS and the fluorescence distribution was visualized using a Zeiss Axiovert confocal scanning microscope (Zeiss, Jena, Germany), under the 60× oil immersion objective.

RNA extraction and cDNA synthesis

RNA was extracted from the whole-U87 cells (24 and 48 h after cell transfection with the target siSURV or siMUT), using the NucleoSpin RNA Isolation Kit (Macherey-Nagel, Düren, Germany), according to manufacturer's recommendations.

After RNA quantification, 300 ng of RNA (extracted from U87 cells 24 and 48 h after cell transfection) were converted to cDNA using the NZY First-Strand cDNA Synthesis Kit (NZYTech, Lisbon, Portugal), by applying the following protocol: 30 min at 50 °C (cDNA synthesis) followed by 5 min at 85 °C (heat-inactivation of the reverse transcriptase). After transcription, the samples were further incubated for 20 min at 37 °C with 0.5 μL of RNase H (from *E.coli*), to specifically degrade the RNA strand in RNA-cDNA hybrids.

The resulting cDNA was further diluted 10 times with RNase-free water prior to quantification by qRT-PCR.

Quantification of mRNA levels by QRT-PCR

Quantitative PCR (QRT-PCR) was performed in a StepOnePlus Real-Time PCR System (Applied Biosystems, USA) using 96-well microtiter plates and the iQ SYBR Green Supermix Kit (Bio-Rad).

Primers for the target gene (survivin) and housekeeping gene (HPRT1) were custom-designed and acquired from Invitrogen. A master mix was prepared for each primer set, containing a fixed volume of SYBR Green Supermix and the appropriate amount of each primer, to yield a final concentration of 150 nM. For each reaction, performed in duplicate, 6 μL of master mix were added to 4 μL of cDNA template. The reaction conditions consisted

of enzyme activation and well-factor determination for 1 min and 30 s at 95 °C, followed by 45 cycles for 10 s at 95 °C (denaturation), 30 s at 55 °C (annealing), and 30 s at 65 °C (elongation). The melting curve protocol started immediately after amplification and consisted of 1 min heating at 55 °C followed by 80 steps of 10 s, with an increase of 0.5 °C in temperature at each step. Threshold values for threshold cycle (Ct) determination were generated automatically by the StepOne Software. Target gene expression was normalized to the amount of total RNA, by comparison with the endogenous reference gene. To determine gene knockdown, survivin gene expression in cells transfected with the target siSURV was compared with the survivin expression in cells treated with siMUT. Gene expression (mRNA fold change with respect to non-transfected control cells) was determined taking into consideration the different amplification efficiencies of both genes in all experiments. The selected housekeeping genes have an amplification efficiency similar to that of the target gene, which was determined according to the formula $E = 10^{-1/S}-1$, where S is the slope of the standard curve obtained for each gene.

Quantification of protein levels by Western blot

Forty-eight hours after U87 cell transfection with siRNA complexes, protein was extracted, at 4 °C, from 12-well microplates using RIPA lysis buffer (50 mM Tris pH 8.0, 150 mM NaCl, 50 mM EDTA, 0.5% sodium deoxycholate, 1% Triton X-100) containing a protease inhibitor cocktail (Sigma), 10 μg/mL DTT and 1 mM PMSF. The protein content of the lysates was quantified using the Bio-Rad protein assay (Bio-Rad) and 30 μg of total protein were resuspended in a loading buffer (20% glycerol, 10% SDS, 0.1% bromophenol blue), denaturated upon 5 min incubation at 95 °C and loaded onto a 12% polyacrylamide gel for electrophoretic separation.

After electrophoresis, the proteins were blotted onto a PVDF membrane according to standard protocols. After 1 h of membrane blocking in 5% nonfat milk, the membrane was incubated with the primary antibody (anti-survivin 1:200, Santa Cruz Biotechnology, Inc., Heidelberg, Germany) overnight, at 4 °C. Following this time period, the membrane was washed three times with TBS/T (25 mM Tris-HCl, 150 mM NaCl, 0.1% Tween) and incubated with the appropriate secondary antibody (1:10000) for 2 h, at room temperature. Then, the membrane was washed three times with TBS/T and incubated with the enzyme substrate ECF (alkaline phosphatase substrate; 20 μL of ECF/cm^2 of membrane) for a maximum of 5 min, at room temperature. Fluorescence detection was achieved at 570 nm using a ChemiDoc™ Touch Imaging System (Bio-Rad). Equal protein loading was shown by

reprobing the membrane with an anti-β-actin antibody (1:1000, Sigma) and with the appropriate secondary antibody. Prior to membrane reprobing, the blots were washed in 40% methanol for 30 min, followed by a fast wash with Milli-Q water. The membrane was then washed with a glycine solution (0.1 M pH 2.5) for 40 min, further washed three times with TBS/T and blocked for 1 h in 5% nonfat milk.

The analysis of band intensity was performed using ImageJ Software (Wayne Rasband National Institutes of Health, USA), and the survivin band intensity was normalized to β-actin in each experiment, in order to correct variations in the total protein content.

Physico-chemical characterization of the complexes: size, zeta potential and siRNA protection determination

The hydrodynamic size distribution of the ternary complexes of surfactant, siRNA and helper lipids was evaluated by dynamic light scattering (DLS). Immediately before analysis, the complexes were prepared as described above and diluted in HBS. The assay was performed using a Submicron Particle Size Analyzer, Beckman Coulter N4 Plus, at 25 °C.

Zeta potential measurement of the complexes was performed in the aqueous buffer HBS, at 25 °C, using a Zetasizer Nano ZS, ZN 3500, with a 532 nm laser (Malvern Instruments, UK). The complexes were prepared immediately before analysis, placed in the measuring cell and an electric current of 3.0 mA was applied.

PicoGreen intercalation assay was used to evaluate the degree of siRNA protection conferred by the delivery system. Complexes containing 14 pmol of siRNA were prepared in a total volume of 100 µl of HBS. After 30 min of incubation, at room temperature, complexes were transferred to a 96-well (black walled) plate (Corning, NY, USA) and 100 µl of PicoGreen (Molecular Probes, Eugene, OR), diluted according to the manufacturer's instructions (1:200 dilution in HBS buffer), were added to each well. Following an incubation period of 5 min, at room temperature, PicoGreen fluorescence, which is directly proportional to the amount of accessible/free nucleic acid, was measured using a SPECTRAmax Gemini EM fluorimeter (Molecular Devices, Union City, CA). The excitation and emission wavelengths were set at 485 and 520 nm, respectively. The fluorescence intensity was measured immediately after complex preparation at 25 °C and 37 °C, and every 10 min for the period of 1 h at 37 °C. The amount of siRNA available to interact with the probe, expressed as a percentage of the maximum fluorescence obtained with naked siRNA, was determined according to the Equation:

$$\% \text{ of free siRNA} = [(F - F_0)/(F_{100} - F_0)] \times 100$$

where F is the fluorescence intensity measured after adding the PicoGreen solution to the complexes, F_{100} (corresponding to 100% of free siRNA) represents the maximum fluorescence intensity, obtained using naked siRNA in the same amount as that associated with the complexes, F_0 (corresponding to 0% of free siRNA) is the residual fluorescence intensity, obtained in the absence of siRNA, which represents the maximum protection of the nucleic acid.

Statistical Analysis

Data are presented as mean ± SD of at least three independent experiments. The significance of the results was statistically analyzed by one-way analysis of variance (ANOVA) with Tukey's multiple pairwise comparison, unless stated otherwise. Statistical significance was set at $p < 0.05$.

4.4. Results

4.4.1. GFP silencing mediated by gemini surfactant-based complexes and cytotoxicity

In order to select an efficient vehicle for siRNAs, used in this work to promote survivin downregulation, studies were initially performed to evaluate the ability of *bis-quats* and serine-derived gemini surfactants to mediate GFP gene silencing in U87 GBM cells, stably transfected to constitutively express GFP (U87-GFP). Flow cytometry analysis was used to assess GFP expression upon cell transfection with gemini surfactant-based complexes carrying anti-GFP siRNA. Parallel cell viability experiments were performed using a modified Alamar blue assay, to evaluate the cytotoxicity associated with the transfection process.

Figure 4.2 shows that complexes containing the cationic gemini surfactant with m=16 and s=2 mediated a significant reduction of GFP expression, displaying the highest transfection efficiency (45.5% of GFP silencing) at the 8/1 (+/-) charge ratio, without causing significant unspecific effects (deduced from the transfection assay in which an oligonucleotide with a scrambled sequence was used, siMUT) or cytotoxicity (86.7% of cell viability). In contrast to 16-2-16, other gemini surfactants of the *bis-quat* family with different tail lengths (m=12, 14 and 18) or with longer spacers (s=5 or 10) showed to be ineffective in promoting GFP silencing (Figure S4.1, Supplementary data).

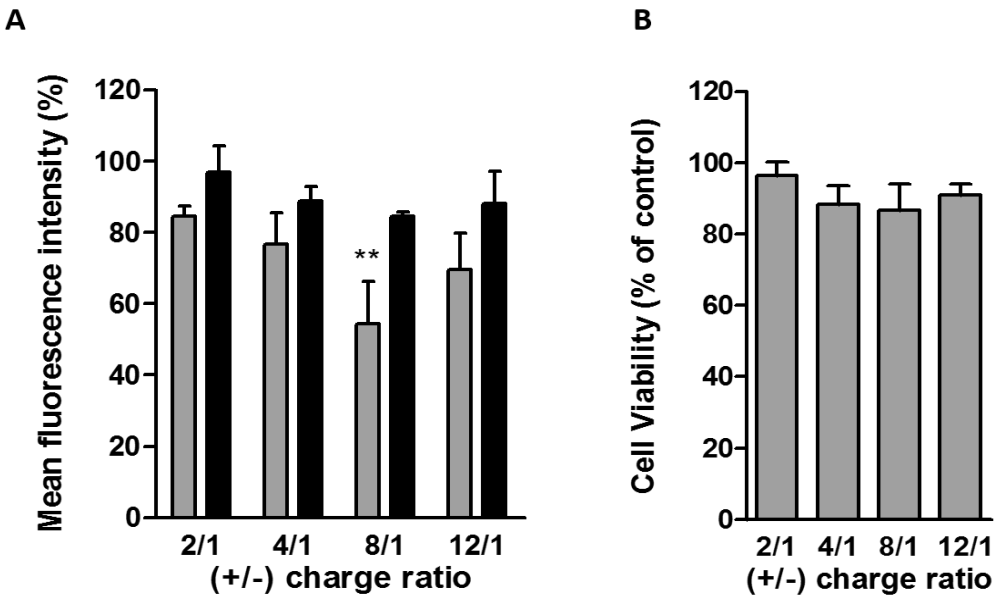

Figure 4.2 - Mean fluorescence intensity (A) and viability (B) of U87-GFP cells transfected with complexes of 16-2-16/siGFP (gray bars) or 16-2-16/siMUT (black bars), at the indicated (+/−) charge ratios. Results of GFP expression are presented with respect to that of a control (nontreated cells, 80% of which express GFP), taken as 100%. Cell viability results are presented as a percentage of the control (nontreated cells, more than 98% of which are

viable), taken as 100%. The results represent the mean ± SD obtained from three independent experiments. Formulations containing siGFP were compared with the corresponding formulation containing siMUT (** $p<0.01$).

Serine-derived gemini surfactants with a 5-carbon spacer, differing in the alkyl tail length (m=12, 14, 16 or 18) showed to be unable *per se* to mediate efficient gene silencing in U87-GFP cells, regardless of the (+/ −) charge ratio (Figure S4.2, Supplementary data). Therefore, the binary complexes (gemini surfactant/siGFP) that induced less cytotoxicity (m=14 and 18) were combined with a mixture of DOPE and Chol, used as helper lipids (HL), in an attempt to improve the ability of gemini surfactant-based complexes to mediate gene silencing.

Figure 4.3 shows the mean fluorescence intensity (A) and viability (B) of U87-GFP cells obtained upon incubation with binary or ternary siRNA complexes based on $(14Ser)_2N5$ and $(18Ser)_2N5$, at the 8/1 and 12/1(+/-) charge ratios and at different HL:gemini surfactant molar ratios. A similar tendency for enhanced transfection efficiency with the increase of the HL:surfactant molar ratio (to a maximum of 4:1), was observed for both gemini sufactants. In fact, $(14Ser)_2N5$/siRNA/HL complexes at the 4:1 HL:surfactant molar ratio and at the 8/1 and 12/1 (+/-) charge ratios displayed the highest transfection efficiency (50% of GFP silencing), without causing significant unspecific effects (as inferred by comparing with siMUT transfection). In addition, at the 12/1 (+/-) charge ratio the complexes induced less cytotoxicity than at the 8/1 (+/-) charge ratio (89.8 and 72.1% of cell viability, respectively).

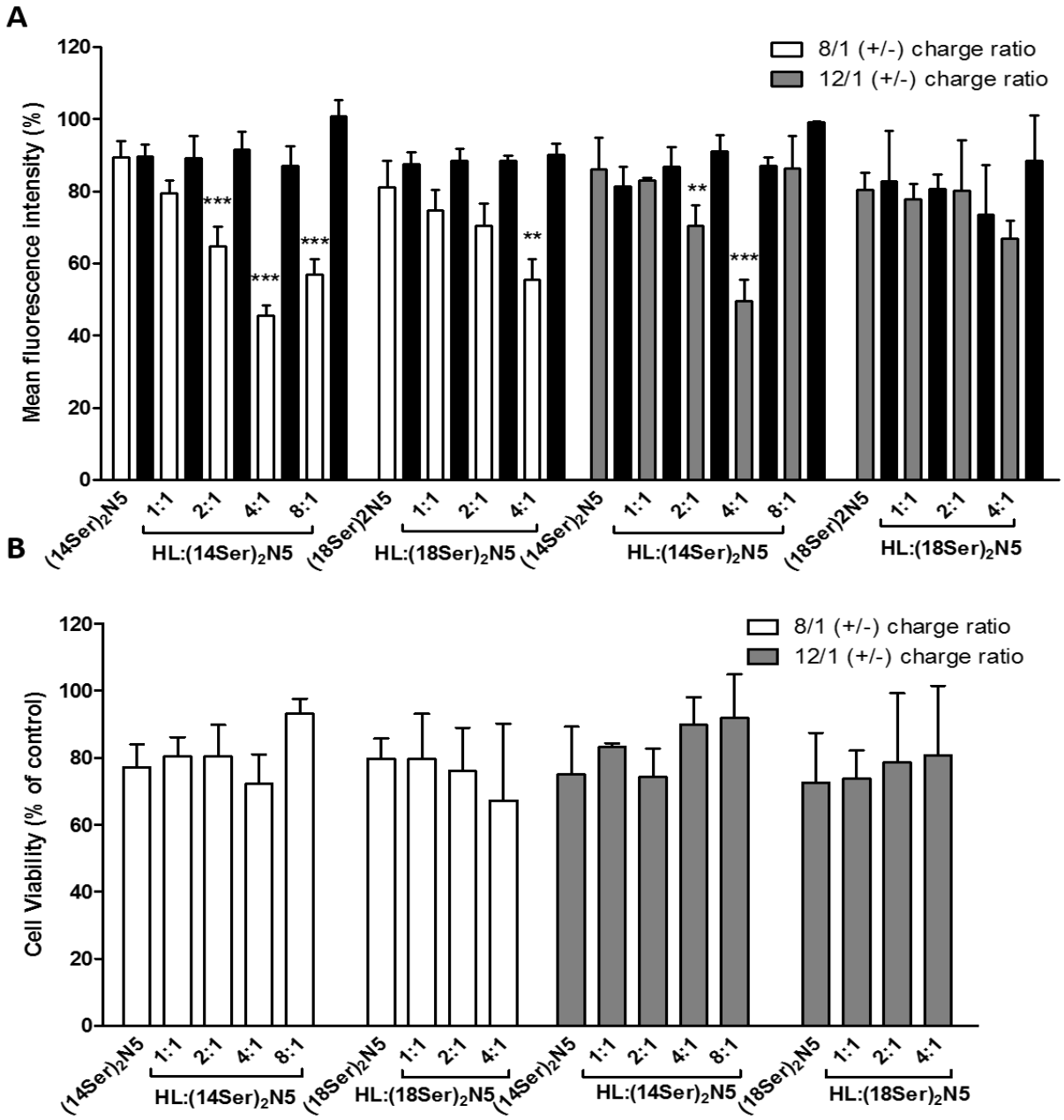

Figure 4.3 - Mean fluorescence intensity (A) and viability (B) of U87-GFP cells, transfected with complexes of $(mSer)_2N5$/siGFP (white and gray bars) or $(mSer)_2N5$/siMUT (black bars), prepared at the 8/1 and 12/1 (+/-) charge ratios, combined with the helper lipids DOPE:Chol (2:1), at the indicated molar ratios of HL: gemini surfactant (HL:$(mSer)_2N5$). Results of GFP expression are presented with respect to that of a control (nontreated cells, 80% of which express GFP), taken as 100%. Cell viability results are presented as a percentage of the control (nontreated cells, more than 98% of which are viable), taken as 100%. The results represent the mean ± SD obtained from three independent experiments. Formulations containing siGFP were compared with the corresponding formulation containing siMUT (black bars) (** $p<0.01$, *** $p<0.001$).

In order to evaluate the capacity of the complexes to overcome the inhibitory effect of serum on transfection, cells were incubated with the complexes in medium containing increasing amounts of serum (10, 20, 30 and 60%) during the period of transfection (4 h). Figure 4.4A shows that serum inhibited transfection mediated by 16-2-16-based complexes, in contrast to the $(14Ser)_2N5$-based formulation, which maintained its transfection ability unchanged up to 20% serum (Figure 4.4C). In either case, the presence of serum did not affect cell viability, as shown in Figure 4.4B and D for cells transfected with 16-2-16-based and $(14Ser)_2N5$-based complexes, respectively.

Since the silencing efficiency of *bis-quat*-based complex (16-2-16/siRNA) revealed to be limited by the presence of serum, serine-derived gemini surfactant-based complexes ($(14Ser)_2N5$/siRNA/HL) were selected for the subsequent experiments.

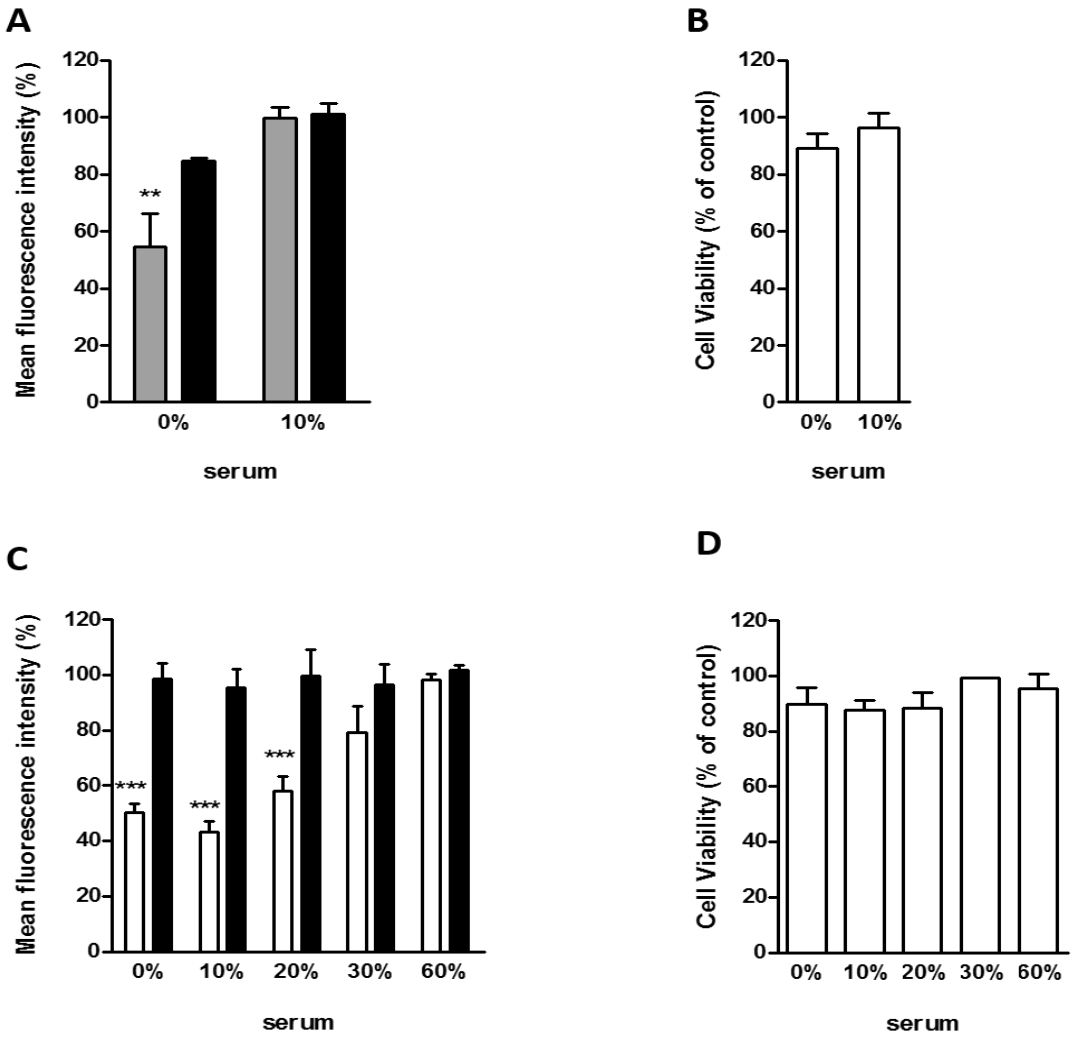

Figure 4.4 - Mean fluorescence intensity (A and C) and viability (B and D) of U87-GFP cells transfected with binary complexes of 16-2-16/siRNA (at the 8/1 (+/-) charge ratio) (A, B) or with ternary complexes of $(14Ser)_2N5$/siRNA/HL (at the 12/1 (+/-) charge ratio and 4:1

HL:surfactant molar ratio) (C, D). Cells were incubated for 4 h with complexes in serum-free medium (0%) or with medium containing 10, 20, 30 or 60% of serum. Then, the medium was replaced by fresh complete medium and, after a further 44 h incubation, data were collected. Results of GFP expression are presented with respect to that of a control (nontreated cells, 80% of which express GFP), taken as 100%. Cell viability results are presented as a percentage of the control (nontreated cells, more than 98% of which are viable), taken as 100%. The results represent the mean ± SD obtained from three independent experiments. Formulations containing siGFP were compared with the corresponding formulation containing siMUT (black bars) (** $p<0.01$, *** $p<0.001$).

4.4.2. Cellular uptake of $(14Ser)_2N5$/siRNA/HL complexes and intracellular distribution of siRNA-DY547

Figure 4.5 shows the intracellular distribution of DY547-labeled siRNAs (red) following transfection of U87 cells mediated by the $(14Ser)_2N5$/siRNA/HL complexes. Confocal microscopy images confirm that, 4 h after transfection, siRNAs efficiently reach the cell cytoplasm, both in the absence and presence of serum. However, particle cytoplasmic distribution in cells transfected in the absence of serum appears in a punctuated pattern indicating that $(14Ser)_2N5$/siRNA/HL complexes may be imprisoned in endocytic vesicles, whereas in the presence of serum the distribution pattern is more diffuse and homogeneous throughout the cytoplasm, suggesting that, under these conditions, the complexes were able to escape from the endosomes or, alternatively, were internalized via non-endocytic pathways.

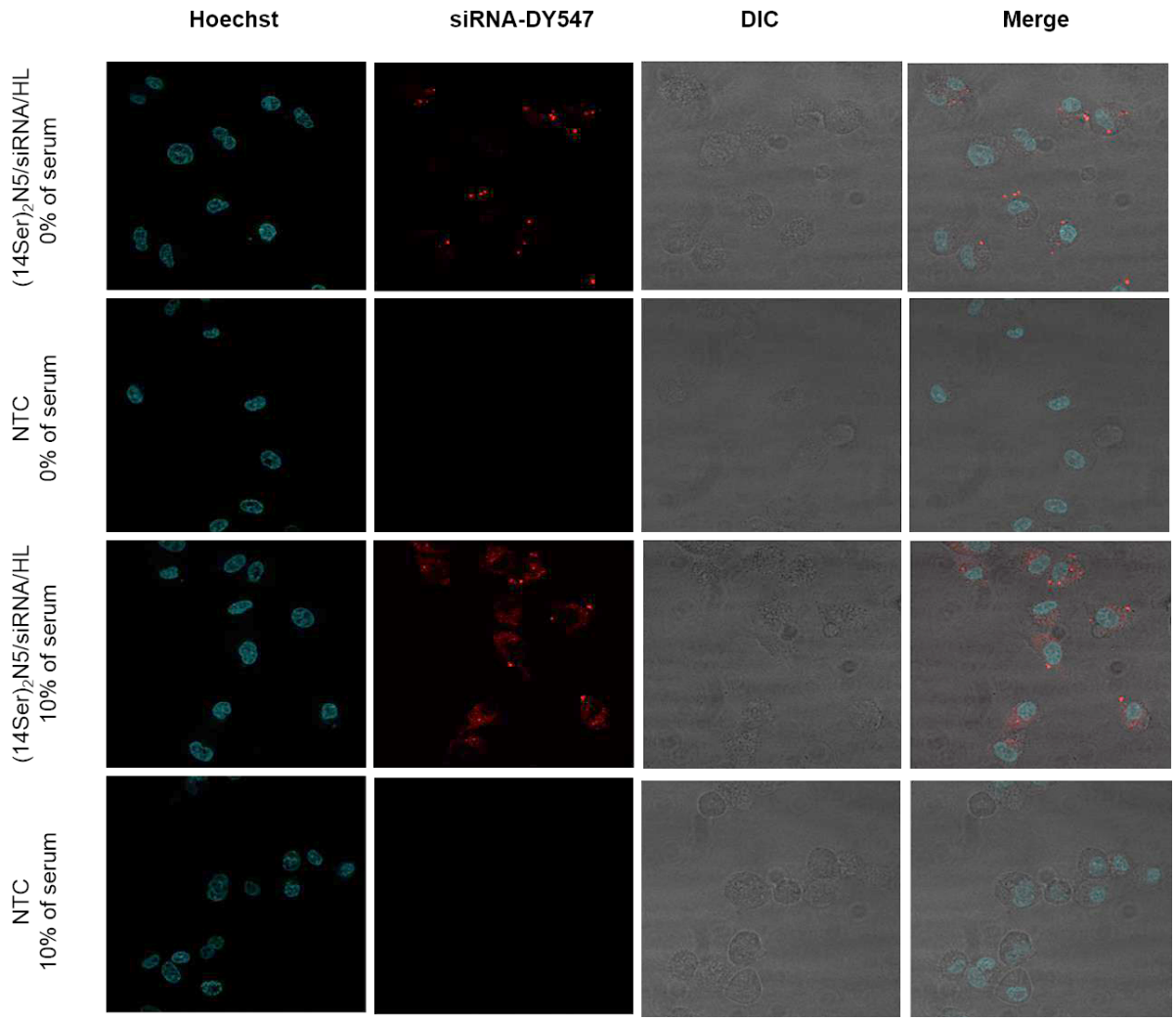

Figure 4.5 - Representative confocal microscopy images of the siRNA distribution in U87 cells, taken 4 h after transfection with $(14Ser)_2N5$/siRNA/HL complexes. U87 cells were transfected in serum-free medium (0%) or in medium containing 10% of serum with complexes containing DY547-labeled siRNA (red). Cell nuclei were labeled blue using the DNA-binding Hoescht 33342 dye and cell limits are visible in differential interference contrast (DIC) images. Non-treated U87 cells (NTC) are shown as a control.

To clarify if endocytosis is involved in the cellular uptake of $(14Ser)_2N5$/siRNA/HL complexes, U87-GFP cells were transfected in the presence and absence of serum, at 37 and 4 °C, and GFP silencing was evaluated by flow cytometry, as previously described (Figure 4.6). In the absence of serum, the reduction of GFP mean fluorescence intensity promoted by siGFP complexes at 4 °C was not significantly different from that induced by the control siMUT complexes, as opposed to what was found at 37 °C (Figure 4.6A). In contrast, in the presence of 10% serum, a specific GFP silencing was obtained at both 4 and 37 °C. In both

conditions (0 and 10% serum), a significant decrease of the specific GFP silencing was found at the low temperature as compared to that observed at the physiological temperature (Figure 4.6B), thus indicating a contribution of temperature-dependent, most likely endocytic, pathways for the internalization of the complexes. However, the observation that at the low temperature GFP silencing was not completely abolished (Figure 4.6A), suggests that non-endocytic mechanisms are also involved in the cell uptake of $(14Ser)_2N5$/siRNA/HL complexes.

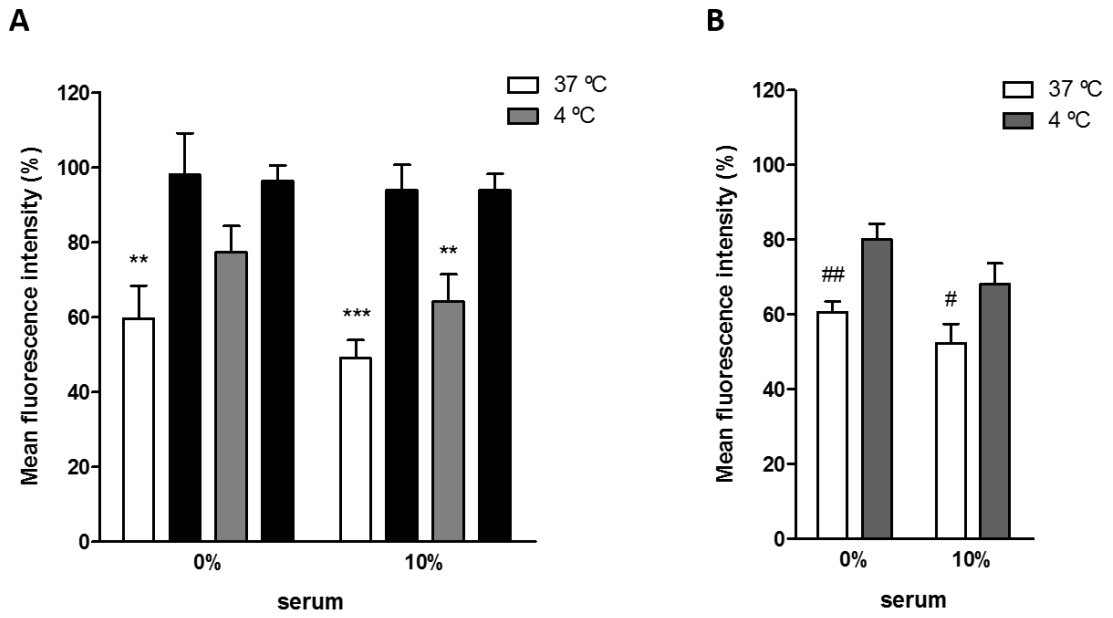

Figure 4.6 - (A) Mean fluorescence intensity of U87-GFP cells transfected with the ternary complexes $(14Ser)_2N5$/siGFP/HL (white and gray bars) or $(14Ser)_2N5$/siMUT/HL (black bars), at the 12/1 (+/-) charge ratio and 4:1 HL:surfactant molar ratio, in the absence and presence of serum, at 37 or 4 °C. (B) Mean fluorescence intensity of U87-GFP cells transfected with the complexes $(14Ser)_2N5$/siGFP/HL, expressed in percentage of the mean fluorescence intensity of the same cells transfected with the complexes $(14Ser)_2N5$/siMUT/HL, in the absence and in the presence of serum, at 37 or 4 °C. Cells were incubated for 2 h with the complexes in serum-free medium (0%) or with medium containing 10% of serum, at 37 or 4 °C, as indicated in the figure. Then, the medium was replaced by fresh complete medium and, after a further 44 h incubation, data of GFP expression were collected and presented with respect to that of a control (nontreated cells, 80% of which express GFP), taken as 100%, (A), and as a percentage of the corresponding formulation containing siMUT (B). The results represent the mean ± SD obtained from three independent experiments. Pairwise comparisons were performed (A) for the reduction of GFP mean fluorescence intensity promoted by formulations containing siGFP and siMUT (**

p<0.01, *** p<0.001) and for the silencing ability of the formulation containing siGFP (expressed in percentage of that containing siMUT) in cells incubated at 4 °C and at 37 °C (# p<0.05, ## p<0.01, using the unpaired t-test).

4.4.3. Physico-chemical characteristics of $(14Ser)_2N5$-based complexes

Gemini surfactant-based complexes were characterized with respect to their hydrodynamic diameter, surface charge and ability to confer protection to the carried siRNAs.

Complexes of $(14Ser)_2N5$/siRNA/HL, prepared at the 12/1 (+/-) charge ratio, displayed an average diameter of 679 nm, although with a polydisperse distribution (PI of 0.655), and a neutral surface charge (Table 4.1).

Table 4.1 - Physico-chemical characteristics of $(14Ser)_2N5$/siRNA/HL complexes.

Complex	Charge ratio (+/-)	HL:surfactant molar ratio	Hydrodynamic diameter / nm	PD index	Zeta potential / mV
$(14Ser)_2N5$/ siRNA/HL	12/1	4:1	679 ± 84	0.655 ± 0.039	+0.4 ± 1.0

The siRNA protection conferred by the $(14Ser)_2N5$/HL carrier was evaluated in the absence and presence of serum (10 and 30%) at 25 and 37 °C (Figure 4.7). At room temperature and in the absence of serum, approximately 50% of the siRNA was inaccessible to the probe, thus indicating a moderate nucleic acid protection (Figure 4.7A), which was maintained for at least one hour when the temperature was increased to 37 °C (Figure 4.7B). In the presence of serum (10 and 30%), siRNA became more accessible to the fluorescent probe, indicating complex destabilization (Figure 4.7A). The disassembly of the complexes and consequent exposure of the siRNA to the probe, at 37 °C and in the presence of serum, revealed to be progressive, being completed after 50 min (Figure 4.7B).

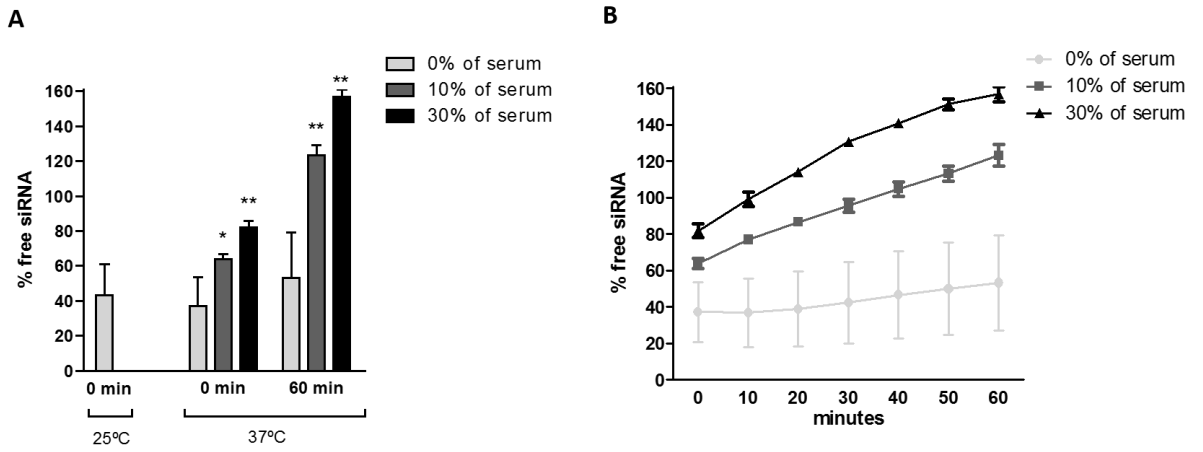

Figure 4.7 - Effect of the temperature and the presence of increasing amounts of serum on siRNA protection conferred by $(14Ser)_2N5$/HL, as assessed by the PicoGreen intercalation assay. Complexes were incubated in HBS containing 0, 10 or 30% of serum and probe accessibility to siRNAs was measured immediately after complex preparation at 25 °C and 37 °C, and after 60 min at 37 °C (A), and every 10 min during a period of 60 min, at 37 °C (B). Data are representative of three independent experiments. Pairwise comparisons were performed in (A) between complexes incubated in the presence of serum and the corresponding complexes incubated in its absence (white bars) (* $p<0.05$, ** $p<0.01$).

4.4.4. Survivin downregulation and effects on cell viability

Transfection experiments using $(14Ser)_2N5$/siRNA/HL complexes, prepared at the 12/1 (+/-) charge ratio, were performed in order to assess their ability to mediate downregulation of an endogenous protein in U87 cells in the presence of serum. For this purpose, siRNA against the messenger RNA (mRNA) of survivin (siSURV), an anti-apoptotic protein overexpressed in cancer, was used to transfect the cells and survivin mRNA levels were evaluated by qRT-PCR. Upon transfection with $(14Ser)_2N5$/siSURV/HL complexes in medium containing 10% of serum, U87 cells presented decreased survivin mRNA levels, by approximately 50 and 60%, 24 and 48 h after transfection, respectively (Figure 4.8 A and C, respectively). In contrast, in the absence of serum, survivin knockdown was not significant when compared to that obtained using complexes prepared with the non-target siRNA (siMUT). The transfection efficiency of $(14Ser)_2N5$-based complexes was compared to that of the commercially available transfection reagent RNAiMAX. Although being able to reduce in 80% the survivin mRNA levels, RNAiMAX transfection resulted in ca. 50% of unspecific effects, as indicated by the silencing effect observed with RNAiMAX/siMUT (Figure 4.8 C). Anti-survivin siRNA delivery mediated by either surfactant-based complexes or RNAiMAX

did not result in any impact on U87 cell viability, neither 24 (Figure 4.8B) nor 48 h (Figure 4.8D) post-transfection.

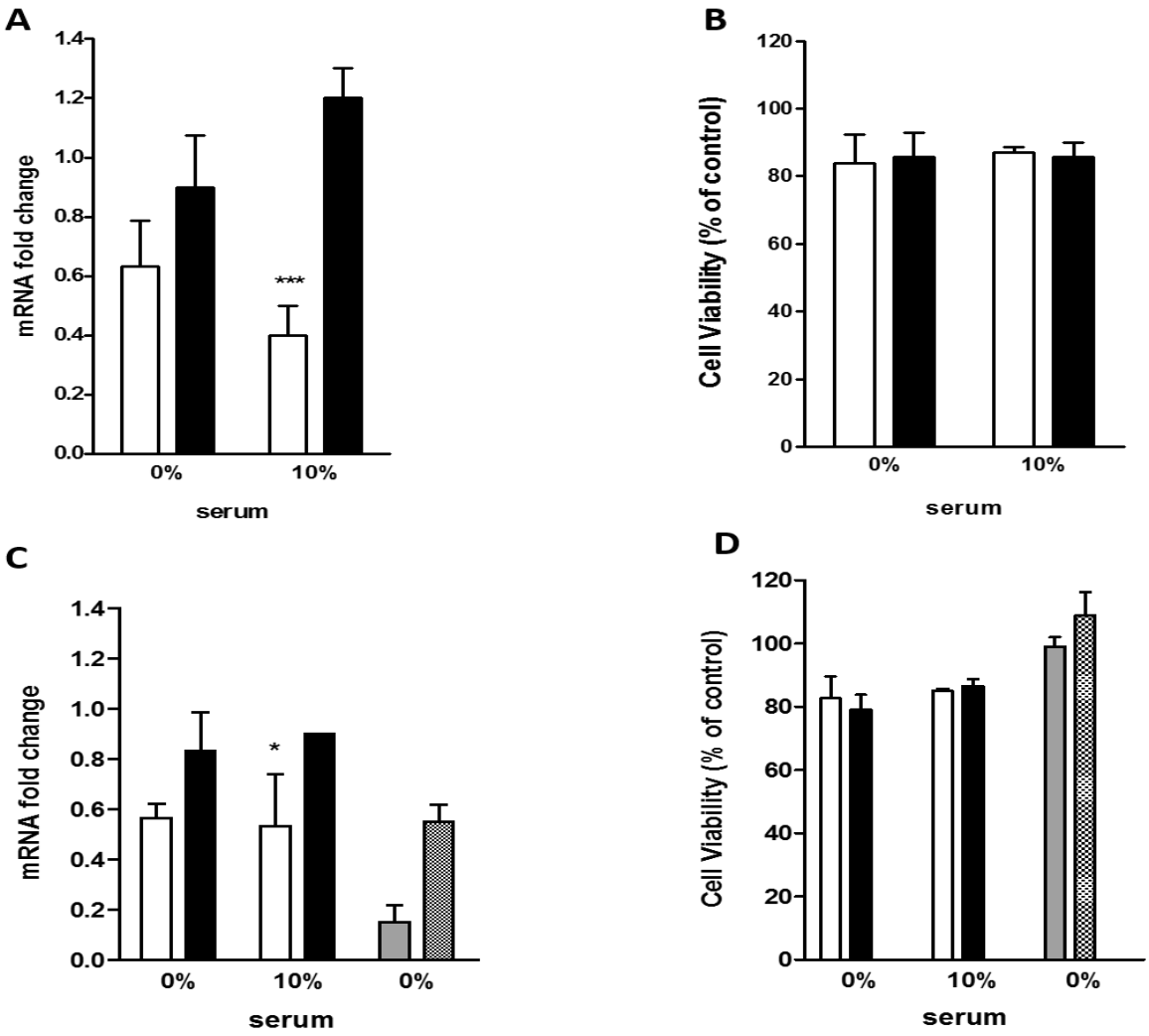

Figure 4.8 - Survivin mRNA levels (A and C) and viability (B and D) of U87 cells 24 (A and B) and 48 h (C and D) post-transfection with complexes of $(14Ser)_2N5$/siRNA/HL, at 12/1 (+/-) charge ratio and combined with helper lipids at the 4:1 (HL:surfactant) molar ratio (white and black bars, for siSURV and siMUT, respectively), or with RNAiMAX/siRNA (gray and dotted bars for siSURV and siMUT, respectively). Transfection was performed in serum-free medium and in medium containing 10% of serum, as indicated in the figure. For determination of survivin mRNA levels, RNA was recovered from U87 cells 24 or 48 h after transfection and converted to cDNA, which was analyzed by qRT-PCR. Survivin mRNA levels, presented as fold change with respect to nontreated control cells, was determined by the ΔΔCt method, as described in Materials and Methods. Cell viability results are presented as a percentage of the control (nontreated cells, more than 98% of which are viable), taken as 100%. Results represent the mean ± SD obtained from three independent experiments.

Survivin mRNA levels of cells transfected with formulations containing anti-survivin siRNA (white and gray bars) were compared with those of cells transfected with the corresponding formulation containing siMUT (black and dotted bars) (* $p<0.05$, *** $p<0.001$).

The reduction of survivin mRNA levels, mediated by $(14Ser)_2N5$/siRNA/HL complexes, in medium containing 10% of serum, was accompanied by the decrease of survivin expression, analyzed by Western blot, 72 h post-transfection (Figure 4.9). In fact, survivin mRNA silencing mediated by $(14Ser)_2N5$/siSURV/HL complexes was able to reduce survivin levels to 60% of those observed for nontreated control cells. In addition, no decrease in survivin expression was observed in cells transfected with the control complexes prepared with siMUT (96% survivin expression), ruling out any unspecific effects.

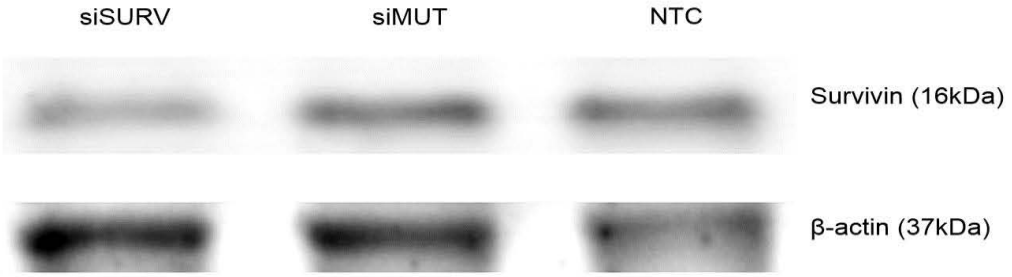

Figure 4.9 - Representative image of survivin knockdown mediated by $(14Ser)_2N5$/siRNA/HL complexes in U87 cells and evaluated by Western blot analysis 72 h after transfection. U87 cells were transfected with $(14Ser)_2N5$/siRNA/HL complexes prepared with siRNA targeting survivin mRNA (siSURV) or with a non-targeting siRNA (siMUT).Non-transfected cells (NTC) are shown as control and β-actin levels are shown as reference for equal amount of protein loaded onto the gel.

4.4.5. Effect of the combination of chemotherapeutics with survivin gene silencing

A combined therapy approach consisting of survivin silencing and chemotherapeutic administration was used to assess the potential of the survivin knockdown strategy to sensitize GBM cells to the anti-cancer drugs temozolomide (TMZ) and etoposide (ETO). For this purpose, survivin silencing with $(14Ser)_2N5$/siRNA/HL complexes was followed by 48 h incubation with TMZ or ETO, and the viability of U87 cells was evaluated using the Alamar blue assay. As observed in Figure 4.10, cell viability was significantly decreased in cells

transfected with anti-survivin siRNA and treated with TMZ or ETO, as compared to cells that were only transfected or treated with each drug alone. TMZ treatment induced only 10% reduction in cell viability, whereas its combination with survivin silencing resulted in approximately 50% of viability loss. Similar results were obtained when cells were incubated with ETO, which *per se* only induced 5% of viability loss, while in cells previously transfected with anti-survivin siRNA, it induced a viability loss of 40%. The combined treatment involving survivin silencing and TMZ or ETO incubation showed a synergistic effect, as concluded by the determined Bliss interaction index (BII), which was higher than 1 (Figure 4.10 B and D) (Olaussen *et al.*, 2009). Parallel transfection experiments with siMUT and drug incubation resulted in a BII around 1, which indicates that cytotoxicity induced by this combination is additive, i.e. results from the sum of the effects of each agent alone.

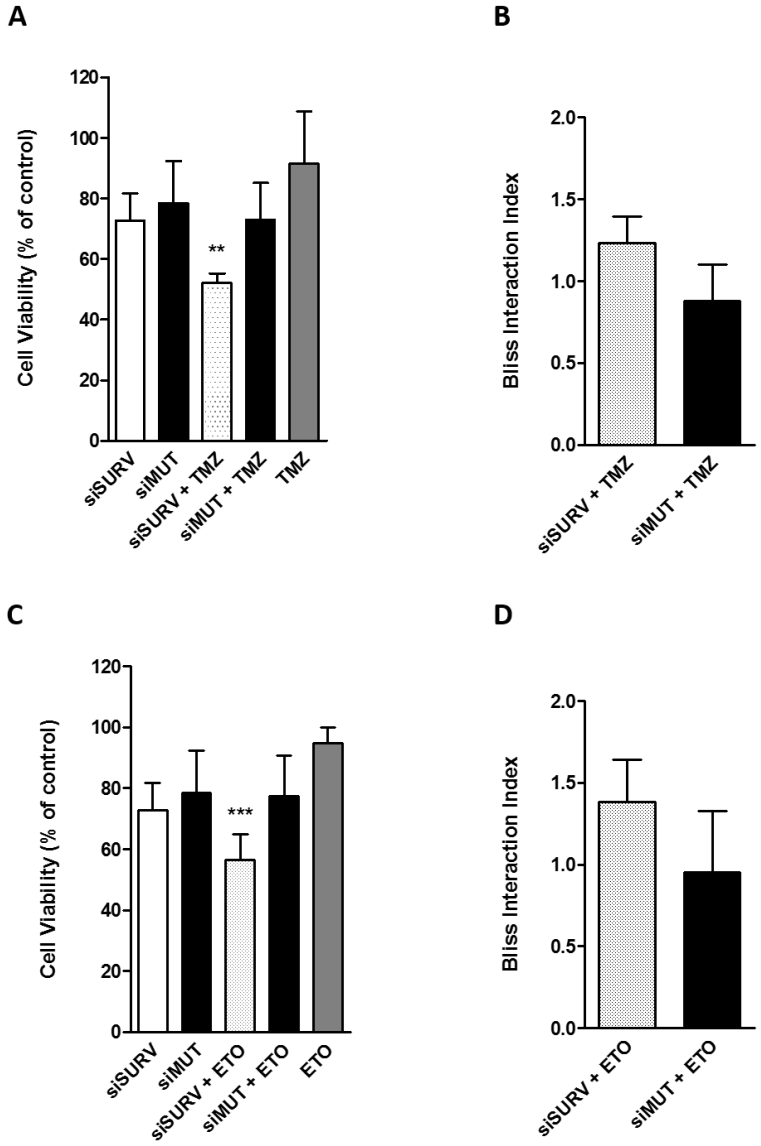

Figure 4.10 - Viability of U87 cells (A and C), assessed by the Alamar Blue assay, 72 h after transfection with siRNA anti-survivin (siSURV) or with siMUT and/or cell incubation with

the chemotherapeutical drugs temozolamide (TMZ) (A) or etoposide (ETO) (C), and Bliss interaction index (B and D) determined for the combined effects on cell viability of survivin silencing plus treatment with each drug. Cells were transfected, for 4 h, with $(14Ser)_2N5$/siRNA/HL complexes and, after an additional period of 20 h, cells were incubated with 400 μM TMZ (A) or 1.5 μM ETO (C), for 48 h. Results, representative of at least three independent experiments, are expressed as a percentage of the nontreated control cells. Combined treatment (dotted bar) was compared with the single drug treatment (gray bar) (** $p<0.01$, *** $p<0.001$).

4.5. Discussion

One of the most concerning hallmarks of GBM is its ability to acquire chemoresistance, which results in a decreased effectiveness of both TMZ, an alkylating agent used as the first-line treatment of GBM, and ETO, an inhibitor of Topoisomerase II enzyme (Sevim *et al.*, 2011) that has also been tested in patients with malignant gliomas. Tumor formation, chemoresistance and radioresistance are phenomena mainly emerging from the combination of genetic and epigenetic events leading to oncogene activation and tumor suppressor gene inactivation. In this context, the deregulation of anti-apoptotic proteins assumes also a crucial relevance (Delbridge, Valente and Strasser, 2012). Survivin, a 16.4 kDa anti-apoptotic protein overexpressed in GBM (George *et al.*, 2010), appears as an extremely promising therapeutic target due to its role in mediating cell proliferation and survival and also in inducing chemoresistance (Mita *et al.*, 2008; Pennati *et al.*, 2008).

In this work, a combined strategy involving survivin silencing followed by treatment with the anti-cancer drugs TMZ or ETO, which have been used as first-line agents in the treatment of GBM, was developed in order to evaluate the efficiency of the knockdown of that oncogenic protein in sensitizing GBM cells to chemotherapeutics. Previous studies in our laboratory using a similar approach have demonstrated an enhancement of the cytotoxicity exerted by doxorubicin and vinblastine in two human cancer cell lines, HeLa (epithelial cervical carcinoma cells) and A549 (breast adenocarcinoma cells), upon survivin knockdown mediated by a commercial transfection reagent (Trabulo *et al.*, 2011). In the present work, a gemini surfactant-based complex combining efficient transfection with low cytotoxicity in GBM cells, was tentatively selected as an anti-survivin siRNA delivery system. With this purpose, an extensive study was performed using two families of gemini surfactants—*bis-quats* (m-s-m) and serine-derived gemini surfactants—that had previously shown to efficiently mediate plasmid DNA delivery in HeLa cells (Cardoso *et al.*, 2011, 2014, 2015a), but whose ability to deliver siRNAs and mediate gene silencing had not been explored. Two gemini surfactant-based formulations, the binary 16-2-16/siRNA and the ternary $(14Ser)_2N5$/siRNA/HL complexes, yielded a remarkable potential to mediate silencing of a reporter gene (GFP), reducing in ca. 50% the green fluorescence of U87-GFP cells (Figures 4.2 and 4.3), without presenting cytotoxicity or unspecific silencing effects (as evaluated with the corresponding complexes formulated with an non-targeting siRNA – siMUT). While 16-2-16/siRNA complexes were able to efficiently mediate gene silencing in the absence of serum, although not in its presence (Figures 4.2 and 4.4), binary complexes of $(14Ser)_2N5$/siRNA were completely ineffective even in the absence of serum. However, the

combination of the latter with the helper lipids DOPE and Chol resulted in an enhancement of transfection efficiency, which was independent of serum presence (up to 20% of FBS). The ability of the helper lipids DOPE and cholesterol to enhance the efficiency of conventional and serine-derived surfactants was previously shown (Cardoso *et al.*, 2014, 2015a) and justified by the propensity of the non-bilayer lipid DOPE to adopt an inverted hexagonal phase, hence promoting nucleic acid escape from the endosome (Hafez and Cullis, 2001; Hui *et al.*, 1996; Koltover *et al.*, 1998; Siegel and Epand, 1997; Zuhorn *et al.*, 2005), and the potential of cholesterol to stabilize the complexes and to prevent their interaction with serum proteins (Crook *et al.*, 1998; Faneca, Simões and Lima, de, 2002; Maslov and Zenkova, 2011; Semple *et al.*, 1996).

The serine-derived gemini surfactant-based complexes $(14Ser)_2N5$/siRNA/HL were selected for the subsequent studies due to their ability to maintain biological activity even in the presence of serum, thus overcoming this important barrier to transfection. Noticeably, confocal microscopy images of cells transfected in the absence or in the presence of 10% FBS with $(14Ser)_2N5$/siRNA/HL complexes prepared with fluorescently labeled siRNAs (Figure 4.6) showed a punctuated distribution of these complexes in the cytoplasm of cells transfected in the absence of serum, whereas in its presence, particle distribution showed a diffuse intracellular pattern. This behavior could indicate that the presence of serum in the transfection medium might alter the pathway of complex uptake, since the punctuated pattern has been assigned to particle entrapment in intracellular vesicles, most likely resulting from the endocytic uptake of the complexes. On the other hand, the diffuse fluorescence distribution observed in the presence of serum may suggest that the complexes have been internalized by non-endocytic pathways, which is consistent with the fact that silencing was not decreased to residual values at 4 °C (Figure 4.6). Alternatively, it is possible that endosomal escape of the complexes and dissociation of siRNAs, which have to be free in order to exert their silencing effect, has been facilitated in the presence of serum. In fact, an early complex disassembly subsequent to the interaction of the complexes with serum components in cell medium is suggested by the siRNA accessibility to the fluorescent probe PicoGreen evaluated over 1 h period (Figure 4.7). The partial disassembly of the complexes promoted by their interaction with serum components and potential alterations of their architecture may facilitate the intracellular release of the nucleic acids. Interestingly, the same formulation containing anti-survivin siRNA, i.e. $(14Ser)_2N5$/siSURV/HL, promoted a significant decrease of survivin mRNA levels in the presence of serum, but not in its absence, thus confirming the importance of siRNA release into the cytoplasm for the success of gene silencing.

Aiming at a future therapeutic application of the $(14Ser)_2N5$/siRNA/HL complexes for gene silencing, further characterization of these complexes was performed. The hydrodynamic diameter and surface charge of the complexes are physical properties that affect the efficiency of the delivery. In fact, although blood capillaries display a 5 μm diameter (Jacobs, Kayser and Muller, 2001), particles larger than 200 nm are not compatible with *in vivo* intravenous administration, being sequestered by the phagocytic system (Gupta and Gupta, 2005). In this regard, although serine-based complexes were found to display a mean diameter larger than this cutoff value (679 nm, see Table 4.1), other routes of administration can be used for the delivery of siRNA complexes, namely intraperitoneal, intramuscular or subcutaneous routes, which are not limited by the size of the particle (Donkuru *et al.*, 2010; Neves *et al.*, 2006; Pfeiffer *et al.*, 2006). In addition, these complexes present a surface charge close to neutrality (Table 4.1), a feature that has been considered ideal to avoid the immune system activation (Li, S. and Huang, 2008).

The therapeutic potential of gemini-based complexes containing siRNAs was tested using siRNAs against survivin, a protein with a recognized role in tumor cell proliferation and viability (Duffy *et al.*, 2007; Mita *et al.*, 2008; Pennati *et al.*, 2008). A significant survivin mRNA silencing (60%, with respect to non-transfected control cells) was observed 24 h after transfection (Figure 4.8) and downregulation of the protein levels (to 60% as compared to non-transfected control cells) was observed 72 h post transfection (Figure 4.9). Although survivin silencing *per se* was unable to impair U87 cell viability, the successful decrease of survivin levels showed to be sufficient for rendering cells more susceptible to a second insult. In fact, cells subjected to the combined approach consisting of survivin knockdown followed by treatment with the chemotherapeutic agents TMZ or ETO displayed a drastic decrease of viability as compared to those exclusively treated with each drug at the same concentration. These results indicate a synergistic effect on the viability of cells whose survivin levels had previously been modulated, when compared to that on cells solely incubated with the drugs (Figure 4.10). On the other hand, cell transfection with the formulation containing the non-targeting siRNA, combined with drug treatment, induced a mere additive cytotoxic effect, which confirms that it was, indeed, the silencing of the anti-apoptotic protein that dramatically impaired the intrinsic chemoresistance of U87 cells.

Overall, these results indicate that cationic gemini surfactants are capable of efficiently delivering siRNA into the cell cytoplasm, even in the presence of serum. The most promising gemini-based complexes, $(14Ser)_2N5$/siRNA/HL, were able to silence the expression of the anti-apoptotic protein survivin, which resulted in a synergistic effect in terms of cytotoxicity induced by the chemotherapeutic drugs TMZ and ETO. Ultimately, this strategy reveals the

potential to improve the therapeutic efficacy of anti-cancer drugs and to allow the reduction of chemotherapeutic doses currently used to tackle GBM, thus also minimizing the side effects associated with cancer treatment.

Acknowledgements

This work is funded by FEDER funds through the Operational Programme Competitiveness Factors - COMPETE and national funds by FCT - Foundation for Science and Technology under the strategic project UID/NEU/04539/2013. C.M.M. and A.M.C. are recipients of fellowships from the FCT with references SFRH/BD/79077/2011 and SFRH/BPD/99613/2014, respectively.

4.6. Supplementary data

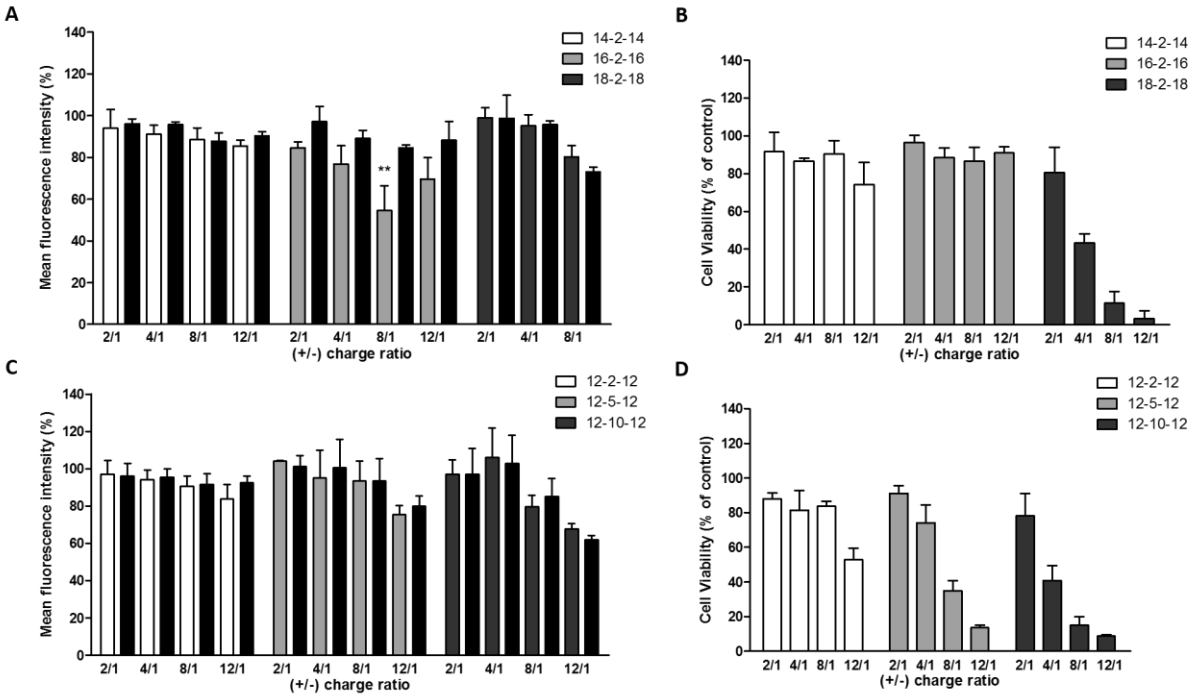

Figure S4.1 - Mean fluorescence intensity (A and C) and viability (B and D) of U87-GFP cells transfected with conventional cationic gemini surfactants-based complexes, differing in the tail and spacer lengths, as indicated in the figure. m-s-m/siGFP (white and gray bars) and m-s-m/siMUT (black bars) were tested at the indicated (+/−) charge ratios. Results of GFP expression are presented with respect to GFP expression of a control (nontreated cells, 80% of which express GFP), taken as 100%. Cell viability results are presented as a percentage of the control (nontreated cells, more than 98% of which are viable), taken as 100%. The results represent the mean ± SD obtained from three independent experiments. Formulations containing siGFP were compared with the corresponding formulation containing siMUT (** $p<0.01$).

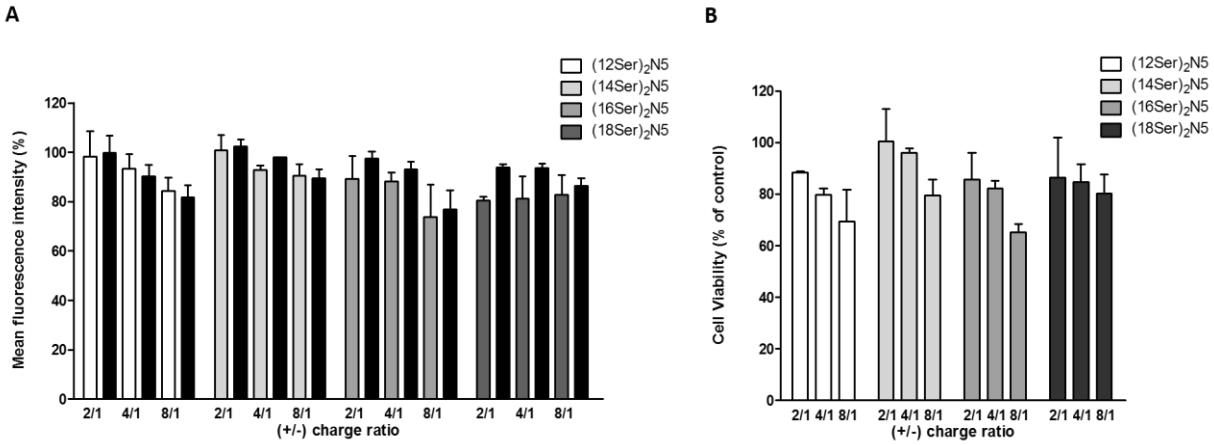

Figure S4.2 - Mean fluorescence intensity (A) and viability (B) of U87-GFP cells transfected with serine derived cationic gemini surfactants-based complexes, differing in the tail length,

as indicated in the figure. $(mSer)_2N5$/siGFP (white and gray bars) and $(mSer)_2N5$/siMUT (black bars) were tested at the indicated (+/−) charge ratios. Results of GFP expression are presented with respect to GFP expression of a control (nontreated cells, 80% of which express GFP), taken as 100%. Cell viability results are presented as a percentage of the control (nontreated cells, more than 98% of which are viable), taken as 100%. The results represent the mean ± SD obtained from two independent experiments.

Chapter 5

Cisplatin delivery to glioblastoma cells mediated by serine-derived gemini surfactant/DNA complexes

The results included in this Chapter are part of the following manuscript in preparation: Rita Q. Cruz, Catarina M. Morais, Ana M. Cardoso, Isabel N. Correia, Sandra G. Silva, Maria L. Vale, Eduardo F. Marques, Maria C. Pedroso de Lima, Amália S. Jurado, "*Cisplatin delivery to glioblastoma cells mediated by serine-derived gemini surfactant/DNA complexes*".

5.1. Abstract

Cisplatin is a chemotherapeutic drug that has a long history of use in the treatment of brain tumors, but whose therapeutic potential is limited by the mechanisms of DNA repair. Mitochondria, which play a crucial role in cell apoptosis, have been actively studied as a potential target for anti-cancer drugs, including those that interfere with DNA, owing to mitochondria dysfunctional nucleotide excision repair mechanisms. Nevertheless, mitochondrial DNA is highly inaccessible due to the double-membrane that surrounds mitochondria, emphasizing the need for designing vectors that can circumvent this barrier. In this work, a cationic serine-derived gemini surfactant that showed to be able to carry a plasmid DNA to mitochondria, mediating mitochondrial expression of GFP, in the human recurrent glioblastoma cell line DBTRG-05MG, was employed to deliver cisplatin intercalated in plasmid DNA to those organelles. Comparative studies on the cytotoxicity induced by complexed and free cisplatin revealed that gemini surfactant-based complexes carrying cisplatin to mitochondria is a promising strategy to fight the intrinsic resistance of glioblatoma to chemotherapy. Moreover, since cisplatin did not impair the translation of plasmid DNA by mitochondria, an innovative therapeutic approach based on gene therapy combined with conventional anti-cancer drugs is proposed in this study to eradicate glioblastoma recurrence.

KEY WORDS: serine, gemini surfactants, cisplatin, mitochondria, chemotherapy, glioblastoma

5.2. Introduction

Cisplatin or cis-diamminedichloroplatinum II (CDDP) was approved by FDA in 1978, to treat testicular and bladder cancer (Galluzzi *et al.*, 2012). Currently, CDDP is also used as a first-line treatment for a broad range of solid tumors such as ovarian, cervical, head and neck, esophageal and lung (Rocha *et al.*, 2014; Todd and Lippard, 2010) and as an adjuvant therapy in recurrent glioblastoma (GBM) (Bent, van den, Hegi and Stupp, 2006; Brandes *et al.*, 2004). Nevertheless, CDDP-doses are restricted by the resulting side-effects, which includes nephrotoxicity (Miller *et al.*, 2010) and neurotoxicity (Amptoulach and Tsavaris, 2011).

Aquated CDDP anti-cancer activity has been described as resulting from its ability to bind to nuclear DNA (El-khateeb *et al.*, 1999), and form CDDP-DNA adducts through intrastrand or interstrand DNA cross-links (Eastman, 1987), which disrupt the structure of the DNA molecule, leading to cell-cycle arrest (Wang, D. and Lippard, 2005). Since, during the cell cycle arrest, CDDP adducts can be recognized and removed by multiple repair pathways (Wang, D. and Lippard, 2005), namely by nucleotide excision repair (NER) (Martin *et al.*, 2008; Rabik and Dolan, 2007), the success of CDDP is also limited by chemotherapy-refractory mechanisms. However, if DNA damage exceeds the repair capacity, cell death supervenes (Galluzzi *et al.*, 2012; Wang, D. and Lippard, 2005). In this context, since mitochondrial DNA (mtDNA) lacks NER (Cullen *et al.*, 2007; Singh and Maniccia-bozzo, 1990) and mitochondria play a central role in cell death mechanisms (Fulda *et al.*, 2010), mtDNA emerges as a promising alternative cellular target for CDDP. Additionally, mtDNA is significantly more susceptible than nuclear DNA (ncDNA) to DNA-binding drugs, due to the lack of histones (Preston *et al.*, 2001).

Noteworthy, mitochondria are surrounded by a double-membrane that restricts the access of a wide range of ions and molecules to their interior. Therefore, there is a need for designing vectors that can surpass this barrier, in order to aid drugs to enter into mitochondrial matrix, when this is the local they exert their activity, namely targeting mtDNA (Smith *et al.*, 2012). The most commonly used mitochondrial-targeting vectors involve the linkage of non-mitochondrial molecules to triphenylphosphonium cation (TTP) (Murphy, 2008), mitochondria-penetrating peptides (MMP) (Horton *et al.*, 2008) or mitochondrial targeting sequences (MTS) (Omura, 1998), taking advantage of the mitochondrial membrane potential (in the case of TTP and MMP) or the mitochondrial protein-import machinery (in the case of MTS) (Murphy, 1997). Additionally, cationic gemini surfactants, which are self-assembling molecules composed of two hydrocarbon chains (tails), two cationic headgroups and a spacer of diverse nature (Littau, 1996; Menger, F and Littau, 1993; Menger, Fredric and Keiper, 2000), have recently shown to mediate efficient delivery

of plasmid DNA into mitochondria, and promote mitochondrial gene expression in HeLa cells (Cardoso *et al.*, 2015b).

In the present work, cationic gemini surfactants derived from the amino acid serine (Figure 5.1) were evaluated regarding their ability to deliver a plasmid of mtDNA (pmtDNA) encoding GFP (pmtGFP), that is specifically translated by mitochondrial machinery (Lyrawati *et al.*, 2011), into mitochondria of human recurrent GBM cells (DBTRG-05MG). The formulation that showed the highest efficiency in promoting GFP expression in mitochondria, without causing a pronounced cytotoxicity, was used to concomitantly deliver CDDP previously intercalated in pmtDNA. Interestingly, our data demonstrated that CDDP benefits from being delivered in the complexed form, i.e. intercalated in pmtDNA, and formulated in a gemini surfactant-based complex, leading to a higher decrease of cell viability and proliferation and a more efficient arrest of cell cycle in the S phase than CDDP administered in the free form, at the same concentration.

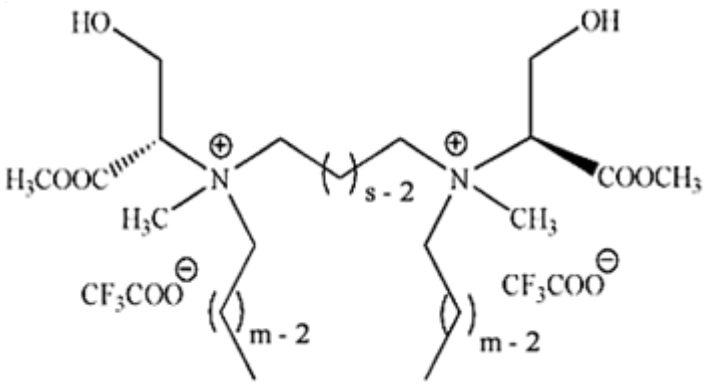

Figure 5.1 - Schematic representation of the general structure of serine-derived gemini surfactants used in this work ($(mSer)_2N5$ with m= 12, 14, 16 and 18).

5.3. Materials and methods

Serine-derived gemini surfactants were synthesized by the method reported by Silva (Silva *et al.*, 2012) and purified by column chromatography. The purity of the compounds was assessed by NMR and mass spectrometry, and the obtained cmc values revealed to be similar to those already reported in the literature (Burrows *et al.*, 2007; Zana, 2002).

The lipids 1,2-dioleoyl-sn-glycero-3-phosphoethanolamine (DOPE) and cholesterol (Chol) were purchased from Avanti Polar Lipids (Alabaster, AL).

Plasmid DNA (pDNA) encoding nuclear GFP (pEGFP-C1, herein designated pncGFP) was obtained from Clontech (CA, USA) and plasmid DNA encoding mitochondrial GFP (pmtGFP) was synthesized and kindly provided by Prof. Diana Lyrawati, Brawijaya University (East Java, Indonesia).

Cisplatin (CDDP) and DMSO (used to prepare CDDP stock solution) were acquired from Sigma (Germany).

Cells and culturing conditions

The human recurrent glioblastoma cell line DBTRG-05MG, kindly provided by Dr. Massimiliano Salerno (Siena Biotech, Italy), was maintained in culture at 37° C, under a humidified atmosphere containing 5% CO_2. DBTRG-05MG cells were grown in monolayer in Roswell Park Memorial Institute 1640 (RPMI, Sigma, R4130) medium, supplemented with 10% (v/v) heat-inactivated fetal bovine serum (FBS; Sigma, St. Louis, MO, USA), 100 units/mL penicillin (Sigma) and 100 µg/mL streptomycin (Sigma) and were detached using enzyme-free cell dissociation buffer at 50–70% confluence. For flow cytometry, DBTRG-05MG cells were plated at a density of $6x10^4$ cells/well, in 1 mL of complete medium supplemented with FBS (10% v/v), in 12-well cell culture plates. For the Alamar blue and sulforhodamine B assays, cells were seeded at a density of $5x10^3$ cells/well, in 100 µL of complete medium, in 96-well plates.

Preparation of binary (gemini/pDNA) and ternary (gemini/pDNA/helper lipids) gemini surfactant-based complexes

Gemini surfactant-based complexes were prepared as previously described (Cardoso *et al.*, 2014). Briefly, an aqueous solution of gemini surfactant was prepared at a concentration of 0.5 mM and filtered through 0.22 µm pore-diameter filters (Schleicher & Schuell, BioScience, Germany). Binary complexes were prepared by mixing an aliquot of gemini solution in HBS with a constant amount of pDNA encoding GFP (pncGFP or pmtGFP to promote nuclear or mitochondrial GFP expression, respectively), in order to obtain the desired

surfactant/pDNA (+/-) charge ratios, followed by incubation at room temperature for 30 min. To produce ternary complexes, a suspension of MLVs composed of DOPE:Chol (2:1 molar ratio) was previously prepared by mixing, at this molar ratio, the helper lipids (HL) DOPE and Chol dissolved in chloroform. The lipid mixture was dried under vacuum in a rotatory evaporator, and the lipid film was hydrated with HBS (pH 11.0) to a final lipid concentration of 0.5 mM. The resulting multilamellar vesicles (MLV) were then sonicated for 3 min, in a sonication bath, and added to surfactant/pDNA complexes previously incubated for 15 min at room temperature, in order to obtain the desired surfactant/HL molar ratios, followed by a further 15 min incubation.

Preparation of gemini surfactant-based complexes containing cisplatin

For the preparation of gemini/pDNA/CDDP complexes, a constant amount of plasmid DNA (1 μg/mL) was mixed with a solution of CDDP in HBS at different concentrations (4, 8 and 16 μM). The mixture was left incubating for 10 min to promote association of the plasmid DNA with CDDP and then added to the gemini surfactant, to obtain the 8/1 surfactant/pDNA (+/-) charge ratio. After an incubation period of 30 min, at room temperature, complexes were added to the cells.

Cell transfection

Twenty-four hours after plating, cell medium was replaced with fresh medium (serum-free OptiMEM medium). Gemini surfactant-based complexes, prepared at different (+/-) charge ratios and containing pDNA encoding GFP, were added to the cells in order to obtain a final pDNA concentration of 1 μg/mL. Following 4 h incubation (in 5% CO_2, at 37 °C), the medium was replaced with fresh medium containing FBS (10% v/v) and antibiotics.

Cell incubation with the drugs

Twenty-four hours after plating, RPMI medium was replaced with OptiMEM, and CDDP, prepared in HBS, was added to 96-well plates to yield the final concentrations of 2, 4, 8, 16, 31, 62.5, 125, 250, 500, 1000 μM. After 4 h of incubation, CDDP-containing medium was replaced with fresh RPMI medium.

Evaluation of cell viability

Cell viability was assessed by a modified Alamar blue assay, as previously described (Konopka *et al.*, 1996). Briefly, an appropriate volume of resazurin dye (10% v/v) in RPMI medium was added to 12-well or 96-well culture plates. After color development, 150 μL of supernatant

were collected from each well, transferred to clear 96-well plates, and the absorbance was measured in a SPECTRAmax PLUS 384 spectrophotometer (Molecular Devices, Union City, CA), at 570 and 600 nm. Cell viability (as a percentage of control cells) was calculated according to the equation:

$$\text{Cell viability (\% of control)} = [(A_{570} - A_{600})/(A'_{570} - A'_{600})] \times 100$$

where A570 and A600 are the absorbances of the treated cells, and A'570 and A'600 are those of the control (nontreated cells), at the indicated wavelengths.

Evaluation of cell proliferation

The sulforhodamine B assay was performed as previously described (Vichai and Kirtikara, 2006). Briefly, immediately or 24, 48, 72 and 96 h after treatment with CDDP, cells were fixed by adding 100 µL of a 1% solution of acetic acid in methanol to each well, followed by 1 h incubation at -20 °C. Cells were then rinsed and left to dry at 37 °C, for 20 min, before being incubated with 200 µL of 0.05% SRB staining solution containing 1% acetic acid, for 1 h at 37 °C. To remove the unbound dye, cells were washed several times with a 1% solution of acetic acid in Milli-Q water and, then, left to dry at 37 °C, for 20 min. The protein-bound dye was solubilized in 10 mM Tris buffer (pH 10) for 15 min, under gentle agitation, and the absorbance was measured at 540 nm in a microplate reader (SPECTRAmax PLUS 384, Molecular Devices, Union City, CA).

Evaluation of transfection efficiency

Forty-eight hours after transfection, cells were detached using enzyme-free cell dissociation buffer (5 min, at room temperature). Cells were then washed by centrifugation (200 *g*, 4 °C, 5 min) in 950 µL of ice-cold PBS and the resulting pellets were resuspended in 200 µL of ice-cold PBS. The cell suspensions were immediately analyzed by flow cytometry using a FACS-Calibur flow cytometer (BD Biosciences, San Jose, CA). To discriminate viable and dead cells and to exclude doublets, cells were appropriately gated by forward/side scattering and from a total of 10,000 events. Data were stored and analyzed using CellQuest software.

Cell cycle analysis

Twenty-four hours after cells were seeded in 12-well plates, the medium was replaced with serum-free medium and cells were transfected with $(18Ser)_2N5$/pDNA or $(18Ser)_2N5$/pDNA/CDDP complexes (at 8 µM CDDP) or treated with free CDDP, at the

same concentration. After 4 h of incubation, the medium was replaced with complete RPMI medium and, forty-eight hours later, cells were detached using enzyme-free cell dissociation buffer (10 min, at room temperature) and washed by centrifugation (300 *g*, 4 °C, 5 min) with ice-cold PBS. The supernatant was discarded and cells were fixed by slowly adding 200 μL of 70% ethanol, while vortexing the mixture at low speed. After 24 h incubation at 4 °C, cells were centrifuged to remove ethanol, and washed once with 2% BSA in PBS. The resulting cell pellet was resuspended in 400 μL of propidium iodide/RNAse solution (Immunostep, Salamanca, Spain). After 15 min incubation under dark at room temperature, cell suspensions were immediately analyzed by flow cytometry using a FACS-Calibur flow cytometer (BD Biosciences, San Jose, CA). To discriminate viable and dead cells and to exclude doublets, cells were appropriately gated by forward/side scattering. Data were collected from at least 10,000 single cell events, stored in CellQuest software and analyzed using ModFit LT 3.0.

Statistical analysis

Data are presented as mean ± SD of at least three independent experiments. The significance of the results was statistically analyzed by one-way analysis of variance (ANOVA) with Tukey's multiple pairwise comparison, unless stated otherwise. Statistical significance was set at $p < 0.05$.

5.4. Results

5.4.1. Transfection Efficiency and Cytotoxicity of Gemini Surfactant-Based Complexes Carrying pmtGFP

Aiming at selecting an efficient vector for pmtDNA, serine-derived gemini surfactants with different hydrocarbon chain lengths (m=12, 14, 16 and 18) were evaluated regarding their ability to mediate mitochondrial expression of GFP, in human recurrent GBM cells (DBTRG-05MG). In parallel, the cell viability was assessed in order to select the formulation that encompasses both the highest transfection efficiency and the lowest cytotoxicity. As observed in Figure 5.2, the highest levels of GFP expression were obtained with complexes displaying the highest (+/-) charge ratio assayed (12/1), regardless of the serine-derived gemini surfactant used for their generation. However, complexes prepared at this (+/-) charge ratio exerted severe effects on cell viability, the reason why they were discarded. At the (+/-) charge ratio of 8/1, the complexes based on the gemini surfactant with 18C-tails showed the highest efficiency in delivering pmtGFP into mitochondria, inducing the expression of GFP protein in 20% of viable cells without causing a severe reduction of cell viability. A further decrease of the (+/-) charge ratio to 4/1 in these complexes did not induce a significant decrease of the cytotoxicity (Figure 5.3A) and significantly reduced their transfection ability (Figure 5.3B). In order to improve the transfection capacity of $(18Ser)_2N5$/pmtGFP complexes (herein designated binary complexes), preformed vesicles of the helper lipids DOPE and Chol at the 2:1 molar ratio (HL) were added to the binary complexes (as described in Material and Methods section), resulting in the formation of ternary complexes with different HL:gemini surfactant molar ratios (1:1, 2:1 and 4:1). Figure 5.3 shows that cell viability decreased with the addition of HL to the complexes, except when they were prepared at 12/1 (+/-) charge ratio. Additionally, HL reduced the efficiency of the complexes to mediate gene expression at all (+/-) charge ratios, being, hence, the binary complexes the most effective formulations. Consequently, $(18Ser)_2N5$/pmtGFP complexes, at 8/1 (+/-) charge ratio, which ally a moderate transfection efficiency (20% of transfected cells) with low cytotoxicity (above 80% of cell viability), were selected for the subsequent experiments.

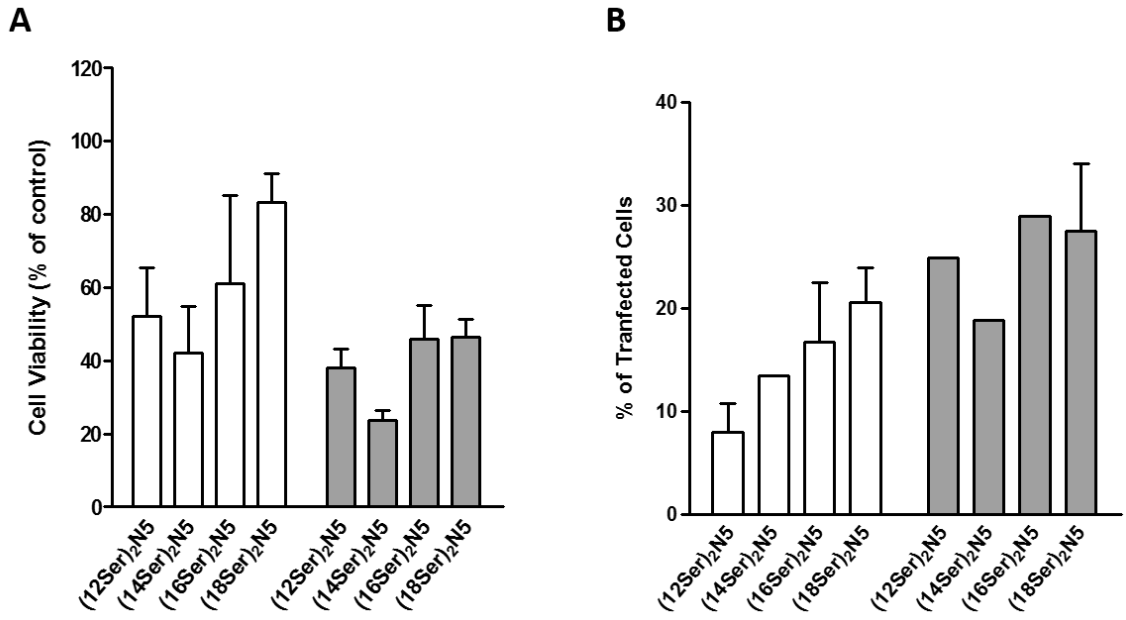

Figure 5.2 - Cell viability (A) and transfection efficiency (B) promoted by complexes of pmtGFP and serine-derived gemini surfactants with different tail length, as indicated in the figure. Cells were incubated for 4 h with the complexes prepared at the 8/1 (white) and 12/1 (gray) (+/−) charge ratios, after which the complex-containing medium was replaced by fresh complete medium. The cells were allowed to further incubate for 44 h. After this period, cell viability was assessed using a modified Alamar blue assay and transfection efficiency was evaluated by flow cytometry as the percentage of transfected viable cells. The results are presented as a percentage of the control (nontreated cells) and represent the mean ± SD obtained from two independent experiments.

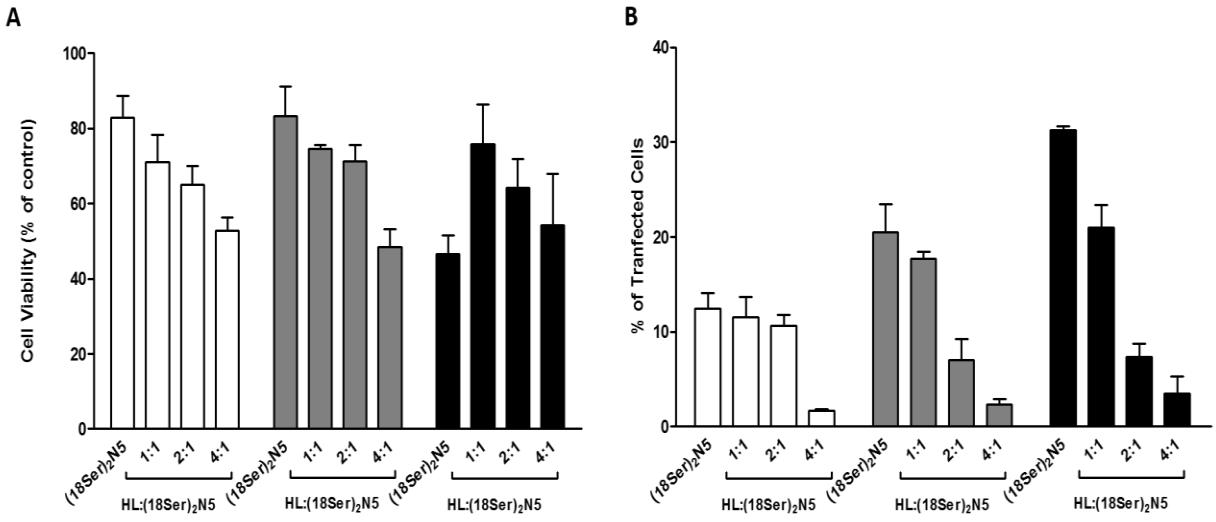

Figure 5.3 - Cell viability (A) and transfection efficiency (B) promoted by $(18Ser)_2N5$-based complexes in the presence and absence of helper lipids (HL) at HL:$(18Ser)_2N5$ molar ratios,

as indicated in the figure. Cells were incubated for 4 h with the complexes prepared at the 4/1 (white), 8/1 (gray) and 12/1 (black) (+/−) charge ratios, after which the complex-containing medium was replaced by fresh complete medium. The cells were allowed to further incubate for 44 h. After this period, cell viability was assessed using a modified Alamar blue assay and transfection efficiency was evaluated by flow cytometry as the percentage of transfected viable cells. The results are presented as a percentage of the control (nontreated cells) and represent the mean ± SD obtained from three independent experiments.

5.4.2. Impact of CDDP and $(18Ser)_2N5$/pmtGFP/CDDP on DBTRG-05MG cell viability and proliferation

To evaluate whether CDDP formulated in $(18Ser)_2N5$/pmtGFP complexes, at 8/1 (+/-) charge ratio, would be more effective than free CDDP in decreasing the viability of DBTRG-05MG GBM cells, cell viability was assessed by Alamar blue assay 48 h after treatment with CDDP, either complexed or in its free form. Initial experiments were performed by exposing DBTRG-05MG cells to different drug concentrations, for 4 h (Figure 5.4), in order to determine the optimal concentration of the drug to be used in the assay. As shown, a moderate decrease in cell viability (*c.a.* 20%) was observed 48 h post-treatment at the concentrations 4, 8 and 16 μM (indicated in the figure in blue color), which were selected for the subsequent experiments.

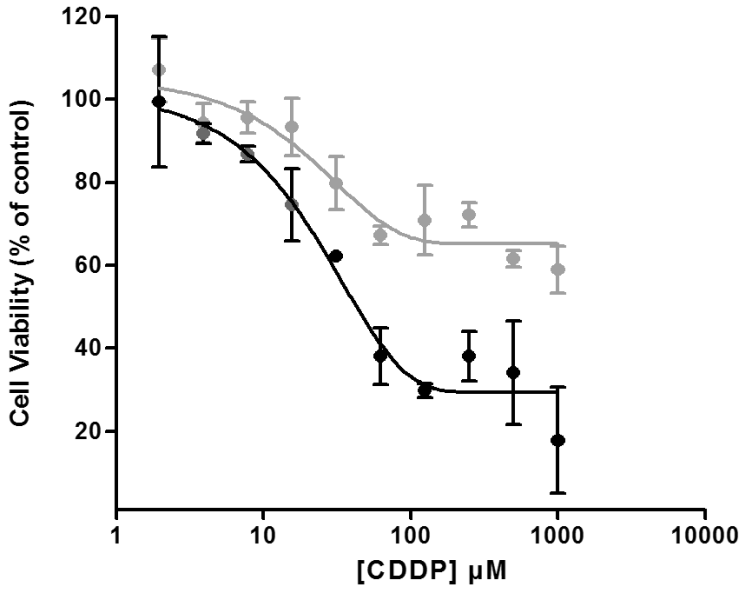

Figure 5.4 - Effect of CDDP on DBTRG-05MG cell viability. Twenty-four hours after plating, cells were exposed to increasing CDDP concentrations, in serum-free medium. After

4 h incubation, CDDP containing medium was replaced with fresh complete medium and, 24 (gray line) and 48 h (black line) later, cell viability was assessed by the Alamar blue assay. The results are presented as a percentage of the control (nontreated cells) and represent the mean ± SD obtained from three independent experiments. The blue points indicate the values of cell viability at the concentrations of CDDP (4, 8 and 16 μM) that were selected for the subsequent experiment.

Figure 5.5 allows to comparing the impact of complexed and free CDDP on the viability of DBTRG-05MG cells, 48 h after treatment. As observed, the percentage of viable cells decreased when CDDP at 4 and 8 μM was carried by $(18Ser)_2N5$/pmtGFP/CDDP complexes, this decrease being much more pronounced than that observed when cells were exposed to free CDDP at the same concentrations. At the highest CDDP concentration assayed (16 μM), the percentages of viable cells exposed to complexed or free CDDP did not show a statistically significant difference. The next experiments were, hence, performed with CDDP at 8 μM.

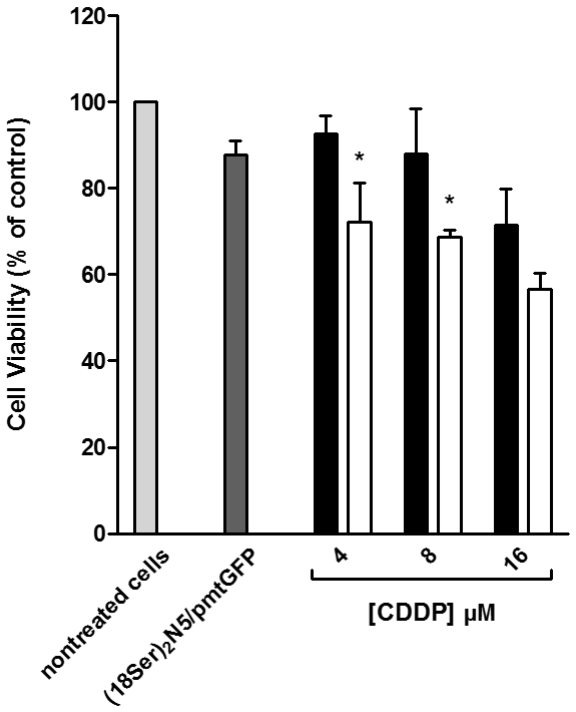

Figure 5.5 - Effect of complexed and free CDDP on DBTRG-05MG cell viability. Viability of DBTRG-05MG cells was assessed by the Alamar blue assay, 48 h after transfection with $(18Ser)_2N5$/pmtGFP (dotted bar) or $(18Ser)_2N5$/pmtGFP/CDDP complexes containing 4, 8 and 16 μM CDDP (white bars) or after treatment with free CDDP (black bars), at the same concentrations. Cells were incubated with the different treatments for 4 h, in serum-free

medium. The results are presented as a percentage of the control (nontreated cells) and represent the mean ± SD obtained from three independent experiments. The viability of cells transfected with complexed CDDP (white bars) were compared with that of cells treated with the corresponding concentrations of free CDDP (black bars) (* $p<0.05$).

In order to compare the effects exerted by complexed and free CDDP at 8 μM on cell proliferation, a sulforhodamine B (SRB) assay was performed to determine the cellular protein content, at different time points, for a 5 day-period after treatment (Figure 5.6). The increase of protein mass, which reflects the increase in cell density, follows the same trend in cultures of nontreated cells and cells treated with free CDDP, although the latter displayed a slower growth rate from 48 h post-treatment and the yield of protein mass at the 96 h time point was significantly lower in this culture than in the culture of nontreated cells. However, cells treated with the complexes containing CDDP showed a lag phase (about 24 h), and 48 h post-treatment cell growth apparently initiated a stationary phase. Remarkably, the yield of protein mass 96 h post-treatment was nearly half of that of nontreated cells and noticeably lower than the one observed when cells were treated with free CDDP, stressing the advantage of delivering CDDP via gemini surfactant-based complexes to promote efficient inhibition of cell proliferation.

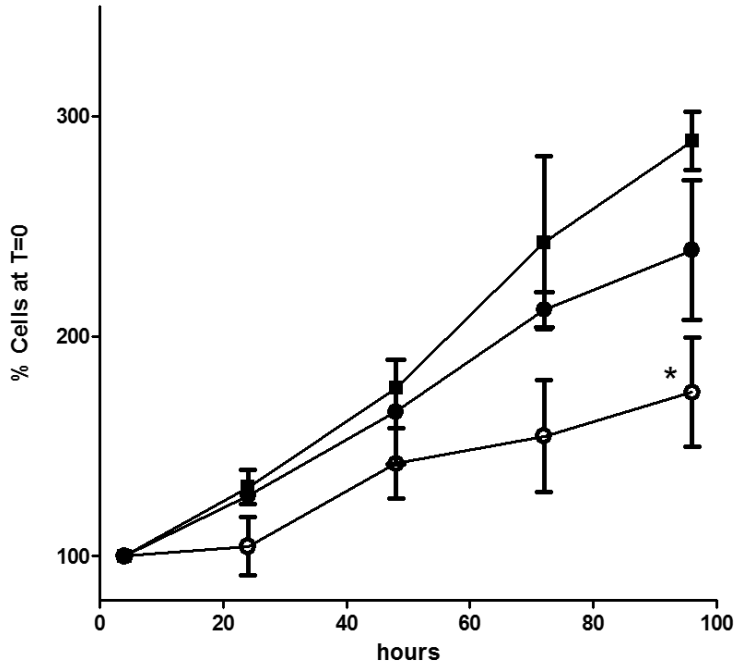

Figure 5.6 - Growth curves of DBTRG-05MG cells, as assessed by sulforhodamine B (SRB) assay. Proliferation of cells transfected with $(18Ser)_2N5$/pmtGFP/CDDP complexes

containing 8 μM CDDP (○) or treated with 8 μM free CDDP (●) is compared with that of control cells (nontransfected and nontreated with CDDP) (■). Cell density was measured at different time points (4, 24, 48, 72 and 96 h) after treatment with CDDP. Density of control cells was measured at the same time points for direct comparison. Proliferation results for each condition are expressed as percentage of the respective cell density at the first time point (set at 100%; T = 0) and represent the mean ± SD obtained from three independent experiments. Pairwise comparisons were performed between each condition and nontreated cells, 96 h post-treatment (* $p<0.05$).

5.4.3. Impact of CDDP and $(18Ser)_2N5$/pmtGFP/CDDP on DBTRG-05MG cell cycle

The distribution of DBTRG-05MG cells along the different phases of the cell cycle (G0/G1, S and G2/M) was analyzed 48 h post-treatment with complexed and free CDDP (Figure 5.7). As observed, 60% of nontreated cells, collected at the same time as those subjected to 4 h treatment with complexed or free CDDP, were found to be in the G0/G1 phase, and a small amount (*c.a.* 7%) in the G2/M phase. As compared to nontreated cells, cells transfected with complexes devoid of CDDP presented a very similar pattern of distribution along the cell cycle phases. However, cell treatment with complexes containing CDDP or with free CDDP resulted in a significant reduction in the percentage of cells in the G0/G1 phase (to around one third) as compared to nontreated cells. Moreover, the percentage of cells in the S phase drastically increased, particularly in the case of cells treated with the complexed CDDP, the majority of which (*c.a.* 70%) were arrested in the S phase. In contrast, the free CDDP allowed a significant amount of cells to pass to the G2/M phase, as compared to nontreated cells or cells transfected with complexes in the presence or absence of CDDP.

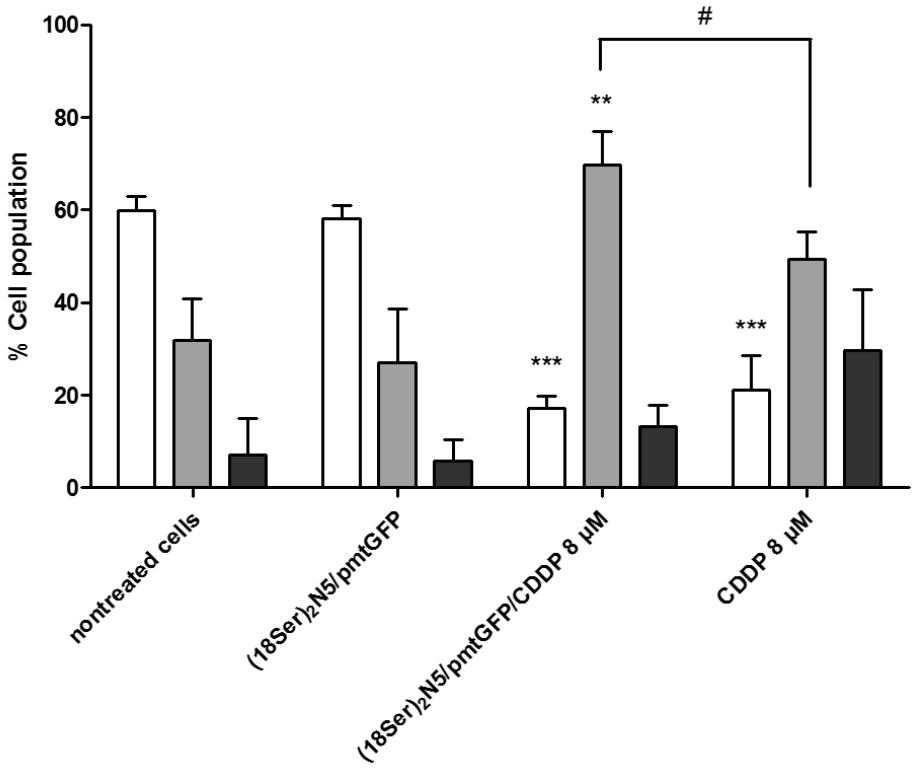

Figure 5.7 - Distribution of DBTRG-05MG cells along the phases of cell cycle. The cell cycle phases, G0/G1 (□), S (▒) and G2/M (■) are indicted in the figure. Forty-eight hours after transfection with complexes of $(18Ser)_2N5$/pmtGFP in the absence or presence of 8 µM of CDDP, cells were fixed and cell cycle was analyzed by flow cytometry. Nontreated cells and cells treated with 8 µM free CDDP are shown as controls. The results represent the mean ± SD obtained from three independent experiments. Pairwise comparisons were performed between each condition and nontreated cells (** $p<0.01$; *** $p<0.001$) and between the complexed CDDP and the free CDDP conditions (# $p<0.05$, using the unpaired t-test).

5.4.4. Impact of CDDP Added to $(18Ser)_2N5$/pGFP Complexes on Transfection Efficiency

To investigate whether the association of CDDP with the plasmid DNA could impair the efficiency of the delivery system, the levels of mitochondrial GFP expression promoted by $(18Ser)_2N5$/pmtGFP and $(18Ser)_2N5$/pmtGFP/CDDP complexes were analyzed by flow cytometry. Additionally, to clarify whether $(18Ser)_2N5$-based complexes would also promote delivery of pDNA into the nucleus, their efficiency to mediate the expression of a pncDNA encoding GFP (pncGFP) was evaluated. Figure 5.8 shows the transfection efficiency of complexes of $(18Ser)_2N5$ with pmtGFP or pncGFP, in the absence or in the presence of 8

μM CDDP. The percentage of transfected cells with $(18Ser)_2N5$/pmtGFP was statistically different from that of cells transfected with $(18Ser)_2N5$/pncGFP, which may indicate that the formulation has a certain mitochondrial tropism. Surprisingly, when CDDP was included in the delivery system, the percentage of transfected cells increased (to about 33%), as compared to that of cells transfected in the absence of CDDP (20% and 7%, when pmtGFP and pncGFP were used, respectively). Therefore, $(18Ser)_2N5$/pDNA/CDDP complexes were able to promote gene expression and, hence, CDDP delivery, both in mitochondria and nucleus.

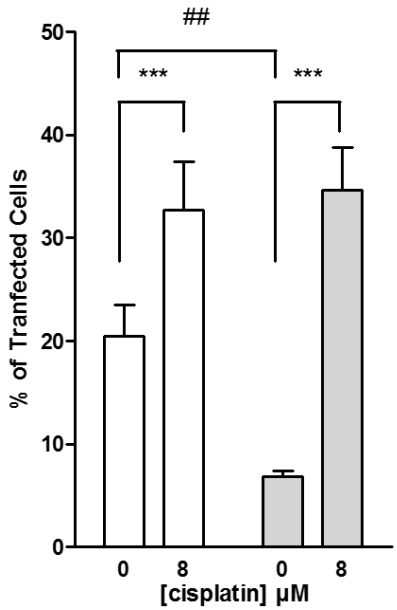

Figure 5.8 - Transfection efficiency of $(18Ser)_2N5$-based complexes carrying mitochondrial or nuclear plasmid in the absence or in the presence of CDDP. The complexes containing pmtGFP (white bars) or pncGFP (gray bars) were prepared at the 8/1 (+/-) charge ratio, in the absence or presence of 8 μM CDDP. The results are presented as a percentage of the control (nontreated cells) and represent the mean ± SD obtained from three independent experiments. Pairwise comparisons were performed between formulations prepared with the same plasmid DNA containing CDDP vs. those not containing CDDP (*** $p<0.001$) and between the formulation prepared with pmtGFP vs. that with pncGFP, in the absence of CDDP (## $p<0.01$, using the unpaired t-test).

5.5. Discussion

The efficacy of the anti-cancer drug cisplatin (CDDP) is considerably restricted by the emergence of secondary effects and the intrinsic drug resistance, resulting from DNA repair mechanisms. Hence, the DNA of mitochondria becomes an attractive target for this drug owing to mtDNA susceptibility to chemical attack, mainly because of the lack of protective histones and the limited ability of mitochondria to repair the damaged DNA (Cullen *et al.*, 2007; Preston *et al.*, 2001; Singh and Maniccia-bozzo, 1990).

Recent studies in our laboratory demonstrated the capacity of gemini-based complexes carrying a plasmid DNA encoding GFP, which is specifically translated by mitochondrial machinery (Lyrawati *et al.*, 2011), to promote the expression of this protein in mitochondria of HeLa cells [4]. In the present work, a formulation based on the cationic serine-derived gemini surfactant $(18Ser)_2N5$, previously selected because of its efficiency in delivering pmtDNA into mitochondria of human recurrent GBM cells (DBTRG-05MG), was employed to transport CDDP to mitochondria of these cells, through its intercalation into pmtDNA carried by the surfactant. The main objective of this approach is to benefit from the ability of $(18Ser)_2N5$/pmtDNA formulation to target mitochondria (inferred from the expression of GFP in mitochondria) in order to carry CDDP to the proximity of mtDNA with two predictable advantages: firstly, the reduction of the anti-cancer drug concentration required to promote a cytostatic effect (arresting cell cycle) or to drive cells to apoptosis, obviating also the extrusion of the drug by cell membrane ABC transporters (Galluzzi *et al.*, 2012); secondly, the possibility of a concomitant transport of a therapeutic gene to mitochondria, rendering these organelles more susceptible to the damage induced by CDDP in the mtDNA.

Although the serine-derived gemini surfactant with 18C hydrocarbon chains showed to promote gene expression in mitochondria in a moderate percentage of viable cells, experiments were conducted aiming at improving the efficiency of $(18Ser)_2N5$ to mediate GFP expression in these organelles, by adding to the formulation the helper lipids (HL) DOPE and Chol at different gemini surfactant/HL molar ratios (Figure 5.3). The role of these lipids in enhancing the transfection activity of conventional and serine-derived surfactants has been demonstrated in our laboratory (Cardoso *et al.*, 2014, 2015b), and attributed to the propensity of DOPE to destabilize endosomal membrane (Hafez and Cullis, 2001; Hui *et al.*, 1996; Koltover *et al.*, 1998; Siegel and Epand, 1997; Zuhorn *et al.*, 2005), and the potential of Chol to stabilize the complexes (Crook *et al.*, 1998; Faneca *et al.*, 2002; Maslov and Zenkova, 2011; Semple *et al.*, 1996). Nevertheless, HL addition to $(18Ser)_2N5$/pmtDNA complexes showed a negative impact on both the viability of DBTRG-05MG cells and the efficiency of

GFP expression in mitochondria, in accordance with previous studies in HeLa cells, which revealed a decrease in the transfection activity of complexes composed of pncDNA and $(18Ser)_2N5$ in the presence of HL (Cardoso *et al.*, 2015a). Since the Zeta potential of gemini surfactant-based complexes was shown to change from positive to negative upon addition of HL (Cardoso *et al.*, 2015a), and mitochondria display a highly negative transmembrane potential, thus counteracting the entry of negative particles into the matrix, the loss of transfection efficiency of the $(18Ser)_2N5$/pmtDNA complexes, when combined with HL, can be putatively attributed to a negative Zeta potential. Indeed, the transfection efficiency of the binary complexes showed to increase with increasing (+/−) charge ratios (Figure 5.2), supporting the need of an overall positive charge to induce mitochondrial gene expression. Moreover, the improvement of the transfection upon CDDP association to the delivery system (Figure 5.8) may be explained by the increase in the overall positive charge of the complexes conferred by the drug, which becomes positively charged in the intracellular environment (Cullen *et al.*, 2007; Rocha *et al.*, 2014).

The advantage of delivering CDDP formulated in $(18Ser)_2N5$/pmtDNA was evaluated by comparing its impact on DBTRG-05MG cell viability and proliferation with that resulting from cell exposure to free CDDP. In fact, when cells were exposed to complexed CDDP, a more drastic decrease of viability was achieved as compared to that observed for cells treated with free CDDP at the same concentrations (Figure 5.5). Indeed, the presence of 8 μM of CDDP in gemini surfactant-based complexes promoted an inhibition of cell viability (*c.a.* 30%), which was only achieved by free CDDP at 16 μM (i.e. twice the concentration).

Nevertheless, the capacity of the $(18Ser)_2N5$/pmtDNA formulation to carry CDDP seems to be dose-limited, since complexed and free CDDP, at the concentration of 16 μM, did not show significantly different effects on cell viability, likely because pmtGFP achieved CDDP-saturation at this concentration. On the other hand, cellular protein content, as assessed by the SRB assay, which reflects the number of cells in culture at each time point (Papazisis *et al.*, 1997), clearly revealed a decrease of cell growth rate upon 48 h of treatment with CDDP formulated in the complexes (Figure 5.6). In contrast, cells treated with free CDDP for the same period of time and nontreated cells exhibited an increase of the growth rate. Remarkably, at the 96 h time point, the cell density attained by cultures grown in the presence of complexed CDDP was approximately half that displayed by nontreated cells and considerably lower than that found for cells treated with free CDDP. The limited growth observed in the presence of complexed CDDP seems to correlate well with the accumulation of cells in the S phase, which were apparently prevented from proceeding to the G2/M phase of the cell cycle (Figure 5.7). Interestingly, the percentage of cells arrested in

the S phase was much lower in cultures treated with free CDDP, a significant number of cells proceeding to the next phase of the cell cycle (G2/M) being observed under these conditions.

Although we cannot definitely attribute the more severe cytotoxicity induced by complexed CDDP, as compared with that of free CDDP, to a higher accessibility to mtDNA or to a lower extrusion of the complexed drug by the cells, our work emphasizes the potential of gemini surfactant-based formulations to efficiently deliver anti-cancer drugs, which deserves to be explored towards an effective therapeutic approach. On the other hand, this study opens windows to a multimodal therapeutic approach against GBM, which allies the gene therapy addressing nuclear and/or mitochondrial genes with key-roles in cancer progression to the use of conventional pharmacological drugs, thus allowing to reduce their therapeutic concentrations and, hence, to attenuate their potential side-effects.

Chapter 6

Concluding remarks and future perspectives

Concluding remarks and future perspectives

The chemoresistance is one of the most remarkable features of GBM, being directly responsible for GBM recurrence upon surgical resection. The overexpression of ABC transporters, which promote the extrusion of chemotherapeutics to the extracellular space, and apoptosis resistance constitute inherent and acquired properties of GBM cells. Additionally, some drugs, such as those forming DNA adducts, may induce mechanisms of DNA repair, which counteract the damage promoted by such drugs.

In this context, the present study opens windows for new strategies, based on gene therapy, that increase GBM cell susceptibility to the action of anti-cancer drugs.

Employing a very well established cell model of human GBM (U87 cells), it was demonstrated that downregulation of the inhibitor-of-apoptosis protein survivin sensitized those cells to the toxicity exerted by the chemotherapeutics temozolomide and etoposide.

On the other hand, treatment of cells derived from patients presenting a recurrent GBM (DBTRG-05MG cells) with CDDP showed to benefit from drug association with a plasmid of mitochondrial DNA formulated in gemini surfactant-based complexes. Moreover, the plasmid DNA associated with CDDP did not lose its capacity to promote gene expression. Therefore, co-delivery of CDDP and a therapeutic gene emerges as a powerful strategy to fight GBM cell chemoresistance.

Importantly, the successful application of the two strategies (survivin downregulation and complex-mediated CDDP delivery) was achieved taking advantage of the versatility and potential of cationic gemini surfactants as drug delivery systems.

Altogether, data provided in this study pave the way for the development of multimodal therapies for GBM, which combine the administration of chemotherapeutics with strategies that render cells more sensitive to drugs, allowing to reduce drug therapeutic doses and, hence, to prevent non-specific toxicity.

However, further studies should be addressed to elucidate the mechanisms through which the delivery of CDDP formulated in complexes of pDNA and gemini surfactant, targeting mitochondria, ensures a more efficient inhibition of cell proliferation and cell cycle progression. Several possibilities can be envisaged: firstly, the cytotoxic activity of CDDP resulting from the formation of DNA adducts can be more severe when targeting mitochondrial genome, as compared to nuclear genome, due to the less efficient mechanisms of DNA repair in mitochondria; secondly, CDDP carried to mitochondria by surfactant-based complexes may escape to the action of ABC efflux pumps, which address cytosolic substrates. In this context, the development of gemini surfactant-based delivery systems with

an evident tropism to mitochondria could be useful to further improve CDDP therapeutic activity.

Due to the relatively low unspecific toxicity exerted by gemini surfactants in GBM cells, a dual delivery of anti-survivin siRNAs in cytoplasm and plasmid mitochondrial DNA associated with CDDP in mitochondria, mediated by distinct gemini surfactant-based systems with adequate delivery features, can also be envisaged. On the other hand, the association to the surfactant-based formulations of targeting peptides such as chlorotoxin, which binds specifically to glioma cells, could ensure a substantial reduction of drug side-effects in healthy cells.

References

ADAMSON, C. *et al.* - Glioblastoma multiforme: a review of where we have been and where we are going. Expert Opinion on Investigational Drugs. 18:8 (2009) 1061–84.

ALMEIDA, P.; VAZ, W.; THOMPSON, T. - Lateral diffusion in the liquid phases of dimyristoylphosphatidylcholine/ cholesterol lipid bilayers: a free volume analysis? Biochemistry. 31:29 (1992) 6739–47.

ALTIERI, D. - Survivin, cancer networks and pathway-directed drug discovery. Nature Reviews. Cancer. 8:1 (2008) 61–70.

AMPTOULACH, S.; TSAVARIS, N. - Neurotoxicity caused by the treatment with platinum analogues. Chemotherapy Research and Practice. (2011) 1–5.

ANDERSON, S. *et al.* - Sequence and organization of the human mitochondrial genome. Nature. 290:5806 (1981) 457–65.

ANTON, K.; BAEHRING, J.; MAYER, T. - Glioblastoma multiforme: overview of current treatment and future perspectives. Hematology/Oncology Clinics of North America. 26:4 (2012) 825–53.

BELL, P. *et al.* - Transfection mediated by gemini surfactants: engineered escape from the endosomal compartment. Journal of the American Chemical Society. 125:6 (2003) 1551–8.

BENT, M. VAN DEN; HEGI, M. E.; STUPP, R. - Recent developments in the use of chemotherapy in brain tumours. European Journal of Cancer. 42:5 (2006) 582–8.

BRANDES, A. *et al.* - First-line chemotherapy with cisplatin plus fractionated temozolomide in recurrent glioblastoma multiforme: a phase II study of the Gruppo Italiano Cooperativo di Neuro-Oncologia. Journal of clinical oncology: official journal of the American Society of Clinical Oncology. 22:9 (2004) 1598–604.

BRITO, R. *et al.* - Physicochemical and toxicological properties of novel amino acid-based amphiphiles and their spontaneously formed catanionic vesicles. Colloids and Surfaces B: Biointerfaces. 72:1 (2009) 80–7.

BURROWS, H. *et al.* - Interplay of Electrostatic and Hydrophobic Effects with Binding of Cationic Gemini Surfactants and a Conjugated Polyanion: Experimental and Molecular Modeling Studies. Journal of Physical Chemistry B. 111:17 (2007) 4401–10.

CALDAS, H. *et al.* - Survivin splice variants regulate the balance between proliferation and cell death. Oncogene. 24:12 (2005) 1994–2007.

CANCER GENOME ATLAS RESEARCH NETWORK - Comprehensive genomic characterization defines human glioblastoma genes and core pathways. Nature. (2008) 1061–8.

CARDOSO, A. *et al.* - Targeted lipoplexes for siRNA delivery. Methods in Enzymology. . 465:09 (2009) 267–87.

CARDOSO, A. *et al.* - Gemini surfactant dimethylene-1,2-bis(tetradecyldimethylammonium bromide)-based gene vectors: a biophysical approach to transfection efficiency. Biochimica et Biophysica Acta. 1808:1 (2011) 341–51.

CARDOSO, A. *et al.* - Bis-quaternary gemini surfactants as components of nonviral gene delivery systems: a comprehensive study from physicochemical properties to membrane interactions. International Journal of Pharmaceutics. 474:1-2 (2014) 57–69.

CARDOSO, A. *et al.* - New serine-derived gemini surfactants as gene delivery systems. European Journal of Pharmaceutics and Biopharmaceutics. 89:- (2015a) 347–56.

CARDOSO, A. *et al.* - Gemini surfactants mediate efficient mitochondrial gene delivery and expression. Molecular Pharmaceutics. 12:3 (2015b) 716–30.

COSTA, P. *et al.* - MicroRNA-21 silencing enhances the cytotoxic effect of the antiangiogenic drug sunitinib in glioblastoma. Human Molecular Genetics. 22:5 (2013) 904–18.

CROOK, K. *et al.* - Inclusion of cholesterol in DOTAP transfection complexes increases the delivery of DNA to cells in vitro in the presence of serum. Gene Therapy. 5:1 (1998) 137–43.

CULLEN, K. *et al.* - Mitochondria as a critical target of the chemotheraputic agent cisplatin in head and neck cancer. Journal of Bioenergetics and Biomembranes. 39:1 (2007) 43–50.

DELBRIDGE, A. R. D.; VALENTE, L. J.; STRASSER, A. - The Role of the Apoptotic Machinery in Tumor Suppression. Cold Spring Harbor Perspectives in Biology. 4:11 (2012) 1–14.

DONKURU, M. *et al.* - Advancing nonviral gene delivery: lipid- and surfactant-based nanoparticle design strategies. Nanomedicine. 5:7 (2010) 1103–27.

DUFFY, M. *et al.* - Survivin: A promising tumor biomarker. Cancer Letters. 249:1 (2007) 49–60.

EASTMAN, A. - The formation, isolation and characterization of DNA adducts produced by anticancer platinum complexes. Pharmacology & Therapeutics. 34:2 (1987) 155–66.

ELBASHIR, S. *et al.* - Duplexes of 21 ± nucleotide RNAs mediate RNA interference in cultured mammalian cells. Nature. 411:- (2001) 494–8.

EL-KHATEEB, M. *et al.* - Reactions of cisplatin hydrolytes with methionine, cysteine, and plasma ultrafiltrate studied by a combination of HPLC and NMR techniques. Journal of Inorganic Biochemistry. 77:- (1999) 13–21.

ESTELLER, M. *et al.* - Inactivation of the DNA-repair gene MGMT and the clinical response of gliomas to alkylating agents. The New England Journal of Medicine. 343:19 (2000) 1350–4.

FALSINI, S. *et al.* - Time resolved SAXS to study the complexation of siRNA with cationic micelles of divalent surfactants. Soft Matter. 10:13 (2014) 2226–33.

FANECA, H.; SIMÕES, S.; LIMA, M. C. P. DE - Evaluation of lipid-based reagents to mediate intracellular gene delivery. Biochimica et Biophysica Acta. 1567:1-2 (2002) 23–33.

FESIK, S. - Promoting apoptosis as a strategy for cancer drug discovery. Nature Reviews. Cancer. 5:11 (2005) 876–85.

FIELDEN, M. *et al.* - Sugar-based tertiary amino gemini surfactants with a vesicle-to- micelle transition in the endosomal pH range mediate efficient transfection in vitro. European Journal of Biochemistry. 268:5 (2001) 1269–79.

FIRE, A. *et al.* - Potent and specific genetic interference by double-stranded RNA in Caenorhabditis elegans. Nature. 391:6669 (1998) 806–11.

FOUGEROLLES, A. *et al.* - Interfering with disease: a progress report on siRNA-based therapeutics. Nature Reviews Drug Discovery. 6:- (2007) 443–53.

FREEMAN, W.; WALKER, J.; VRANA, K. - Review Quantitative RT-PCR: Pitfalls and Potential. BioTechniques. 26:1 (1999) 112–22.

FULDA, S.; GALLUZZI, L.; KROEMER, G. - Targeting mitochondria for cancer therapy. Nature Reviews Drug Discovery. 9:6 (2010) 447–64.

FULTON, D.; URTASUN, R.; FORSYTH, P. - Phase II study of prolonged oral therapy with etoposide (VP16) for patients with recurrent malignant glioma. Journal of Neuro-Omcology. 27:- (1996) 149–55.

FURNARI, F. *et al.* - Malignant astrocytic glioma: genetics, biology, and paths to treatment. Genes & Development. 21:21 (2007) 2683–710.

GALLUZZI, L. *et al.* - Molecular mechanisms of cisplatin resistance. Oncogene. 31:15 (2012) 1869–83.

GEORGE, J.; BANIK, L.; RAY, K. - Survivin knockdown and concurrent 4-HPR treatment controlled human glioblastoma in vitro and in vivo. Neuro-Oncology. 12:11 (2010) 1088–101.

GROSMAIRE, L. *et al.* - Alkanediyl-alpha,omega-Bis(dimethylalkylammonium bromide) Surfactants 9. Effect of the spacer carbon number and temperature on the enthalpy of micellization. Journal of Colloid and Interface Science. (2002) 175–81.

GROTH, C. *et al.* - Kinetics of the Self-Assembly of Gemini Surfactants. Journal of Surfactants and Detergents. 7:3 (2004) 247–55.

GUPTA, A. K.; GUPTA, M. - Synthesis and surface engineering of iron oxide nanoparticles for biomedical applications. Biomaterials. 26:18 (2005) 3995–4021.

HAFEZ, I.; CULLIS, P. - Roles of lipid polymorphism in intracellular delivery. Advanced Drug Delivery Reviews. 47:2-3 (2001) 139–48.

HANNON, G. - RNA interference. Nature. 418:6894 (2002) 244–51.

HANNON, G.; ROSSI, J. - Unlocking the potential of the human genome with RNA interference. Nature. 431:7006 (2004) 371–8.

HORTON, K. L. *et al.* - Mitochondria-penetrating peptides. Chemistry & Biology. 15:4 (2008) 375–82.

HUI, S. *et al.* - The role of helper lipids in cationic liposome-mediated gene transfer. Biophysical Journal. 71:2 (1996) 590–9.

JACOBS, C.; KAYSER, O.; MULLER, R. - Nanosuspensions as particulate drug formulations in therapy Rationale for development and what we can expect for the future. Advanced Drug Delivery Reviews. 47:1 (2001) 3–19.

KAINA, B. *et al.* - MGMT: key node in the battle against genotoxicity, carcinogenicity and apoptosis induced by alkylating agents. DNA Repair. 6:8 (2007) 1079–99.

KARABORNI, S. *et al.* - Simulating the self-assembly of gemini (dimeric) gurfactants. Science. 266:5183 (1994) 254–6.

KARLSSON, L.; EIJK, M. VAN; SÖDERMAN, O. - Compaction of DNA by gemini surfactants: effects of surfactant architecture. Journal of Colloid and Interface Science. 252:2 (2002) 290–6.

KAY, M. - State-of-the-art gene-based therapies: the road ahead. Nature Reviews Genetics. 12:5 (2011) 316–28.

KIM, D.; ROSSI, J. - Strategies for silencing human disease using RNA interference. Nature Reviews Genetics. 8:3 (2007) 173–84.

KIRBY, A. *et al.* - Gemini surfactants: new synthetic vectors for gene transfection. Angewandte Chemie (International ed. in English). 42:13 (2003) 1448–57.

KOLTOVER, I.; SALDITT, T.; RA, J. - An inverted hexagonal phase of cationic liposome–DNA complexes related to DNA release and delivery. Science. 281:5373 (1998) 78–81.

KONDO, S. *et al.* - Combination therapy with cisplatin and nifedipine induces apoptosis in cisplatin-sensitive and cisplatin-resistant human glioblastoma cells. British Journal of Cancer. 71:2 (1995) 282–89.

KONOPKA, K. *et al.* - Human immunodeficiency virus type-1 (HIV-1) infection increases the sensitivity of macrophages and THP-1 cells to cytotoxicity by cationic liposomes. Biochimica et Biophysica Acta. 1312:2 (1996) 186–96.

KUMAR, N.; TYAGI, R. - Industrial applications of dimeric surfactants: a review. Journal of Dispersion Science and Technology. 35:2 (2014) 205–14.

LI, H. *et al.* - PDCD5 promotes cisplatin-induced apoptosis of glioma cells via activating mitochondrial apoptotic pathway. Cancer Biology & Therapy. 13:9 (2012) 822–30.

LI, S.; HUANG, L. - Pharmacokinetics and biodistribution of nanoparticles. Molecular Pharmaceutics. 5:4 (2008) 496–504.

LI, W. *et al.* - Co-delivery of thioredoxin 1 shRNA and doxorubicin by folate-targeted gemini surfactant-based cationic liposomes to sensitize hepatocellular carcinoma cells. Journal of Materials Chemistry B. 2:- (2014) 4901–10.

LITTAU, F. M. M. And C. A. - Gemini surfactants: Synthesis and Properties. 2 (1996) 1451–1452.

LIU, L. - DNA topoisomerase poisons as antitumor drugs. Annual Review of Biochemistry. 58:- (1989) 351–75.

LOUIS, D. *et al.* - The 2007 WHO classification of tumours of the central nervous system. Acta Neuropathol. 114:2 (2007) 97–109.

LYRAWATI, D.; TROUNSON, A.; CRAM, D. - Expression of GFP in the mitochondrial compartment using DQAsome-mediated delivery of an artificial mini-mitochondrial genome. Pharmaceutical Research. 28:11 (2011) 2848–62.

MAHMOOD, T.; YANG, P.-C. - Western blot: technique, theory, and trouble shooting. North American Journal of Medical Sciences. 4:9 (2012) 429–34.

MAHOTKA, C. *et al.* - Differential subcellular localization of functionally divergent survivin splice variants. Cell Death and Differentiation. 9:12 (2002) 1334–42.

MARTIN, L.; HAMILTON, T. C.; SCHILDER, R. J. - Platinum resistance: the role of DNA repair pathways. Clinical Cancer Research. 14:5 (2008) 1291–5.

MASLOV, M.; ZENKOVA, M. - Non-Viral Gene Delivery Systems Based on Cholesterol Cationic Lipids: Structure-Activity Relationships. Non-Viral Gene Therapy. 2011).

MENGER, F; LITTAU, C. - Gemini Surfactants: A New Class of Self-Assembling Molecules. Journal of the American Chemical Society. 115:22 (1993) 10083–90.

MENGER, Fredric; KEIPER, J. - Gemini Surfactants. Angewandte Chemie (International ed. in English). 39:11 (2000) 1906–20.

MILLER, R. P. *et al.* - Mechanisms of Cisplatin nephrotoxicity. Toxins. 2:11 (2010) 2490–518.

MITA, A. *et al.* - Survivin: key regulator of mitosis and apoptosis and novel target for cancer therapeutics. Clinical Cancer Research. 14:16 (2008) 5000–5.

MOUNTAIN, A. - Gene therapy: the first decade. Trends Biotechnology. 18:3 (2000) 119–28.

MURPHY, M. - Selective targeting of bioactive compounds to mitochondria. Trends in Biotechnology. 15:30 (1997) 326–30.

MURPHY, M. - Targeting lipophilic cations to mitochondria. Biochimica et Biophysica Acta. 1777:7-8 (2008) 1028–31.

NEVES, S. *et al.* - Transfection of oral cancer cells mediated by transferrin-associated lipoplexes: mechanisms of cell death induced by herpes simplex virus thymidine kinase/ganciclovir therapy. Biochimica et biophysica acta. 1758:11 (2006) 1703–12.

NOTON, E. *et al.* - Molecular analysis of survivin isoforms: evidence that alternatively spliced variants do not play a role in mitosis. The Journal of Biological Chemistry. 281:2 (2006) 1286–95.

OHGAKI, H.; KLEIHUES, P. - Genetic pathways to primary and secondary glioblastoma. The American Journal of Pathology. 170:5 (2007) 1445–53.

OHGAKI, H.; KLEIHUES, P. - The definition of primary and secondary glioblastoma. Clinical cancer research : an official journal of the American Association for Cancer Research. 19:4 (2013) 764–72.

OKADA, H.; MAK, T. - Pathways of apoptotic and non-apoptotic death in tumour cells. Nature Reviews Cancer. 4:8 (2004) 592–603.

OLAUSSEN, K. *et al.* - Synergistic proapoptotic effects of the two tyrosine kinase inhibitors pazopanib and lapatinib on multiple carcinoma cell lines. Oncogene. 28:48 (2009) 4249–60.

OMURA, T. - Mitochondria-targeting sequence, a multi-role sorting sequence recognized at all steps of protein import into mitochondria. Journal of Biochemistry. 123:6 (1998) 1010–6.

OPALINSKA, J.; GEWIRTZ, A. - Nucleic-acid therapeutics: basic principles and recent applications. Nature Reviews Drug Discovery. 1:7 (2002) 503–14.

PAI, S. I. *et al.* - Prospects of RNA interference therapy for cancer. Gene therapy. 13:6 (2006) 464–77.

PAN, Q. *et al.* - Chemoresistance to temozolomide in human glioma cell line U251 is associated with increased activity of O6-methylguanine-DNA methyltransferase and can be overcome by metronomic temozolomide regimen. Cell Biochemistry and Biophysics. 62:1 (2012) 185–91.

PAPAZISIS, K. T. *et al.* - Optimization of the sulforhodamine B colorimetric assay. June (1997).

PENNATI, M.; FOLINI, M.; ZAFFARONI, N. - Targeting survivin in cancer therapy. Expert Opinion on Therapeutic Targets. 12:4 (2008) 463–76.

PÉREZ, L. *et al.* - Investigation of the micellization process of single and gemini surfactants from arginine by SAXS, NMR self-Diffusion, and light scattering. American Chemical Society. 111:39 (2007) 11379–87.

PFAFFL, M. W. - A new mathematical model for relative quantification in real-time RT – PCR. Nucleic Acids Research. 29:9 (2001) 16–21.

PFEIFFER, T. *et al.* - Lipoplex gene transfer of inducible nitric oxide synthase inhibits the reactive intimal hyperplasia after expanded polytetrafluoroethylene bypass grafting. Journal of Vascular Surgery. 43:5 (2006) 1021–7.

PRESTON, T. *et al.* - Mitochondrial contributions to cancer cell physiology: potential for drug development. Advanced Drug Delivery Deviews. 49:1-2 (2001) 45–61.

PURVES, D. *et al.* - Neuroscience. 3rd. ed. Massachusett, U.S.A : Sinauer Associates Inc. Publishers, 2004. ISBN 0-87893-725-0.

RABIK, C.; DOLAN, M. - Molecular mechanisms of resistance and toxicity associated with platinating agents. Cancer Treatment Reviews. 33:1 (2007) 9–23.

ROBINSON, L. - Catalysis of nucleophilic substitutions by micelles of dicationic detergents. The Journal of Organic Chemistry. 36:16 (1971) 2346–50.

ROCHA, C. *et al.* - Glutathione depletion sensitizes cisplatin- and temozolomide-resistant glioma cells in vitro and in vivo. Cell Death & Disease. 5:e1505 (2014) 1–10.

ROSENZWEIG, H.; RAKHMANOVA, V.; MACDONALD, R. - Diquaternary ammonium compounds as transfection agents. Bioconjugate Chemistry. 12:2 (2001) 258–63.

RYAN, B.; O'DONOVAN, N.; DUFFYG, M. - Survivin: A new target for anti-cancer therapy. Cancer Treatment Reviews. 35:7 (2009) 553–62.

SCHWARTZBAUM, J. *et al.* - Epidemiology and molecular pathology of glioma. Nature Clinical Practice. Neurology. 2:9 (2006) 494–503.

SEMPLE, S.; CHONN, A.; CULLIS, P. - Influence of Cholesterol on the Association of Plasma Proteins with Liposomes. Biochemistry. 35:8 (1996) 2521–5.

SEVIM, H.; PARKINSON, J.; MCDONALD, K. - Etoposide-mediated glioblastoma cell death: dependent or independent on the expression of its target, topoisomerase II alpha? Journal of Cancer Research and Clinical Oncology. 137:11 (2011) 1705–12.

SIEGEL, D.; EPAND, R. - The mechanism of lamellar-to-inverted hexagonal phase transitions in phosphatidylethanolamine: implications for membrane fusion mechanisms. Biophysical Journal. 73:6 (1997) 3089–111.

SILVA, S. *et al.* - Towards novel efficient monomeric surfactants based on serine, tyrosine and 4-hydroxyproline: synthesis and micellization properties. Tetrahedron. 65:21 (2009) 4156–64.

SILVA, S. *et al.* - Serine-Based Bis-quat Gemini Surfactants: Synthesis and Micellization Properties. European Journal of Organic Chemistry. 2012:2 (2012) 345–52.

SIMÕES, S. *et al.* - Cationic liposomes for gene delivery. Expert Opinion Drug Delivery. 2:2 (2005) 237–54.

SINGARE, P.; MHATRE, J. - Cationic Surfactants from Arginine: Synthesis and Physicochemical Properties. American Journal of Chemistry. 2:4 (2012) 186–90.

SINGH, G.; MANICCIA-BOZZO, E. - Evidence of lack of mitochondrial DNA repair following cis-dichlorodiammineplatinum treatment. Cancer Chemotherapy and Pharmacology. 26:2 (1990) 97–100.

SMITH, R. *et al.* - Mitochondrial pharmacology. Trends in Pharmacological Sciences. 33:6 (2012) 341–52.

SNUDERL, M. *et al.* - Mosaic amplification of multiple receptor tyrosine kinase genes in glioblastoma. Cancer Cell. 20:6 (2011) 810–7.

STOMMEL, J. *et al.* - Coactivation of receptor tyrosine tumor cells to targeted therapies. Science. 318:5848 (2007) 287–90.

STUPP, R. *et al.* - Radiotherapy plus Concomitant and Adjuvant Temozolomide for Glioblastoma. The New England Journal of Medicine. 352:- (2005) 987–96.

SZAKÁCS, G. *et al.* - Targeting multidrug resistance in cancer. Nature reviews. Drug discovery. 5:3 (2006) 219–34.

SZERLIP, N. *et al.* - Intratumoral heterogeneity of receptor tyrosine kinases EGFR and PDGFRA amplification in glioblastoma defines subpopulations with distinct growth factor response. Proceedings of the National Academy of Sciences of the United States of America. 109:8 (2012) 3041–6.

TANAKA, S. *et al.* - Diagnostic and therapeutic avenues for glioblastoma: no longer a dead end? Nature Reviews Clinical Oncology. 10:1 (2013) 14–26.

TODD, R.; LIPPARD, S. - Inhibition of transcription by platinum antitumor compounds. Metallomics. 1:4 (2010) 280–91.

TRABULO, S. *et al.* - Survivin silencing as a promising strategy to enhance the sensitivity of cancer cells to chemotherapeutic agents. Molecular Pharmaceutics. 8:4 (2011) 1120–31.

VERHAAK, R. *et al.* - Integrated genomic analysis identifies clinically relevant subtypes of glioblastoma characterized by abnormalities in PDGFRA, IDH1, EGFR, and NF1. Cancer Cell. 17:1 (2010) 98–110.

VERMA, I.; SOMIA, N. - Gene therapy – promises , problems and prospects. Nature. 389:6648 (1997) 239–42.

VICHAI, V.; KIRTIKARA, K. - Sulforhodamine B colorimetric assay for cytotoxicity screening. Nature Protocols. 1:3 (2006) 1112–6.

WANG, C. *et al.* - Investigation of complexes formed by interaction of cationic gemini surfactants with deoxyribonucleic acid. Physical Chemistry Chemical Physics. 9:13 (2007) 1616–28.

WANG, D.; LIPPARD, S. - Cellular processing of platinum anticancer drugs. Nature Reviews Drug discovery. 4:4 (2005) 307–20.

WANG, L.; SETLOW, R. B. - Inactivation of 06-alkylguanine-DNA alkyltransferase in HeLa cells by cisplatin. Carcinogenesis. 10:9 (1989) 1681–4.

WARE, M.; BERGER, M.; BINDER, D. - Molecular biology of glioma tumorigenesis. Histology Histopathology. 18:1 (2003) 207–16.

WEIHS, D. *et al.* - Self-aggregation in dimeric arginine-based cationic surfactants solutions. Colloids and Surfaces A: Physicochemical and Engineering Aspects. 255:1-3 (2005) 73–8.

WISNOVSKY, S. P. *et al.* - Targeting mitochondrial DNA with a platinum-based anticancer agent. Chemistry & biology. 20:11 (2013) 1323–8.

YOON, Y.; KOOB, M.; YOO, Y. - Re-engineering the mitochondrial genomes in mammalian cells. Anatomy & Cell biology. 43:2 (2010) 97–109.

ZANA, R. - Dimeric (gemini) surfactants: effect of the spacer group on the association behavior in aqueous solution. Journal of Colloid and Interface Science. 248:2 (2002) 203–20.

Zeta Sizer Nano Series User Manual. Chapters 1 and 13, United Kingdom: Malvern Instruments, Issue 1.1 (2014).

ZHANG, J.; STEVENS, M.; BRADSHAW, T. - Temozolomide: mechanisms of action, repair and resistance. Current Molecular Pharmacology. 5:1 (2012) 102–14.

ZHENG, Y. *et al.* - A novel gemini-like cationic lipid for the efficient delivery of siRNA. New J. Chem. 38:10 (2014) 4952–62.

ZUHORN, I. *et al.* - Nonbilayer phase of lipoplex-membrane mixture determines endosomal escape of genetic cargo and transfection efficiency. Molecular Therapy. 11:5 (2005) 801–10.